Resource localization and multimodal flight control in *Drosophila melanogaster*

Thesis by
Seth A. Budick

In Partial Fulfillment of the Requirements for the
Degree of Doctor of Philosophy

California Institute of Technology
Pasadena, CA

2007
(Defended May 23, 2007)

Acknowledgements

I wish to thank Titus Neumann for his assistance with the free-flight fly visualization system and with German language translation. I also thank Andrew Straw for his help in programming the pulse generating system used in the free-flight experiments and for his design of the fly visualization system used in the magnetically tethered flight experiments. I thank John Bender for assistance with the magnetic tether apparatus and William Dickson for useful discussion on the mechanics of magnetically tethered flight. I thank Michael Dickinson and Michael Reiser for their assistance in building the rigidly tethered flight apparatus, Dan Rizzuto for his implementation of the non-parametric test for circular mean differences, and Don Lifke for suggestions on statistical analysis. Finally, I thank the members of my thesis committee, Masakazu Konishi, John Allman, Gilles Laurent, and Michael Dickinson for their valuable input on all aspects of this thesis.

Abstract

Upwind flight is a common strategy among insects searching for the sources of attractive odors. While much is known about the behavior of male Lepidoptera tracking female pheromone plumes, data on odor localization in other taxa, including the model organism *Drosophila melanogaster*, have been relatively lacking. The work presented in this thesis provides a description of the multimodal control of forward flight in *D. melanogaster*, including olfactory mediated flight during the localization of attractive resources.

Here it is shown that *D. melanogaster* responds rapidly to the onset of olfactory stimulation by turning upwind and increasing its airspeed, yielding an upwind surge. Following plume loss, flies, like many moths, often cast—flying perpendicular to the wind while making iterated large-angle turns. Flies, however, are anemotactic even in the absence of odor, and unlike many Lepidoptera, they also fly fast and straight upwind in a homogenous odor cloud. Though they respond rapidly to odor contact and loss, flies thus do not require intermittent olfactory stimulation in order to sustain upwind flight.

The results of tethered-flight experiments are largely in accord with those from free-flight. Pulsed and continuous olfactory stimuli elicit qualitatively similar responses in the wing kinematics of tethered flies, suggesting that the intermittency of the odor plume is not a key parameter in modulating flight behavior. At the same time, a tethered-flight analogue of casting may preferentially follow exposure to brief odor pulses, suggesting that pulse duration is an important factor in shaping flight trajectories.

The role of mechanosensory cues in the orientation of flying insects has been the focus of relatively little research. The results presented here suggest that a strong mechanosensory response orients flying flies into an oncoming wind, as would be experienced during forward flight. This response is mediated by the Johnston's organs and may play an essential role during forward flight. Expanding visual stimuli, which necessarily accompany forward translation, normally elicit a robust turning response in flies. The wind orientation response described here is sufficient to suppress this visual reflex, however, potentially explaining how flies are able to successfully fly forward while searching for attractive resources.

Contents

List of Figures

List of Tables

CHAPTER 1

Introduction

Flying insects demonstrate a remarkable ability to localize the resources necessary for their survival and reproduction. In doing so successfully, they must integrate the input of multiple sensory modalities. Insects have thus served as model systems in neuroethological studies on the control of locomotion, particularly with respect to the role of the visual and olfactory systems. The work in this thesis pertains to the multimodal control of flight in *Drosophila melanogaster*, but our understanding of flight control draws on a diverse literature, from the level of sensory input all the way to theoretical models of optimal search behavior.

1.1 Search strategies

Analyses of the search strategies used by insects to locate resources generally divide those searches into two main classes: those in which a conspicuous olfactory signal permits detection of a distant resource, and those where the resource must be detected at relatively close range (the "range of detection" or "active space" of the resource). For resources that do not advertise themselves via olfactory cues, theoretical studies have described optimal search strategies for contacting a resource's active space. This type of non-directed search is often referred to as "ranging" and has been most extensively described by Dusenberry (1989b; 1992).

When a chemical stimulus is borne on a current, the range of detection becomes asymmetric. That is, the axis of the resulting plume lengthens along the direction of flow, creating an elongated active space. For a plume that is longer than it is wide, search becomes optimal at a course heading of 90° relative to the direction of the current, with the relative advantage of cross-current movement increasing as a function of flow velocity (Dusenberry, 1989a). It is thus not surprising that many flying insects apparently search for plumes by flying perpendicular to the wind line (Kennedy et al., 1981; Kuenen and Cardé, 1994; Zanen et al., 1994).

An additional complication arises, however, due to fluctuations in wind direction. In winds shifting over ±30° relative to the mean direction, the time-averaged plume becomes wider than it is long, and the optimal search orientation switches from cross-wind to one directed upwind or downwind (Dusenberry, 1989a; Sabelis and Schippers, 1984). In at least two species of *Drosophila*, this closely matches an observed change in search strategies in shifting winds (Zanen et al., 1994).

1.2 Plume structure

Time-averaged plume analyses imply a uniformity of the stimulus environment within that space. In fact, plume structure is often highly non-homogeneous, with filaments containing high concentrations of odorant interspersed with large volumes of relatively clean air (Murlis et al., 1992). This distribution results from the two distinct mixing mechanisms that affect odorant molecules: molecular and turbulent diffusion. The root mean square (rms) 3-D displacement of a molecule by molecular diffusion is equal to $(6*D*t)^{\frac{1}{2}}$, where D is the diffusion coefficient and t is time. Even for a very small molecule like CO_2, the rms displacement after one minute is only 7.6 cm, illustrating the relatively limited movement resulting from this process on a time scale of seconds. Turbulent diffusion, meanwhile, may have a much greater effect on plume structure over similar durations.

Turbulence, the fluctuating component of wind velocity, results in the mixing of air at a variety of spatial scales (Hanna and Insley, 1989; Murlis et al., 1992). When the ground is irradiated by the sun, convective energy is injected into giant vortices, whose energy is transferred to progressively smaller eddies. At large scales—hundreds to thousands of meters—eddies cause long-term shifts in wind direction. On the scale of meters, eddies may cause plumes to undulate and meander, yet still do relatively little to disrupt their fine spatial structure. This is because at a characteristic size, the Kolmogorov length, vortices lose their energy in the form of heat due to the air's viscosity. Below the Kolmogorov length, mixing is a function of molecular rather than turbulent diffusion.

If a plume was to emanate from a point source, its width would expand, driven by molecular diffusion, until it reached the Kolmogorov length, at which point individual plume filaments may be stretched and stirred (Jones, 1983). Studies indicate that plumes may therefore often be composed of multiple coherent filaments, while the plume as a whole undulates due to large-scale eddies (Murlis et al., 1992; Murlis et al., 2000). An insect may thus be likely to encounter a plume as a series of discrete odor packets, and this realization has shaped a great deal of current research on olfactory localization (e.g., Mafra-Neto and Cardé, 1994; Murlis et al., 1992; Vickers and Baker, 1994).

1.3 Evidence from Lepidoptera

For a variety of reasons, not least their extremely robust responses to simple blends of pheromones, several species of Lepidoptera have served as behavioral and physiological models of olfactory mediated search (see papers in Cardé and Minks, 1997). It was using mosquitoes, however, that Kennedy (1940) first showed that insects, activated by an olfactory stimulus, fly upwind by using visual motion to maintain their groundspeed, a behavior known as "optomotor anemotaxis." This finding was later extended to male moths tracking a pheromone plume, but unlike mosquitoes, these insects did not proceed directly

upwind, instead zigzagging while following a generally upwind trajectory (Marsh et al., 1978).

Interestingly, moths also counterturn following odor loss, but with progressively larger magnitudes, leading to "casting"—flight directed across the wind-line with iterated large magnitude turns (Kennedy et al., 1980; Kennedy et al., 1981). These results led to the hypothesis that in addition to optomotor anemotaxis, pheromone contact triggers a self-steered counterturning program which nevertheless is also subject to modulation by additional stimuli, such as odor concentration (Kennedy, 1983; Kuenen and Baker, 1983).

While this general model of Lepidoptera flight is still largely accepted, recent results have suggested a greater role for plume fine structure in shaping flight trajectories (Baker et al., 1985). Baker & Haynes (1987), showed that male moths of the species *Grapholita molesta* surge upwind in response to individual instances of plume contact and rapidly shift to cross-wind flight following plume loss. This result led Baker (1990) to formulate a model for moth behavior whereby contact with an odor plume initiates both a phasic upwind surge and a tonically activated, long-lasting, internal counterturn-generating program. The rapidly adapting phasic response suppresses the tonic one, giving rise to upwind surges immediately following plume contact. On plume loss, the tonic program is expressed, yielding casting flight. This model also accounts for the observation that many moth species enter a period of sustained casting when flying in a homogenous plume (Kennedy et al., 1980; Willis and Baker, 1984). Interestingly, theoretical models for optimal search during upwind flight in an intermittent plume suggest that such a "surge and cast" pattern may maximize the efficiency of locating an odor source (Balkovsky and Shraiman, 2002).

The Baker model predicts that an insect encountering a plume that is pulsed at the appropriate frequency may respond by flying straight upwind. That is, successive pulses may elicit iterated upwind surges, but avoid adaptation of the phasic response, and thus the expression of the counterturning program. Indeed, at least two species of moths have subsequently been shown to be capable of straight upwind flight under these conditions, providing support for the Baker model (Mafra-Neto and Cardé, 1994; Vickers and Baker, 1994). Nevertheless, the

applicability of this model to flight in other insect orders has yet to be extensively tested.

1.4 The *Drosophila* olfactory system and relevant comparisons to other insect species

It is important to consider these behaviors in light of the function and constraints of insect olfactory systems. Enormous progress has been made in recent years in understanding how insects process olfactory stimuli. In *Drosophila*, olfactory receptor neurons (ORNs) are located on the antennae (about 1200 ORNs) and maxillary palps (about 120 ORNs). These neurons are compartmentalized in olfactory sensillae with up to four ORNs housed within individual sensillae (de Bruyne et al., 1999; de Bruyne et al., 2001). Olfactant molecules enter the sensillae through cuticular pores and diffuse across the sensillar lymph, possibly with the aid of odorant binding proteins (Rützler and Zwiebel, 2005), before activating olfactory receptor proteins on the ORN dendrites. The 62 members of the odorant receptor family are seven transmembrane domain G protein coupled receptors, and their activation triggers a transduction cascade that leads to depolarization of the ORN (Robertson et al., 2003).

The secondary olfactory neuropil, the antennal lobe (AL), is composed of about 43 discrete units, the glomeruli. With very few exceptions, a single ORN expresses only one olfactory receptor protein and, for the most part, a single ORN projects to just one glomerulus in the AL (Couto et al., 2005; Fishilevich and Vosshall, 2005). Furthermore, a given glomerulus receives ORN input from cells expressing only a single olfactory receptor, resulting in a precise spatial map of ORN activity in the AL. Individual olfactory receptor types are tuned to specific classes of odorants. For instance, multiple glomeruli have strong preferences for esters, yet different glomeruli respond maximally to carbon chains of different lengths (Couto et al., 2005; de Bruyne et al., 2001; Hallem et al., 2004). At the same time, there is overlap in the sensitivities of different olfactory

receptors, and their corresponding ORNs, such that stimulation with even a single odorant evokes a broad pattern of activation across the AL (Wang et al., 2003; Wilson et al., 2004).

The question of how the brain is able to extract an odorant's identity has been the subject of much recent research. In the glomeruli, ORNs synapse on projection interneurons (PNs) which project to downstream targets in the mushroom bodies and lateral horn of the protocerebrum. A single PN innervates only one glomerulus, but local interneurons (LNs) make substantial lateral inhibitory contacts between glomeruli. The degree to which PN output matches ORN input to its respective glomerulus is still somewhat unclear. Optical imaging of PN activity has indicated a relatively faithful transmission of the signal from ORN input to PN output (Ng et al., 2002; Wang et al., 2003). Electrophysiological recordings, however, have suggested that PNs are more broadly tuned and have very different dynamics than their corresponding ORNs, suggesting an important role for the LNs in integrating activity across the AL (Wilson et al., 2004).

The transduction mechanics of the olfactory system are especially important to consider in regards to plume tracking. As mentioned above, recent studies have indicated that the behavioral response of a male moth tracking a pheromone plume may depend strongly on the precise frequency of interception of odorant pulses, at rates up to 10Hz (Mafra-Neto and Cardé, 1994; Vickers and Baker, 1994). The speed of the olfactory system and its "flicker-fusion" rate may thus play a central role in determining the moth's behavioral response dynamics. In cockroaches for example, ORNs are able to track olfactory stimulation at rates up to 40Hz (Lemon and Getz, 1997) while PNs can track pulses at 5–10Hz (Lemon and Getz, 1998). In the moth *Antheraea polyphemus*, olfactory receptors are able to detect individual pheromone pulses up to 10Hz (Rumbo and Kaissling, 1989), while PNs can resolve pulses at the same frequency in *Manduca sexta* (Christensen and Hildebrand, 1988). It thus appears as though insect olfactory systems, at the sensory and central levels, are capable of the high-frequency performance implied by these behavioral results. Unfortunately, no analogous work yet exists for *Drosophila melanogaster*.

1.5 Visual control of *Drosophila* flight

D. melanogaster has been a model organism in the study of the visual control of behavior. The optomotor response, for instance, was described very early in this species (Götz, 1964). In this paradigm, an animal responds to rotation of the visual field by turning syndirectionally, and at the same angular velocity as the stimulus, compensating for rotation that could otherwise have been generated by an unintended turn, perhaps due to a wind gust. Besides this large-field response to spatially extended patterns, *D. melanogaster* is also highly responsive to local visual stimuli, strongly fixating vertical edges in a tethered-flight paradigm (Götz, 1987). This response is mediated by a neural pathway that is distinct from the one underlying the large-field response, at least in the flies *Musca domestica* and *Calliphora erythrocephala* (Egelhaaf, 1985a; Egelhaaf, 1985b; Egelhaaf, 1987).

In recent years, another robust, visually evoked behavior has been described in *D. melanogaster*: the expansion avoidance response. It has become apparent, both from free- and tethered-flight experiments, that visual expansion is an extremely potent aversive stimulus, eliciting avoidance responses in the form of saccades (high angular-velocity turns) when the angle subtended by an approaching object reaches a critical size (in tethered-flight) (Bender and Dickinson, 2006b), or when the total visual expansion exceeds a threshold value (in free-flight) (Tammero and Dickinson, 2002b).

This expansion avoidance response would seem to be an intuitive behavioral strategy since it reduces the likelihood of collisions with looming objects. At the same time, flies must sometimes land on these objects, such as an odorous piece of necrotic fruit, rather than saccading away from them. Thus, an alternate neural pathway must be triggered some fraction of the time upon approach to an expanding visual stimulus. Tethered-flight experiments have demonstrated that the relative likelihood of a saccade or landing response depends on the expanding object's position on the fly's retina, such that objects

looming in front of the fly are relatively more likely to elicit landing, whereas those expanding laterally favor saccades (Tammero and Dickinson, 2002a).

Forward flight would thus appear to be a problematic goal for a fly intent on avoiding visual expansion. A fly translating forward will inevitably encounter expansion, the most potent stimulus for eliciting avoidance responses in tethered-flight. Recent work has demonstrated that this paradox may be partially explained by considering behavior in a more realistic visual setting.

If a tethered fly is presented with a periodic pattern of vertical stripes expanding from a focus of expansion (FOE), its orientation towards the FOE depends on the temporal frequency of the stimulus. Thus, at an expansion rate above approximately 1 Hz, *D. melanogaster* orients instead towards a focus of contraction (FOC), but at lower temporal frequencies, the avoidance of the FOE largely disappears, or even reverses (Reiser, 2007). Thus, depending on realized expansion rates in free-flight, this dependence may help to explain real world behavior.

Further, it may be the case that in free-flight, a good deal of flight is "goal-directed" in that flight control may often be dominated by object fixation rather than large-field responses. Thus, when a vertical bar is superimposed on the FOE, that pole becomes much less aversive (Reiser, 2007). In this thesis, I will further explore the role that wind plays in overcoming this strong intrinsic aversion.

1.6 Olfactory mediated flight in *Drosophila*

From the above descriptions, it might appear as though mechanisms of plume tracking are largely consistent across the Lepidoptera. While it is easy to over-generalize, there is a fair degree of stereotypy among those species that have been studied, raising the question of whether this represents shared evolutionary origins, or convergence on an optimal strategy of plume localization. For this reason, it is especially interesting to consider odor localization in unrelated species such as *D. melanogaster*.

Despite its role as a model species in genetics, neurobiology, and behavior, odor tracking has been relatively unstudied in *D. melanogaster*. David (1982), showed that *Drosophila hydei*, in general, maintains a preferred groundspeed despite fluctuations in windspeed, as is also the case in mosquitoes (Kennedy, 1940). Wright & colleagues presented anecdotal evidence that *D. melanogaster* responds to narrow odor plumes by flying convoluted upwind trajectories, and by flying straight upwind in a homogeneous plume (Kellogg et al., 1962; Wright, 1964). On odor loss, flies flew across or downwind.

When searching for the source of an attractive odor while flying in still air, *D. melanogaster* increases its rate of saccades (high angular-velocity turns) when near the odor source, while decreasing its velocity (Frye et al., 2003). *D. melanogaster* also executes saccades sooner when flying away from an odor source, suggesting perhaps that saccades are initiated in response to the perception of decreasing odor concentration (Frye et al., 2003). The interpretation of results in still air is difficult, however, since the precise nature of the odor environment is hard to ascertain, making wind-tunnel studies with a well-defined plume structure desirable.

1.7 Mechanosensation and the paradox of upwind flight

Among the sensory modalities discussed thus far, vision has received perhaps the greatest degree of attention in studies of insects orienting with respect to the local environment. As mentioned earlier, Kennedy (1940) first showed that mosquitoes make use of visual cues to set their groundspeed during upwind flight by maintaining a consistent velocity relative to the visual environment.

In addition to simply setting groundspeed, it has also been suggested that insects use visual cues to maintain a consistent orientation in the presence of an externally imposed wind (Marsh et al., 1978). If an insect's flight trajectory (course angle) is not parallel to the wind direction, it will drift sideways, resulting in image flow over its ventral and dorsal ommatidia; a signal that could be

decomposed into its longitudinal and transverse components. In theory, an insect could thus maintain an upwind heading by minimizing transverse flow. Alternatively, if the insect's goal was to maintain a trajectory at some consistent angle relative to the wind, it could hold transverse flow at a constant value for a given wind velocity. In the case of a counterturning moth, the sign of the transverse flow could then be iteratively reversed (David, 1986).

The role of mechanosensory cues in orienting insect flight has received relatively little attention however. A wind-borne insect cannot use mechanosensory information to detect the direction or velocity of the ambient air (David, 1986). It is entirely possible however, and in fact quite likely, that insects do use mechanosensory cues to detect their own velocities relative to the ambient air, as well as yaw deviations from the direction of their thrust vectors.

The first indication that insects use mechanosensory information in flight orientation came from Weis-Fogh's work on the paired beds of trichoid sensillae in *Schistocerca gregaria* (Weis-Fogh, 1948; Weis-Fogh, 1949). Weis-Fogh observed that tethered insects, subjected to asymmetric wind stimulation on their heads, tended to orient into the direction of the oncoming wind. Thus, if a flying insect was temporarily yawed relative to its direction of motion, as appears to be the case in locusts, where an individual's yaw may average 5.2^{o} relative to its direction of flight (Baker et al., 1981), the resulting side-slip could induce a mechanical stimulus leading to an orientation response.

Gewecke (1970) demonstrated that locust antennae also contribute to wind detection. In insects that had their antennae glued at the level of the pedicellus-flaggellum joint (eliminating input to antennal mechanoreceptors), wing stroke amplitude showed a significantly smaller decline in response to increasing wind velocity than in control animals. Arbas (1986) showed that the antennae also act as wind direction sensors in *Schistocerca gregaria*, but in an apparently antagonistic capacity to the hair beds. Locusts with their antennae and sensillae immobilized tended to turn into the direction of an oncoming wind, while those with only the hair beds immobilized turned away from the wind.

Similar results have been obtained in a variety of species and insect orders, including Diptera (Gewecke, 1967b; Schneider, 1953), Hymenoptera (Heran,

1959), and Lepidotera (Gewecke and Niehaus, 1981; Niehaus, 1981). Nevertheless, it has been difficult to ascribe the role of wind detection to any one sensory structure within the antennae. In most cases, multiple structures, including the Johnston's organs (JOs), campaniform sensillae, and other chordotonal organs respond to deviations of the flagellum relative to the pedicel. Wind-mediated orientation in *D. melanogaster*, where the JO is the only mechanoreceptive organ present at this junction, has not been tested however.

Finally, as described above, flies avoid expanding visual stimuli in free- and tethered-flight, though recent experiments have indicated that this response is dampened under certain visual conditions. In tethered-flight however, wind-induced mechanical feedback cues are absent, and it is possible that these are required to suppress the powerful expansion avoidance response. That is, the perception of a headwind, as would be experienced during forward flight, may be necessary in order to tolerate the accompanying visual expansion.

1.8 Plan for thesis

The goal of this thesis is to describe the use of olfactory, visual, and mechanosensory cues in structuring the flight trajectories of *D. melanogaster*. In Chapter 2, I describe the methods used in free- and tethered-flight studies to test fly responses in naturalistic and controlled conditions. In Chapter 3, I document the free-flight behavior of flies responding to plumes of attractive odors. The results of these experiments have previously been published by Budick & Dickinson (2006). In Chapter 4, I examine the tethered-flight responses of flies exposed to odor plumes similar to those encountered in the free-flight experiments. In Chapter 5, I then test the additional role of mechanosensory stimuli in orienting flight trajectories, particularly in the context of competing visual stimuli. Those results have recently been submitted for publication (Budick et al., in review).

CHAPTER 2

Experimental methods

2.1 Free-flight experiments

2.1.1 Wind tunnel

An open-circuit, closed-throat wind tunnel was built commercially to custom specifications (Engineering Laboratory Design, Inc., Lake City, MN). At the intake end, air was drawn through a honeycomb and screen pack followed by a 6.25:1 contraction and then a 1.55 m long working section, constructed from acrylic, with a width and height of 0.305 m (Fig. 2.1A). The working section was followed by a diffuser and then the fan. At the upwind and downwind ends of the working section, 1 mm mesh prevented the flies from escaping from the tunnel. All ducts were fabricated of fiberglass-reinforced plastic.

The floor of the tunnel was painted black with acrylic paint to aid in fly visualization as described below. The walls of the tunnel were covered by a random pattern consisting of black and white squares of length 1.4 cm. At this size, a square normal to the fly would subtend 5° of visual space when viewed from the midline of the tunnel. The checkerboard patterns were perforated at half their height to allow for illumination via infrared diodes positioned outside the tunnel, again to aid in fly visualization.

In experiments utilizing wind, the velocity was set to 0.4 m sec^{-1}. This value was selected as odor source localization was robust at that speed while

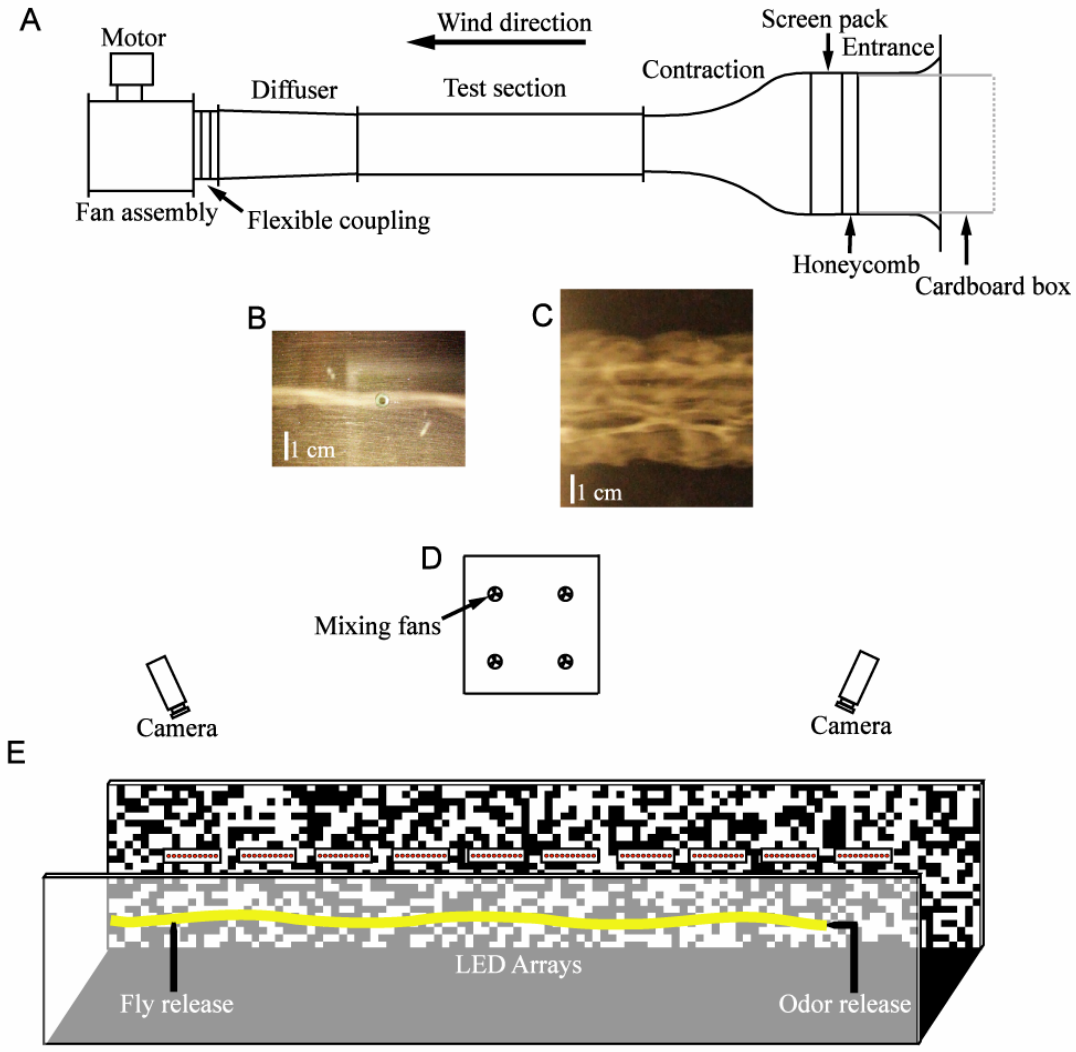

Figure 2.1. (A) Schematic profile view of the full wind tunnel. Gray/dotted line at upwind end represents the 76 cm cardboard box used for generation of the homogeneous cloud. Smoke visualization of the ribbon (B) and large diameter (C) plumes. (D) Front view of the 76 cm cardboard box with 4 mixing fans. (E) Schematic representation of the working section of the wind tunnel. Flies were introduced via a pipette tip glued to the end of a tube at the downwind end of the tunnel; odor was introduced via a second tube at the upwind end. The floor of the tunnel was painted black and the walls were covered with a random checkerboard pattern. Arrays of IR diodes illuminated the tunnel which was visualized by two IR sensitive cameras positioned above it (camera positions not to scale).

being inhibited at higher velocities. Furthermore, our own observations of wind velocities in an orange orchard in which *Drosophila* spp. were active indicated that this value was well within the normal range of variation both beneath individual orange trees and in the open spaces between trees (mean velocity 0.37 ± 0.35 m sec^{-1}).

2.1.2 Odor

Banana odor was produced by macerating ripe banana, together with distilled H_2O and bakers yeast in the ratio 1g banana:1 ml H_2O:0.02 g yeast. This recipe was chosen on the basis of its demonstrated ability to lure wild flies to outdoor traps and is derived from standard *Drosophila* bait recipes (e.g., Carson and Heed, 1986). This mixture was allowed to ferment for 45 minutes at approximately 25°C and was then filtered through 0.1 mm mesh for an additional hour. The filtrate was produced in quantities of 0.5–1 L and frozen immediately for later use.

Fly responses were tested in three differently structured odor plumes. In ribbon plume experiments, air was bubbled through the banana mixture at a rate of 0.3 L min^{-1} by means of a volume flow controller (Sierra Side Trak, Monterey, CA). The banana mixture was contained within a polypropylene vial with clean air passing into the vial via a 3 mm diameter brass tube that penetrated the vial's lid. The tube descended slightly less than the height of the vial such that the air emerging from it bubbled through 50 mL of the banana mixture. The scented air then passed out of the vial via a PVC tube attached to the vial's lid and passed into an acrylic tube of 3 mm diameter that penetrated the tunnel floor 13 cm from the upwind end of the working section, halfway between the two tunnel walls. This acrylic tube was bent 90° at a height of 15.25 cm, half the height of the tunnel, and a polypropylene nozzle, diameter 2 mm, was glued to the end of the tube. In wide plume experiments, air was injected into the banana mixture at 1.0 L min^{-1} and passed down a 3 mm diameter brass tube that penetrated the tunnel floor in the same position as in the ribbon plume experiments. This brass tube was then inserted in, and glued to, the end of a 7

mm diameter acrylic tube, 157 mm in length, parallel to the tunnel floor. This tube was perforated by a 1 mm diameter hole at its downwind end and three additional sets of 4 concentric holes, with one set each at 5, 10 and 15 cm along its length. Due to the pressure differential along the length of this tube, gas exiting the more proximal holes was projected further from the tube, resulting in a diffuse cylindrical plume. The wide plume was either produced continuously, or was pulsed via a three-way solenoid valve (Valve Driver II, General Valve Corp., Fairfield, NJ) controlled by custom software running on a PC. This valve was downstream of the flow controller and switched a clean air input between one output that led to the vial containing the banana odor and a second output which simply consisted of a PVC tube. Those two output lines were then reunited via a Y junction just prior to reaching the brass tube that passed through the tunnel floor, thus switching the odor and clean air inputs to the tunnel. In the pulsed plume, the banana odor alternated with clean air at 1 sec intervals. By switching the input to clean air, the odor was evacuated very rapidly from the tube following the truncation of each pulse, producing very sharp boundaries at both the leading and lagging edges of the pulse, as judged from smoke visualization.

To visualize the odor plume produced by these delivery systems, we generated a smoke plume by pumping mineral oil through a hypodermic needle across which we placed a high voltage that burned the oil. The smoke thus generated was then injected into the tunnel under the same conditions as in the odor plume experiments and the plume's trajectory and dimensions were measured. The ribbon plume was slightly sinuous, with a mean instantaneous diameter of 0.68 ± 0.09 cm, measured at 10 1 cm intervals along its length (Fig. 2.1B). The envelope described by the undulating plume, along this same length, was 1.01 cm and thus for analytical purposes, we modeled the plume as a 1 cm diameter cylinder. We similarly measured the mean instantaneous diameter of the large diameter plume as 4.84 ± 0.24 cm and this plume was thus modeled as a 4.84 cm diameter cylinder (Fig. 2.1C). The position of the plume within the tunnel was determined by recording its position at its upwind entrance and at the downwind exit and linearly interpolating between the two.

Homogeneous odor cloud experiments used the same banana odor, but in this case, air was pumped into 100 mL of the filtrate at 25.5 L min^{-1}. A large cardboard box, 76 cm square, was inserted into the tunnel inlet and served as a mixing chamber for the odor. Four computer fans were positioned approximately equidistant from each other and from the walls of the cardboard box (Fig. 2.1D). Four PVC tubes carried the odor from the vial to the cardboard box where the odor was released immediately upstream of the four small fans and was mixed thoroughly in the mixing chamber (as judged by experiments with smoke tracers). By the time it reached the working section however, the smoke plume was too diffuse to visualize. Normalizing the odor density of the ribbon plume to 100%, the calculated densities of the wide plume and homogeneous cloud were 18% and 11% respectively.

2.1.3 Animals

Experiments were performed at approximately 25°C on 3–5 day old female fruit flies, *Drosophila melanogaster* Meigen, descended from a wild-caught population of 200 mated females. Animals were deprived of food, but not water, for 20–24 hours prior to experimentation in order to motivate flight. On the day of experimentation, approximately 100 flies were kept in a 50 ml vial beneath the tunnel where they acclimated for 10 minutes to two hours, depending on when they were introduced into the tunnel, as described below, with an experiment lasting approximately two hours. This vial was connected, via a stop cock, to an acrylic tube of diameter 5 mm that penetrated the floor of the tunnel at a distance 16.7 cm from the downwind end of the working section. This tube was capped by a pipette tip such that flies emerging from the tube were positioned halfway between the tunnel walls and at approximately half the height of the tunnel. Flies were introduced into the tunnel individually such that the odor plume intercepted the fly release tube at approximately the height of the emerging flies, immediately exposing them to the odor. If a fly did not take flight shortly after emerging into the tunnel, one or more flies were introduced in order to increase the probability that one would do so. Flies were captured by

the imaging system from takeoff at the release tube or shortly after takeoff. Individual trajectories were often recorded as several trajectory fragments due to loss of the fly by the visualization system. As such, a single mean value based on all trajectory fragments was calculated for each trajectory parameter for each fly, except as noted below. In all experiments, flies were recorded until they landed. The flies were vacuumed out of the tunnel approximately every ten minutes.

2.1.4 Tunnel illumination and fly visualization

The tunnel was illuminated by a linear array of 10 halogen bulbs on each side yielding a luminance of 60 to 120 lux within the working section. IR LEDs (HSDL-4200, Hewlett Packard, Palo Alto, CA) positioned at the mid-height of the tunnel provided illumination for two near IR sensitive cameras (SSC-M350, Sony, Tokyo, Japan) positioned 1.27 m above the tunnel at a distance of 1.82 m from each other (Fig. 2.1E). The 3-dimensional flight trajectories were sampled at 60 frames s^{-1} and reconstructed with commercially available software, Trackit 3-D (Fry et al., 2000). In the pulsed plume experiments, the state of the solenoid valve was recorded at every time point together with the 3-dimensional fly position. We were thus able to determine the location of all pulses in the tunnel at any given time as well as the fly's position relative to them. This allowed us to determine the moment of plume entry and plume loss. The fly trajectories were smoothed to remove digitization errors by low-pass filtering with a fifth order Butterworth filter using a frequency cutoff of 7.5 Hz.

All analyses of fly trajectories made use of software written using Matlab (Mathworks). Only trajectories longer than 0.42 sec were analyzed in order to be of sufficient length for low-pass filtering. Flies approaching the odor source generally slowed down and ceased to respond with upwind surges, due either to the visual effects of the plume source, changes in plume dynamics, or both. Because of these qualitative changes in flight trajectories as the animals approached and landed on the odor release site, flight within the most upwind 0.25 m of the tunnel was excluded from quantitative analyses. In order to

visualize the distribution of flies within the wind tunnel, individual trajectories (Fig. 2.2A) were overlaid (Fig. 2.2B), and plotted as pseudocolor transit probability histograms (Fig. 2.2C). Flight trajectories were described in terms of a number of variables that were calculated at every frame in the flight trajectory (Fig. 2.3). Groundspeed was determined from the distance that the animal traveled in the horizontal plane between samples. Cross-wind velocity and upwind velocity were the components of groundspeed directed across the width of the tunnel and up its long axis, respectively. Vertical velocity was determined from the distance that the animal traveled in the vertical plane between samples. Three-dimensional heading was the angle formed by the tangent to the flight trajectory and the long axis of the tunnel, such that 0° corresponded to straight upwind and 180° was straight downwind. Three-dimensional heading is thus intentionally underdefined in that a value of 90° could correspond to any vector within the transverse vertical plane of the fly. Heading (track angle) was the projection of three-dimensional heading in the horizontal plane of the fly and is equivalent to the angle between the groundspeed vector and the long axis of the tunnel. Airspeed was calculated trigonometrically using groundspeed, wind speed, and heading and is the velocity of the animal in the horizontal plane relative to the wind. Finally, plume distance was defined as the shortest absolute 3-D distance between the fly and the plume. Substantial variability in the overall shape of flight trajectories, relative to published trajectories for moths, made it difficult to assign meaningful parameters to the counterturning behavior, such as turn frequency or inter-reversal distance.

2.1.5 Statistical analysis

All linearly distributed trajectory parameters were compared using heteroscedastic t-tests whereas count data were compared with χ^2 tests. Heading data were circularly distributed and thus required treatment with the appropriate statistical methods. For each trajectory, a mean heading was calculated by treating the instantaneous heading between each pair of frames as a unit vector with angle θ_i. The rectangular components of this unit vector are

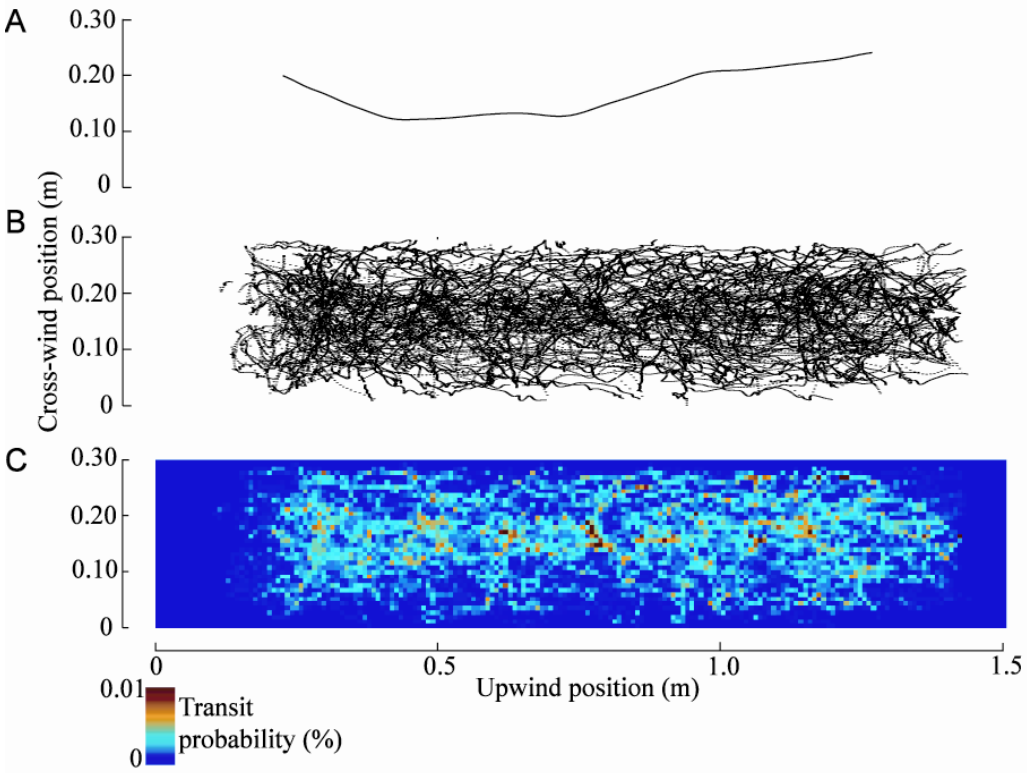

Figure 2.2 (A) A sample trajectory in a no odor, control treatment. (B) 386 overlaid trajectory fragments from the same treatment. (C) A transit probability histogram derived from the trajectories in B. Transit histograms were derived by dividing two dimensional views of the wind tunnel into 7220 squares with side lengths of 0.8 cm. Within a given treatment, the number of fly occurrences within each square was summed and divided by the total number of fly occurrences in all squares to yield a probability of square occupancy, where the total probability summed to one.

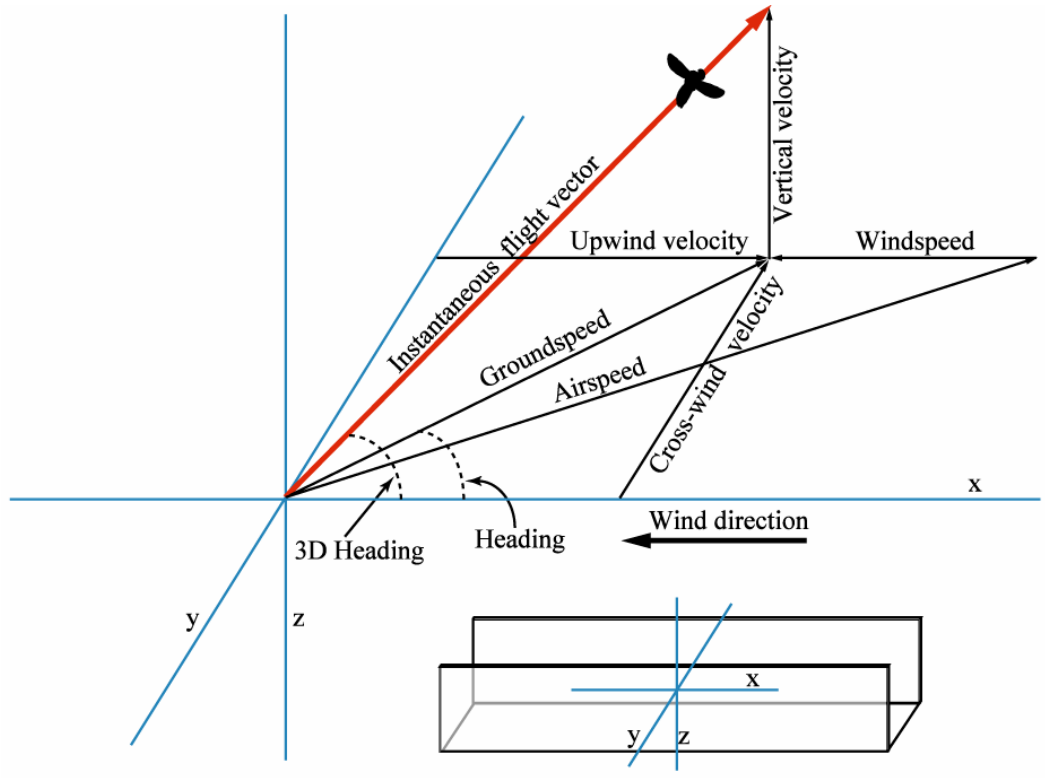

Figure 2.3. Trajectory parameters subjected to analysis (explanations in text).

then: $C_i = \cos\theta_i$ and $S_i = \sin\theta_i$. Summing over the entire trajectory and dividing by trajectory length yields the rectangular coordinates of the mean vector: $\overline{C} = \frac{1}{n}\sum_{i=1}^{n} C_i$, $\overline{S} = \frac{1}{n}\sum_{i=1}^{n} S_i$. The angle of the mean vector, $\overline{\theta}$, is then calculated as:

$$\overline{\theta} = \begin{cases} \tan^{-1}(\overline{S}/\overline{C}) \text{ if } \overline{C} > 0 \\ \tan^{-1}(\overline{S}/\overline{C}) + 180° \text{ if } \overline{C} < 0 \\ 90° \text{ if } \overline{C} = 0 \text{ and } \overline{S} > 0 \\ 270° \text{ if } \overline{C} = 0 \text{ and } \overline{S} < 0. \end{cases}$$

The length of the mean vector, r, is calculated as $r = \left[\overline{C}^2 + \overline{S}^2\right]^{1/2}$. This value varies between 0 and 1 and is a measure of the dispersion around the mean heading (Batschelet, 1981). The mean angular deviation, a quantity equivalent to the standard deviation in linear statistics, is then defined as $s = \left[2(1-r)\right]^{1/2}$. Circular means are thus reported here as mean$\pm s$ while means of linear parameters are reported with the standard deviation.

To test for differences in mean direction between experimental conditions, we implemented the non-parametric test for common mean direction suggested by Fisher (1993, Pp. 115–117). To test for differences in the angular dispersions of two samples about their respective means, we used the non-parametric test suggested by Batschelet (1981, Pp. 124–126). Non-parametric tests were used due to their limited assumptions about angular distributions, namely that the data need not be fit by von Mises distributions.

In several cases, mean trajectory headings did not appear to be unimodally distributed so we tested the fit of one or more von Mises distributions using the method of moments suggested by Fisher (1993, Pp. 100–102). A von Mises distribution is described by two parameters, μ and κ. For a given distribution, the maximum likelihood estimate of μ is $\overline{\theta}$ while κ is estimated as the solution of the equation: $A_1(\kappa) = r$ where $A_1(x) = I_1(x)/I_0(x)$, the ratio of two modified Bessel functions. We begin by fitting a single von Mises distribution (1VM) to a sample of mean heading vectors, estimating μ and κ and testing the goodness of fit (*gof*) of a unimodal model. The goodness of fit statistic U^2 is calculated as: $U^2 = \left[\sum_{i=1}^{n}(z_i - (2i-1)/2n)^2\right] - n(\overline{z} - \frac{1}{2}) + (1/12n)$ where n is the sample size and

the z_i are the cumulative frequency values of the individual mean trajectory headings rearranged into ascending order. In successive iterations, we fit a model containing one additional mode (2VM, etc.), estimate the values of μ and κ for each mode and the proportion of the total sample represented by each. The *gof* of the new model is calculated to obtain U^2_{VM}. To assess the significance probability of the fit, we generate 100 parametric bootstrap samples of the same size as the original dataset. For each sample, we estimate μ and κ and calculate the corresponding *gof*. The significance probability of the fit (P_{VM}) is then estimated as $P_{VM} = \frac{N_{U^2}}{100}$ where N_{U^2} is the number of bootstrap samples for which the *gof* exceeds U^2_{VM}. All statistical analyses were conducted using custom routines written in Matlab.

2.2 Rigidly-tethered experiments

2.2.1 Animals, tethering

All experiments used female flies 3–5 days post-eclosion from the same population as that described in §2.1.3. Flies were deprived of food, but not water, for 4–6 hours prior to experimentation. Flies were anaesthetized by chilling to approximately 4°C and tethered to 0.1 mm diameter tungsten rods with UV sensitive glue (see Dickinson et al., 1993; Lehmann and Dickinson, 1997). Flies were mounted in a wingbeat analyzer (described below) that was itself placed within the wind tunnel described in §2.1.1, such that the fly was positioned halfway between the tunnel walls at a height of 36 cm (approximately half the tunnel's height) and 26.7 cm from the downwind end of the tunnel. Experiments were performed at approximately 25°C.

2.2.2 Odor delivery

Flies were presented with the same odor stimulus described in §2.1.2, but the delivery was slightly different here, with air again being injected into 50 mL

of the banana mixture at 1.0 L min^{-1}. The odor dispenser again consisted of a 3 mm diameter brass tube which now penetrated the tunnel floor 34.9 cm upwind of the fly. This tube was inserted in and glued to a 7 mm diameter acrylic tube, 5.1 cm in length, parallel to the tunnel floor. The acrylic tube was laterally perforated at its downwind end by 4 orthogonal 1.9 mm holes. The odor was thus distributed in the form a large diameter turbulent plume, as determined by smoke visualization, that fully engulfed the tethered fly. As in the free-flight experiments, flow through the delivery system was controlled via a three-way solenoid valve (Valve Driver II, General Valve Corp., Fairfield, NJ) which was now controlled by a digital stimulator (PG4000, Neuro Data Instruments Corp.).

The duration of plume pulses was set by programming the digital stimulator. For a variety of reasons, including the latency in opening and closing the solenoid valve, the actual pulse durations did not match those output by the digital stimulator, particularly at the shortest durations. In order to quantify the pulse durations, we used a digital camera running at 100 Hz (A602f, Basler, Ahrensburg, Germany) to visualize smoke pulses produced under identical conditions. Mean realized pulse durations were calculated based on measurements of five presentations of each nominal pulse duration.

2.2.3 Wingbeat analyzer

The wingbeat amplitude and frequency of tethered flies were measured via a wingbeat analyzer that has been used extensively in studies of wing kinematic responses to visual stimuli in *D. melanogaster* (Fig. 2.4) (Dickinson et al., 1993; Tammero et al., 2004). Briefly, flies are tethered such that an infrared light source illuminates the fly from above, casting shadows of the two wings on a pair of infrared photodiodes positioned below the fly. The fly is positioned such that the sensors are maximally adumbrated by the wings when they are in their most ventral position (at the end of the downstroke) and least obscured when the wings are in their most dorsal position (at the end of the upstroke). The photodiode thus produces a periodic voltage signal where successive peaks correspond to the termination of individual wing stroke cycles, allowing an analog

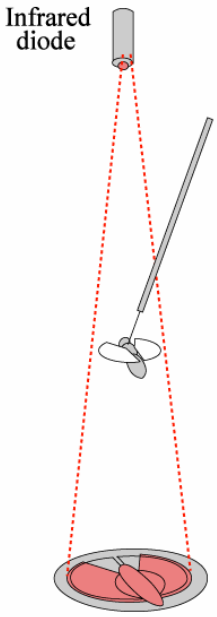

Figure 2.4. Schematic representation of the wingbeat analyzer used in rigidly tethered flight experiments. Figure is derived from Reiser (2007).

circuit to identify individual wing strokes (based on a peak detection algorithm). The amplitude of each downstroke can thus be measured in the form of a voltage signal (based on the fraction of the mask occluded by the wing), as well as the wingbeat frequency. While this quantification of wing stroke amplitude is a simplification of 3-D wing kinematics, the signal is proportional to true wing stroke amplitude (Dickinson et al., 1993). Importantly, subtracting the right wingbeat amplitude from the left (L–R) yields a signal that is proportional to yaw torque (Tammero et al., 2004) and thus to a fly's rotational response to visual or olfactory stimuli. Statistical analyses of these signals made use of SPSS (SPSS, Inc.).

2.3 Magnetically-tethered experiments

2.3.1 Animals, tethering

Females aged 3–5 days post-eclosion, derived from the same population as in §2.1.3, were deprived of food, but not water, for 4–6 hours prior to experimentation. For experiments, flies were glued to steel pins and positioned between two magnets, allowing rotation around the functional yaw axis as described in Bender & Dickinson (2006b) except that in this study, the magnet located beneath the flies consisted of a stack of five 3.8 cm diameter ring magnets. Briefly, the end of the steel pin was positioned in a sapphire V-aperture bearing that was glued to the upper magnet, minimizing friction and allowing the fly to rotate around an axis parallel to the magnetic field lines.

2.3.2 Fly visualization and visual stimulus presentation

A ring of 880 nm LEDs around the lower magnet provided illumination for the IR visualization system used to track fly orientation. Tethered flies were tested in a visual arena similar to that described in Bender & Dickinson (2006b)

except that the arena used in the present experiments had a circumference of 160 and a height of 24 LEDs. A detailed technical description of the modular display system is provided in Reiser & Dickinson (in review). The 24 columns of LEDs at the up and downwind ends of the arena were removed to allow wind to flow through the arena, impinging on the tethered fly (Fig. 2.5).

The visual arena was placed in a wind tunnel based on the one described in §2.1.1. The only differences here were that the length of the working section was 91.4 cm, the floor was transparent, the walls were covered with white paper, and no lighting, besides that from the visual arena and the IR LEDs, was provided. Flow through the arena appeared laminar when visualized with a smoke plume. Experiments were performed between 23.5 and 25°C.

The fly visualization system used by Bender & Dickinson (2006b) was modified so that the camera, positioned under the floor of the plexiglass tunnel, directly visualized the fly through the hole in the center of the circular magnets at a framerate of 100Hz. The visual arena was controlled, as described in Reiser & Dickinson (in review), by a dedicated controller board operating under the command of a PC. All statistical analyses of fly orientation were performed using SPSS (SPSS, Inc.) or JMP (SAS Institute, Inc.).

2.3.3 Wind velocity control

Wind velocity was controlled by custom software which regulated the tunnel's motor speed via a voltage signal to the motor controller. This PC also recorded the tunnel's actual motor speed and the position of the visual stimulus at 12 Hz, as well as the fly orientation at 100 Hz. To change tunnel speed, the tunnel motor followed a constant acceleration trajectory. Wind velocity was validated by smoke visualization, an ultrasonic anemometer, and a thermistor-based anemometer.

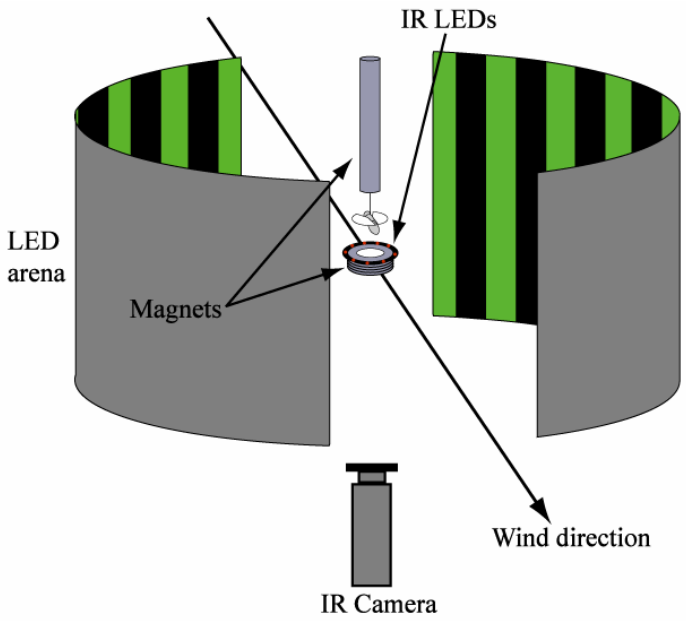

Figure 2.5. Schematic view of visual arena. The arena had a circumference of 160 and a height of 24 rows of LEDs with 24 columns removed at the up and downwind ends to allow smooth airflow over the fly. Flies were glued to a steel pin, positioned between two magnets, allowing rotation around the functional yaw axis. A camera positioned below the tunnel visualized the fly at 100 Hz through a hole in the center of a set of ring magnets.

CHAPTER 3

Free-flight responses to olfactory and visual stimuli

A great deal is known about mechanisms of olfactory mediated flight in a variety of species of Lepidoptera, but this topic has been the subject of relatively little research in other insect orders. While the effects of olfactory stimulation on *Drosophila* free-flight trajectories have been studied in still-air (Frye et al., 2003), it is somewhat difficult to relate behavior to short-term olfactory experience in this paradigm, since the precise distribution of the olfactory stimulus is unknown. For this reason, we studied the free-flight behavior of *Drosophila melanogaster* in a low velocity wind tunnel, where the interaction between the animal and odor plume could be described with better precision. This chapter describes the results of those free-flight experiments.

Since the effect of wind alone on the flight behavior of *Drosophila* has not previously been described, we first tested the impact of wind on flight trajectories in the absence of odor. We then compared the relative strength of wind-based orientation to a visually mediated orientation mechanism, object fixation, in structuring flight trajectories.

We next tested the additional effect of an olfactory cue superimposed on a wind stimulus by examining the short term effects of plume contact on flight trajectories. Because contact with a narrow odor plume subjects an animal to near simultaneous plume contact and loss, we explicitly tested the effects of plume loss by truncating a large diameter odor plume in which insects had been flying. Finally, because recent work on flight in Lepidoptera has placed great

emphasis on the influence of intermittent olfactory stimulation on flight trajectories, we examined *Drosophila* flight within homogeneous odor plumes. The results of four experiments are thus presented. In all experiments involving odor, flies were restricted to one treatment per day to avoid odor contamination. The results presented in this chapter have been previously published (Budick and Dickinson, 2006).

3.1 Anemotaxis

3.1.1 Experimental design

Flies were flown in two conditions: (a) no wind, no odor, or (b) 0.4 m s^{-1} wind, no odor.

3.1.2 Results

In a low-velocity wind (0.4 m s^{-1}), hungry flies readily took flight and flew upwind in the wind tunnel. In still air, flies tended to remain in the vicinity of their emergence point into the tunnel (Fig. 3.1A), while in the presence of wind, flies were distributed relatively uniformly along the length of the wind tunnel (Fig. 3.1B). In both cases, flies preferentially flew down the center of the tunnel, reminiscent of the "centering response" described by Srinivasan and colleagues in honeybees (Srinivasan et al., 1991). Because this centering response could have resulted from an attraction to the visually conspicuous fly or odor releasing tubes, the analysis was restricted to the central 0.5 m of the tunnel (Fig. 3.1C).

While it appeared as though wind biased flight towards the upwind end of the tunnel, it is possible that this was an artifact of a wind-induced increase in activity levels rather than unidirectional upwind flight. Mean trajectory headings for each fly, however, manifested a clear bimodal distribution in the absence of wind, as flies were likely to fly in either direction along the longitudinal axis of the tunnel (Fig. 3.1D). In the presence of wind, flies were instead unimodally

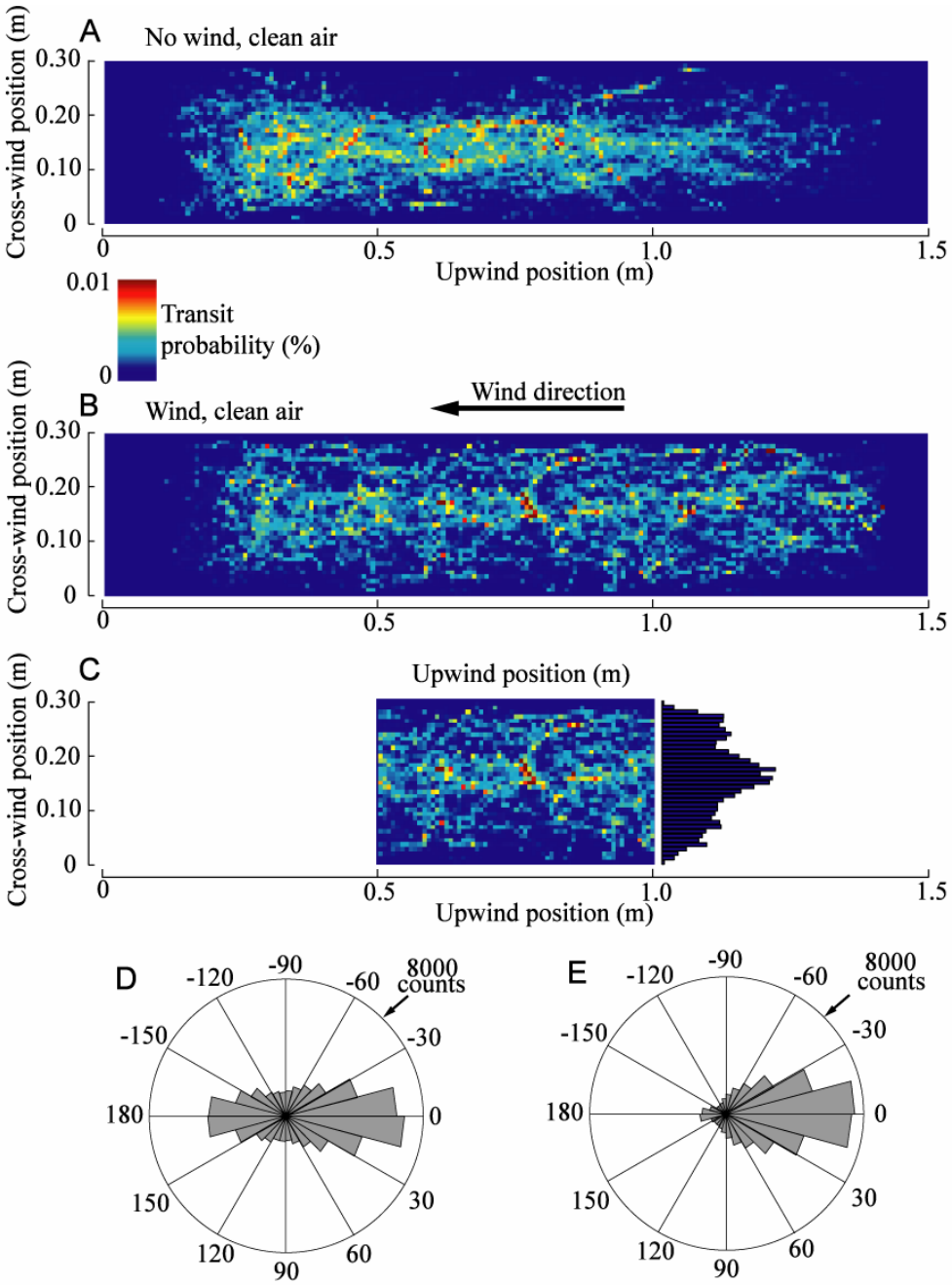

Figure 3.1 *D. melanogaster* are anemotactic and manifest a centering response. Transit histograms, viewed from above, of flies released at the downstream end of the tunnel in still air (A, 132 flies) and in the presence of a 0.4 m sec-1 wind (B, 80 flies). (C) A histogram of the distribution of flies across the tunnel's width indicates that flies manifested a centering response within the central 0.5 m of the tunnel in a 0.4 m sec-1 wind. Flight in only the central section was analyzed in order to minimize the visual effects of the odor and fly releasing tubes.Based on a mixture of von Mises distributions, flight headings were bimodally distributed up (-2.91±28.30°) and down (177.72±32.45°) the longitudinal axis of the tunnel in still air (D), but were unimodally centered on 1.46±13.67° in the presence of wind (E). Raw counts of instantaneous heading values are plotted in D and E, but all statistical analyses are on mean trajectory headings which were significantly more dispersed in the absence of wind (N=80, U=2730, P<0.0001).

distributed around an upwind orientation (Fig. 3.1E). To quantify these distributions, we tested unimodal and bimodal fits of von Mises distributions to the mean heading data in the presence and absence of wind (Tables 3.1 and 3.2). In both cases, the data were significantly better fit by bimodal distributions, although in the absence of wind, the mode directed towards upwind (-2.91±28.30°) accounted for only 58% of the data (Table 3.1) while in its presence, 93% of the data were captured by the mode with its mean at 1.46±13.67° (Table 3.2). Non-parametric circular tests indicated that the mean trajectory orientation did not differ between the two treatments (d.f.=1, Y_2=0.025, P=0.87), but headings were significantly more dispersed around their mean in still air (N=80, U=2730, P<0.0001).

Table 3.1. *Fitting a mixture of von Mises distributions to mean heading vectors of flies in a -odor, -wind environment*

Mode	*gof* (U^2)	P	μ_1	s	p_1	μ_2	s	p_2
1VM	0.644	<0.01	1.26±178.3	74.51°	1.00	-	-	-
2VM	0.098	0.16	-2.91±6.55°	28.30°	0.58	177.72±8.83°	32.45	0.42

For each model, a goodness of fit was calculated and significance tested against a parametric bootstrap as described in the methods. The mean direction of each mode (μ±95%CI) as well as the angular standard deviation (s) and proportion of data fit by that mode (p_n) are shown. The fitting of mixtures was stopped when the probability exceeded 10%. P represents the probability that the data are better fit by a model containing the corresponding number of modes than by a model containing additional modes.

Table 3.2. *Fitting a mixture of von Mises distributions to mean heading vectors of flies in a –odor, +wind environment (details as in Table 3.1)*

Model	*gof* (U^2)	P	μ_1	s	p_1	μ_2	s	p_2
1VM	1.250	<0.01	-	31.16°	1.00	-	-	-
2VM	0.126	0.16	1.46±3.14°	13.67°	0.93	-145±36.20°	39.96°	0.07

3.2 Anemotaxis vs. object-mediated orientation

3.2.1 Experimental design

Flies were flown in two conditions, in both, a black post, 1.27 cm in diameter and spanning the full height of the working section, was positioned halfway along the length of the tunnel and 6.35 cm from the nearest wall. Flies were flown with (a) no wind, no odor, or (b) 0.4 m s^{-1} wind, no odor.

3.2.2 Results

The structure of the visual environment, particularly the presence of high-contrast objects, clearly plays a substantial role in shaping flight trajectories, even in the presence of odor (Frye et al., 2003). Because the anemotactic response is also able to exert a powerful effect on orientation, we tested the relative strength of this behavior, and the preference for conspicuous visual objects, in structuring flight. In the absence of wind, flies were clearly drawn to a black post positioned halfway along the tunnel's length, with 26% of all transit in the wind tunnel occurring within a cylindrical volume of radius 14.5 cm surrounding the post (from which distance, the post would subtend 5° on the fly's retina (Fig. 3.2A). When the wind velocity was increased to 0.4 m s^{-1} however, this attraction was largely suppressed by the anemotactic response, with only 11% of fly transit occurring within the same volume as the flies largely ignored the post while they flew upwind (Fig. 3.2B).

3.3 Flight in a narrow banana odor plume

3.3.1 Experimental design

Flies were flown in two conditions: (a) 0.4 m s^{-1} wind, clean air ribbon plume, or (b) 0.4 m s^{-1} wind, banana odor ribbon plume.

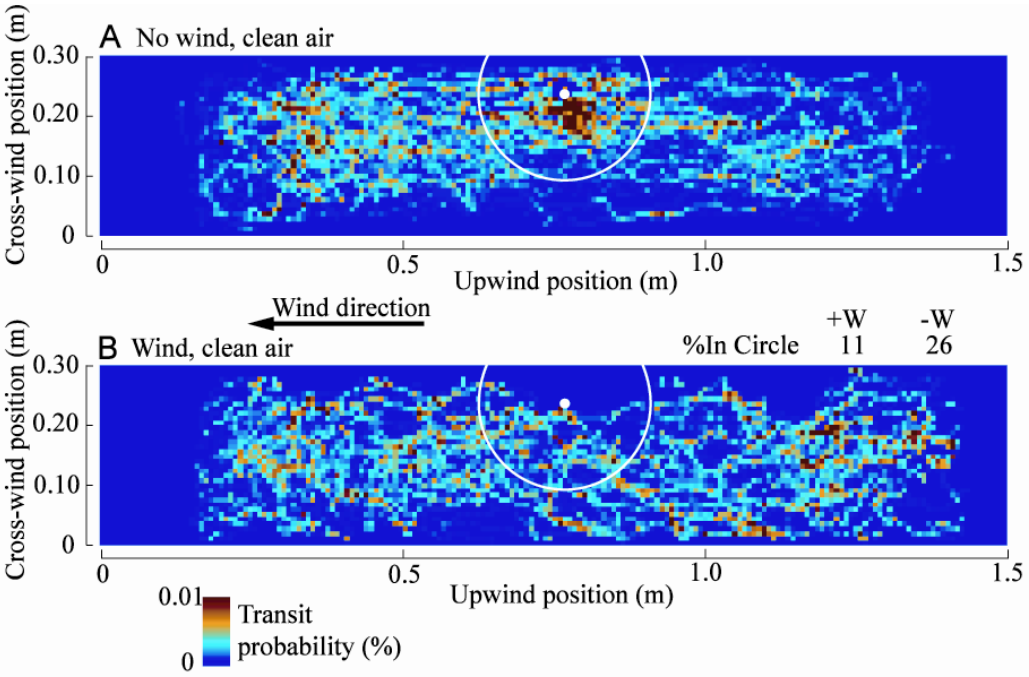

Figure 3.2. Flies orient towards a conspicuous visual object, a black post (white dot), in the absence, but not in the presence of wind. Transit histograms, with flies viewed from above, in no wind (A, 67 flies) and in a 0.4 m sec-1 wind (B, 39 flies). The white circle represents the distance from which the post would subtend 5° on a fly's retina. Without wind, 26% of total fly transit within the tunnel was located within the circle, but with wind this probability dropped to 11%.

3.3.2 *Results*

When exposed to a narrow plume of banana odor, flies rapidly took flight and flew upwind, generally landing on either the odor release tube or the screen at the upwind end of the wind tunnel. The highly reproducible flow structure within the wind tunnel allowed us to quantify fly behavior as a function of contact with the odor plume. The odor plume was modeled, based on smoke visualization experiments, as a 1 cm diameter cylinder that descended slightly along the length of the working section.

While the effects of plume contact were often dramatic, they were also somewhat variable, as indicated by the eight trajectory examples shown in Fig. 3.3. In some cases, flies proceeded relatively straight upwind while increasing their airspeed (e.g., Fig. 3.3A, D, F), while in others the trajectories were somewhat sinuous, or manifested looping turns during flight in a generally upwind direction (e.g., Fig. 3.3C, G). In some cases, upwind flight was also interrupted by cross-wind casting, as flies flew roughly perpendicular to the wind line, executing large magnitude turns (e.g., Fig. 3.3A, B, D). Despite this variability, however, it is clear that flies tended to respond to plume contact, in the short term, by shifting from cross-wind to upwind flight and simultaneously increasing their airspeeds.

It is useful to visualize the effects of plume contact by plotting transit probability histograms of flight trajectories in the presence and absence of the narrow banana plume. We partitioned flight trajectories into "pre-contact" and "post-contact" fragments with histograms of the "post-contact" portions shown in Fig. 3.4. It is clear that flies were able to track the banana plume along its entire length as they followed it to its source (Fig. 3.4A, B). In a clean air plume, flies did not systematically fly in the center of the wind tunnel, indicating that this response cannot be explained by the turbulence created by the plume or by a visual, centering response (Fig. 3.4C, D).

To quantify the effects of plume contact, we analyzed the "pre-contact" and "post-contact" portions of flight trajectories separately. Prior to plume contact, flight trajectories tended to be oriented either upwind or across wind

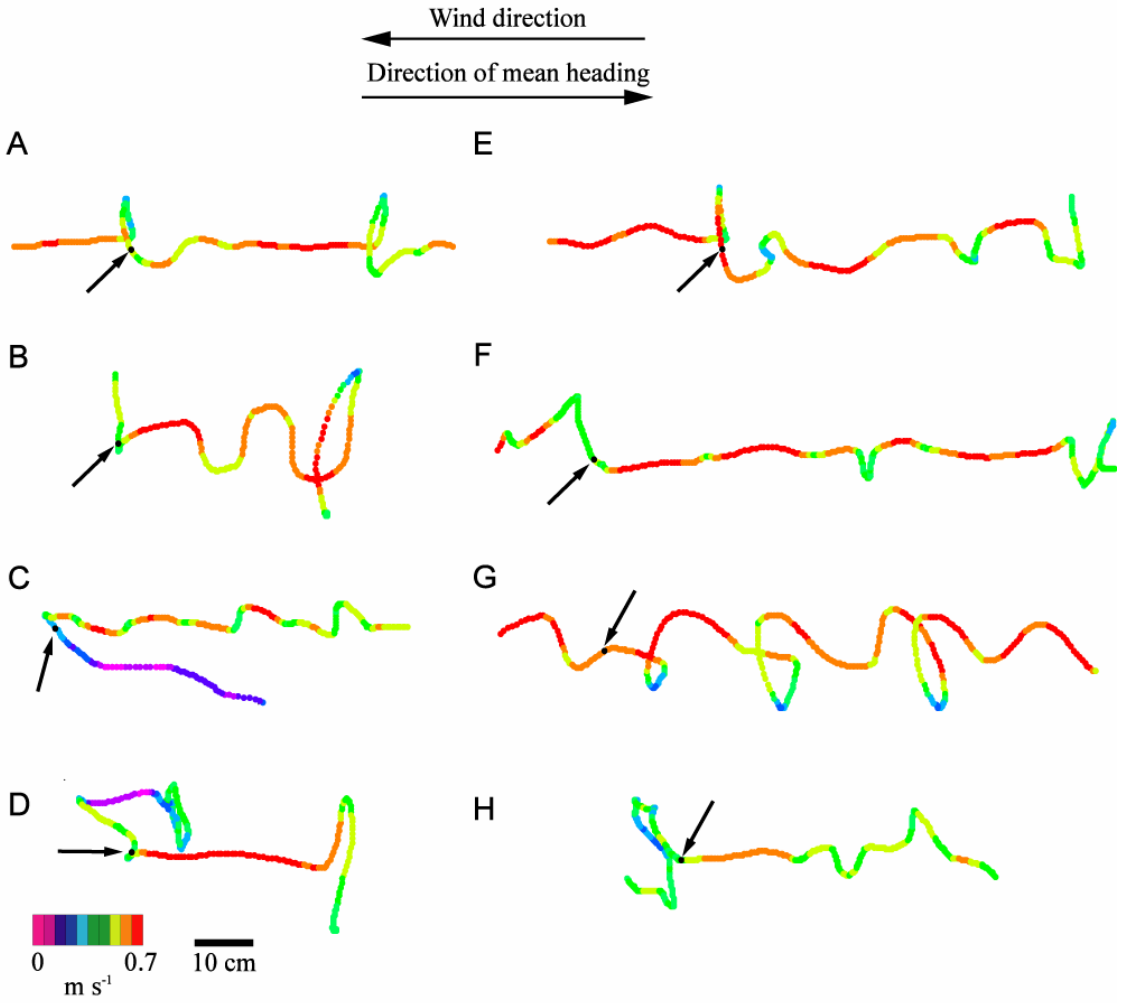

Figure 3.3. Eight examples of odor-mediated upwind flight with airspeed encoded by color. The odor of fermented banana was presented to the flies in the form of a ribbon (1 cm diameter) plume. Flight trajectories, viewed from above, showed substantial variability following plume contact (plume contact indicated by arrow and black dot). Several features are often salient, however, including a shift from cross-wind to upwind flight as well as a fast upwind surge. Upwind progress is often interrupted by looping counterturns and casting flight directed across wind.

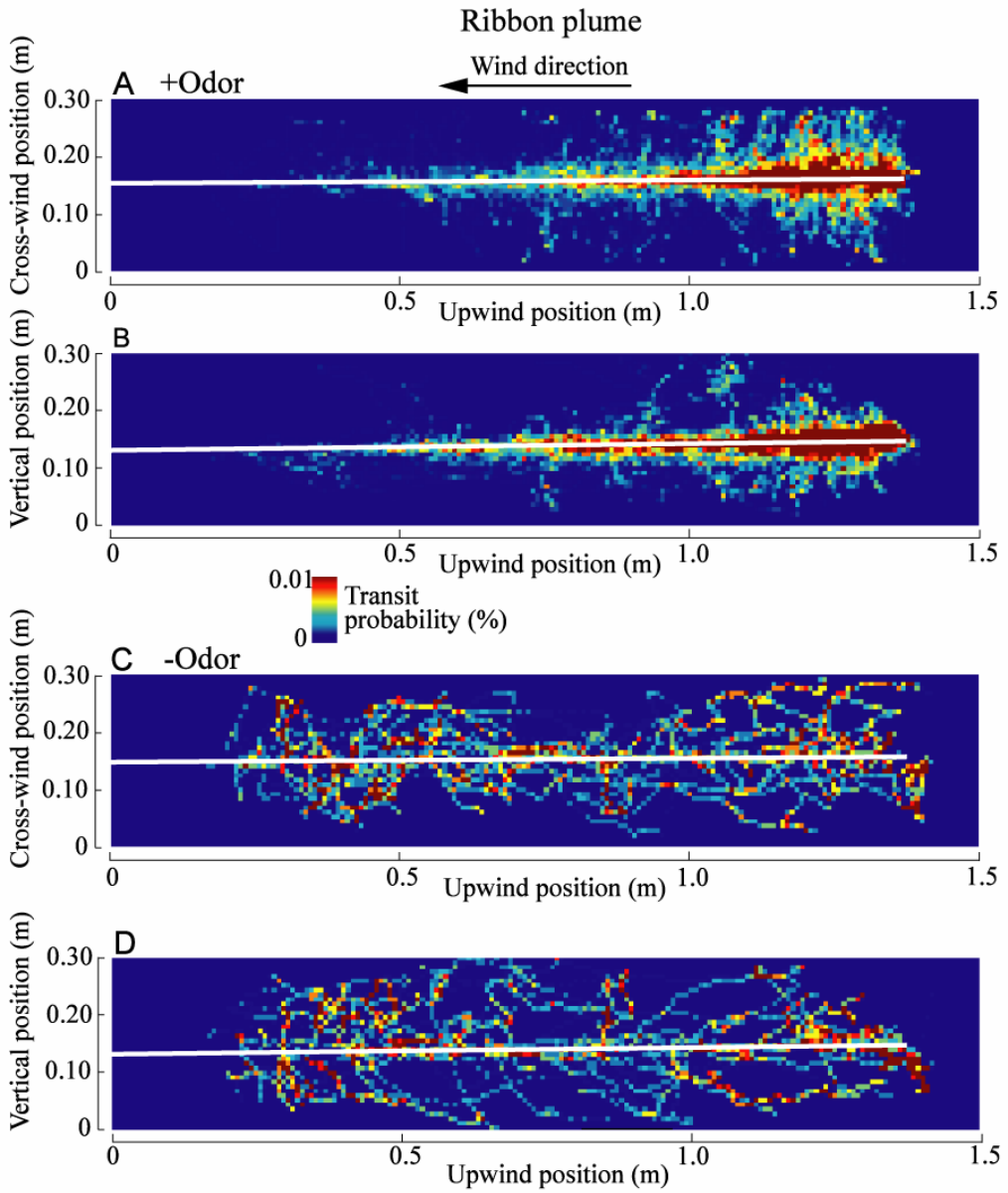

Figure 3.4. Flies localize a ribbon plume of banana odor. Trajectories were partitioned into "pre-contact" and "post-contact" fragments. Transit histograms of post-contact flight indicate that flies localized and maintained close proximity to the plume (white bar) both in the horizontal (A) and vertical (B) dimensions (278 episodes of plume contact from 127 flies). In the absence of an odor plume, flies distributed much more uniformly throughout the tunnel (C and D, horizontal and vertical dimensions respectively, 51 episodes of "plume contact" from 36 flies). Note that the plume did descend slightly along the tunnel's length and that the white bar accurately represents the approximate plume extent.

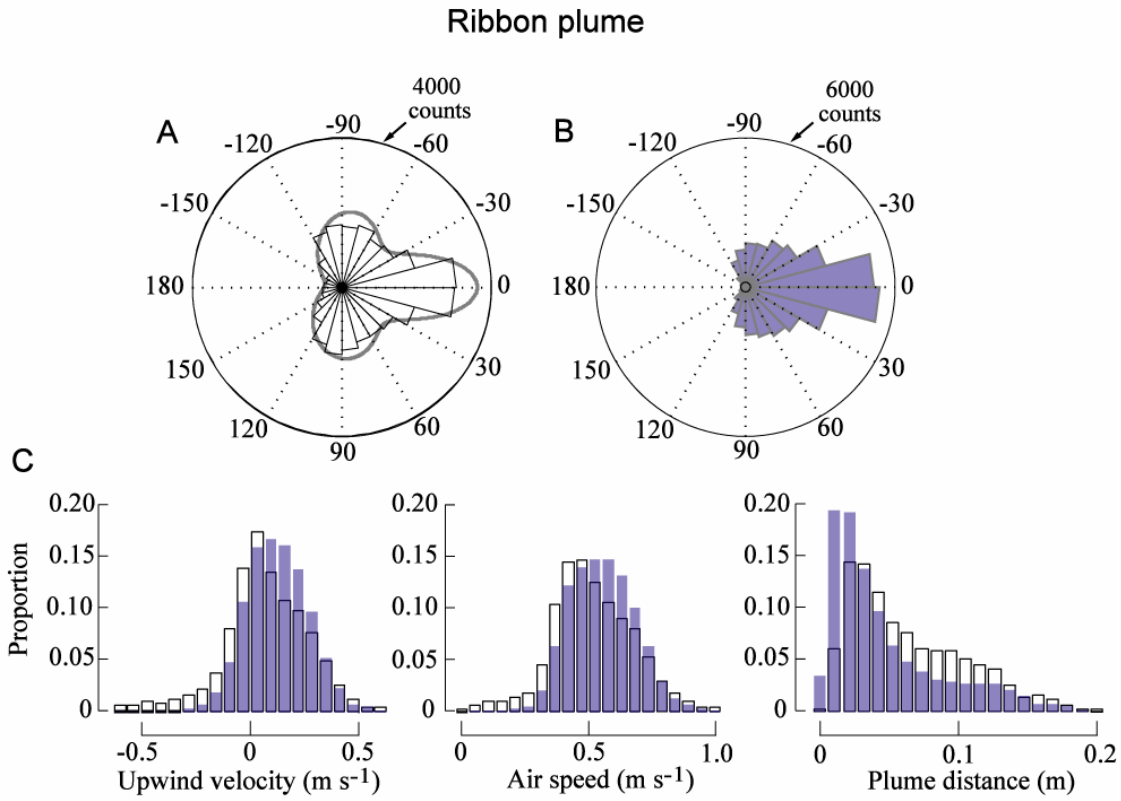

Figure 3.5. Following plume contact, flies fly faster, straighter upwind. (A) Prior to plume contact, flight headings were distributed trimodally, with modes at 0.00±18.16°, 84.77±49.35° and -80.89±41.79°, based on the fit of a mixture of three von Mises distributions to the raw counts of instantaneous heading vectors. The shaded curve represents the trimodal model fit. (B) Following plume contact, flight was unimodally directed upwind (2.18±55.92°). For statistical analysis, mean pre and post-contact headings were calculated for each fly. Mean pre-contact headings were significantly more dispersed than the corresponding post-contact means (N=138, U=5507, P<0.0001). (C) Proportions of the total counts of instantaneous trajectory values for upwind velocity, air speed and plume distance. Comparing trajectory means for each fly, upwind velocity increased following plume contact (t=4.53, d.f.=223.11, P<0.0001) as did airspeed (t=3.71, d.f.=250.94, P<0.001), while the flies remained closer to the plume, (t=5.46, d.f.=273.31, P<0.0001) (pre-contact, empty bars; post-contact, filled bars, 138 flies).

(Fig. 3.5A), whereas post-contact flight was unimodally directed upwind (Fig. 3.5B). Because this cross-wind component tends to be obscured when taking mean trajectory headings (i.e., flight with iteratively reversing cross-wind legs yields a mean orientation of 0°), the instantaneous heading angles are plotted in Fig. 3.5. Because those headings are not statistically independent, tests on their distributions are not valid. Nevertheless, fitting a mixture of three Von Mises distributions to these data yielded modes oriented towards 0.00±18.16°, 84.77±49.35° and -80.89±41.79°; that is, either across or upwind. A non-parametric test of the dispersion of mean pre- and post-contact trajectory headings, based on all episodes of plume contact for each fly, indicates that pre-contact flight was significantly more highly dispersed around its mean of -4.98±47.21° than was flight following plume contact around its mean of 4.52±22.03° (N=138, U=5507, P<0.0001).

In addition to the significant effect on heading, flight following plume contact had significantly higher upwind velocity (pre-contact: 0.090±0.140 m sec^{-1}, post-contact: 0.153±0.083 m sec^{-1}) (t=4.53, d.f.=223.11, P<0.0001) and airspeed (pre-contact: 0.55±0.11 m sec^{-1}, post-contact: 0.59±0.08 m sec^{-1}) (t=3.71, d.f.=250.94, P<0.001), as well as being significantly closer to the plume (pre-contact: 0.053±0.024 m, post-contact: 0.037±0.023 m), (t=5.46, d.f.=273.31, P<0.0001) (Fig. 3.5C). Thus, flies were able to track the odor plume while simultaneously increasing their flight velocities.

While the transit probability histogram is a useful means of depicting general trends in flight trajectories, it is not ideal for representing the fine modulations that accompany plume contact. For this reason, 35 randomly selected episodes of plume contact are plotted in Fig. 3.6, where the pre- and post-contact fragments are translated and aligned to better visualize the effects of plume contact. Prior to contact, flight tended to be directed either across or upwind, with plume contact being followed by a bout of upwind flight and occasional instances of cross-wind flight (Fig. 3.6A). Viewed from the side, trajectories tended to remain near the altitude of the plume both prior to and following contact, with a few conspicuous exceptions. In a clean air control,

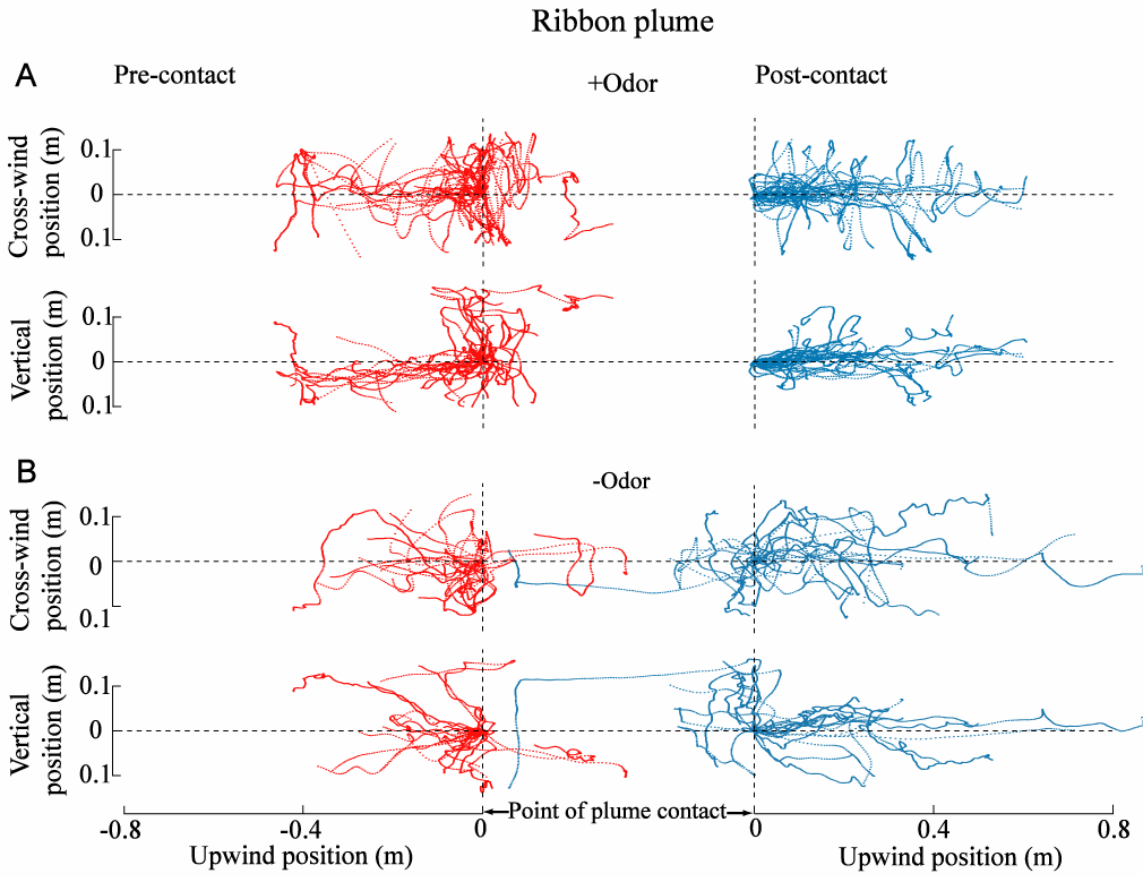

Figure 3.6. Plume contact results in trajectories oriented along the plume line. Thirty five randomly selected episodes of plume contact were translated and aligned at the point corresponding to entrance into the plume cylinder in the banana odor ribbon plume and in a no odor control. (A) In the banana odor plume, pre-contact flight was largely directed across-wind whereas plume contact was followed by a shift towards upwind progress while maintaining close proximity to the plume-line with flies occasionally casting across wind. (B) In the absence of an odor plume, "plume" contact lacked consistently similar effects on trajectory structure.

there were few consistent trends in trajectory structure either before or after "contact" with a clean air plume (Fig. 3.6B). This again suggests that the behavioral responses observed in the context of the narrow banana plume were in fact the consequence of contact with an attractive odor.

The short-term effects of plume contact on a variety of trajectory parameters were quantified in order to extract a profile of the mean plume contact response. The time-series averages for the first episode of plume contact by each fly, aligned relative to the moment of plume contact, are plotted in Fig. 3.7. It is apparent that while there are substantial changes in a variety of these parameters following plume contact, they are often accompanied by slower changes, with the same sign, in the control group. It probably should not be surprising that similar effects are evident in both groups, simply as a result of tunnel geometry. For instance, in both groups, cross-wind velocity apparently peaked at the time of plume contact. In order to encounter the plume, an insect flying upwind needs to displace laterally (or vertically, though that is apparently less common, see Fig. 3.6), yielding an increase in cross-wind velocity. This trajectory modification is likely to evoke a collision avoidance response as the fly approaches the tunnel wall, with the resulting turn tending to be biased towards upwind as a result of the anemotactic response described earlier.

Nevertheless, to test for significant differences between these two groups, we compared the changes from baseline, in all parameters, 250 and 500 ms after plume contact. These time points were selected since they represented the approximate latencies at which the changes in trajectory parameters were most apparent in the experimental and control groups respectively. In the presence of odor, flies significantly decreased their cross-wind velocity and increased their upwind velocity within 250 ms of plume contact, a period corresponding to roughly 50 wingbeats (Table 3.3). The combined effect of these responses was to orient the flies significantly more upwind. Flies also significantly increased their airspeeds during this "upwind surge." Groundspeed and vertical velocity meanwhile were not significantly changed relative to controls, suggesting relatively stable control of these flight parameters. After 500 ms, however, flies exposed to the banana odor were not significantly different from the control

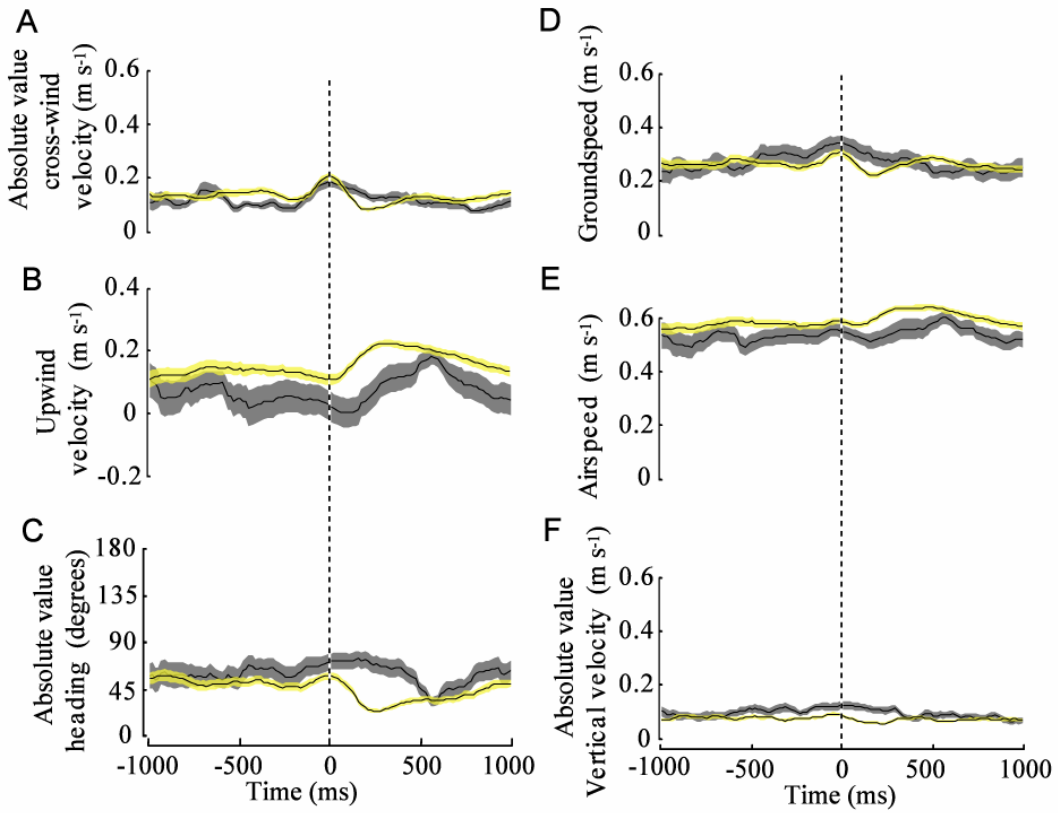

Figure 3.7. Effects of contact with a ribbon plume of banana odor on kinematic parameters. The mean and standard error envelope are plotted for one second of flight prior to and following the first episode of plume contact in the banana odor ribbon plume (yellow error envelope, 124 flies) and in a no odor control (gray error envelope, 44 flies). Because not all trajectories consisted of at least 1 second of flight prior to and following plume contact, means and standard errors were calculated at all time points from all trajectories whose durations met or exceeded that threshold length.

group in any of these metrics. Thus, while the experimental group manifested a rapid surge response to odor contact, the changes to the trajectory were eventually matched by the control group, indicating that visual reflexes were able to produce a slower, "surge-like" response under the appropriate conditions. This visually mediated behavior is likely to also have been a component of the response to odor contact.

Table 3.3. *Comparisons of changes in mean trajectory values from baseline in the narrow banana odor plume and a clean air control for six flight parameters at 250 and 500 following plume contact*

	250 ms			500 ms		
	d.f.	t	P	d.f.	t	P
Cross-wind velocity	86.64	2.54	<0.01	62.33	0.52	0.30
Upwind velocity	65.29	2.03	<0.05	75.48	1.29	0.10
Heading	58.47	3.55	<0.001	67.40	1.20	0.12
Groundspeed	81.57	0.37	0.35	58.36	1.20	0.12
Airspeed	60.10	1.93	<0.05	62.78	1.37	0.09
Vertical velocity	62.63	0.59	0.28	50.34	0.38	0.35

All values are calculated using one-tailed, heteroscedastic t-tests.

3.4 Responses to a homogeneous odor plume

3.4.1 Experimental design

Flies were flown in two conditions: (a) 0.4 m s^{-1} wind, no odor, or (b) 0.4 m s^{-1} wind, homogenous banana odor plume.

3.4.2 Results

Because of the anemotactic response, flight in the presence of wind is already strongly polarized in the upwind direction (Fig. 3.1). Nevertheless, when

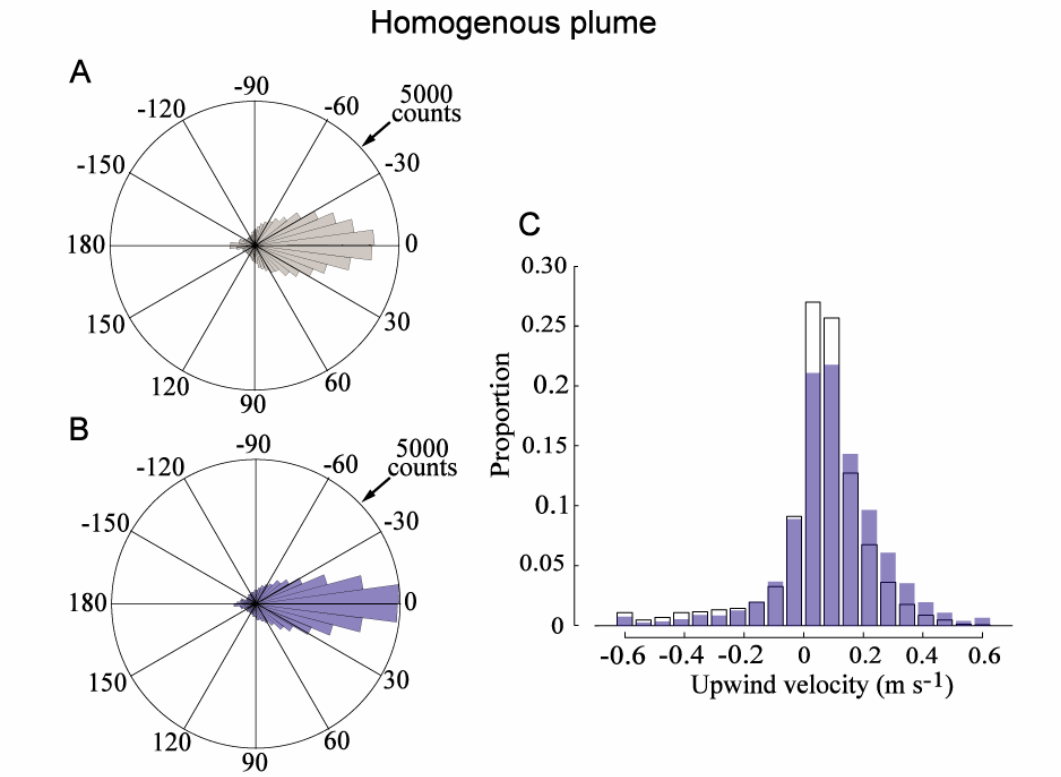

Figure 3.8 In a homogeneous cloud, flight is directed almost completely upwind. (A) In a no odor control, wind polarized flight upwind (0.49±21.98°, 80 flies), but still resulted in greater dispersion of mean heading angles (N=80, U=2995, P<0.05) than in a homogeneous odor cloud (B, -1.16±31.16°, 94 flies). Note that raw heading counts are plotted, but only mean trajectory headings are analyzed statistically. Upwind flight was also significantly faster in the homogeneous cloud (d.f.=171.84, t=4.57, P<0.0001) (C, no odor, empty bars; homogeneous cloud, filled bars).

a homogeneous odor cloud was superimposed on that wind stimulus, flies flew upwind with trajectories that were even less dispersed around their mean orientation of 0.49±21.98° than in wind alone (-1.16±31.16°; N=80, U=2995, P<0.05) (Fig. 3.8A, B). Indeed these trajectories were directed the most consistently upwind of those that we observed in any condition. While flying in the homogeneous plume, flies also significantly increased their upwind velocities relative to the clean air control (clean air: 0.053±0.105 m sec^{-1}, homogeneous cloud: 0.131±0.120 m sec^{-1}) (d.f.=171.84, t=4.57, P<0.0001) (Fig. 3.8C). It should be noted that while smoke visualization indicated that the plume had been mixed to the limits of visual resolution, it is possible that some fine structure remained intact.

The effects of the homogenous plume can be seen in a few "post-contact" trajectories (where contact is defined based on the position of the narrow plume) where flight tended to be oriented more directly upwind than in clean air (Fig. 3.9A, B). Further, flies in the homogenous plume rarely performed the cross-wind "casts" that were often conspicuous in the narrow banana plume (Fig. 3.9C). The fact that casts were apparently elicited in the presence of the narrow banana plume, and not in the homogenous cloud, suggests that they were not a consequence of sustained plume contact, but were instead causally related to plume loss.

3.5 Responses to pulsed and continuous plumes

3.5.1 Experimental design

Flies were flown in three conditions: (a) 0.4 m s^{-1} wind, clean air, pulsed, large-diameter plume, (b) 0.4 m s^{-1} wind, banana odor, pulsed, large-diameter plume, or (c) 0.4 m s^{-1} wind, banana odor, continuous, large-diameter plume.

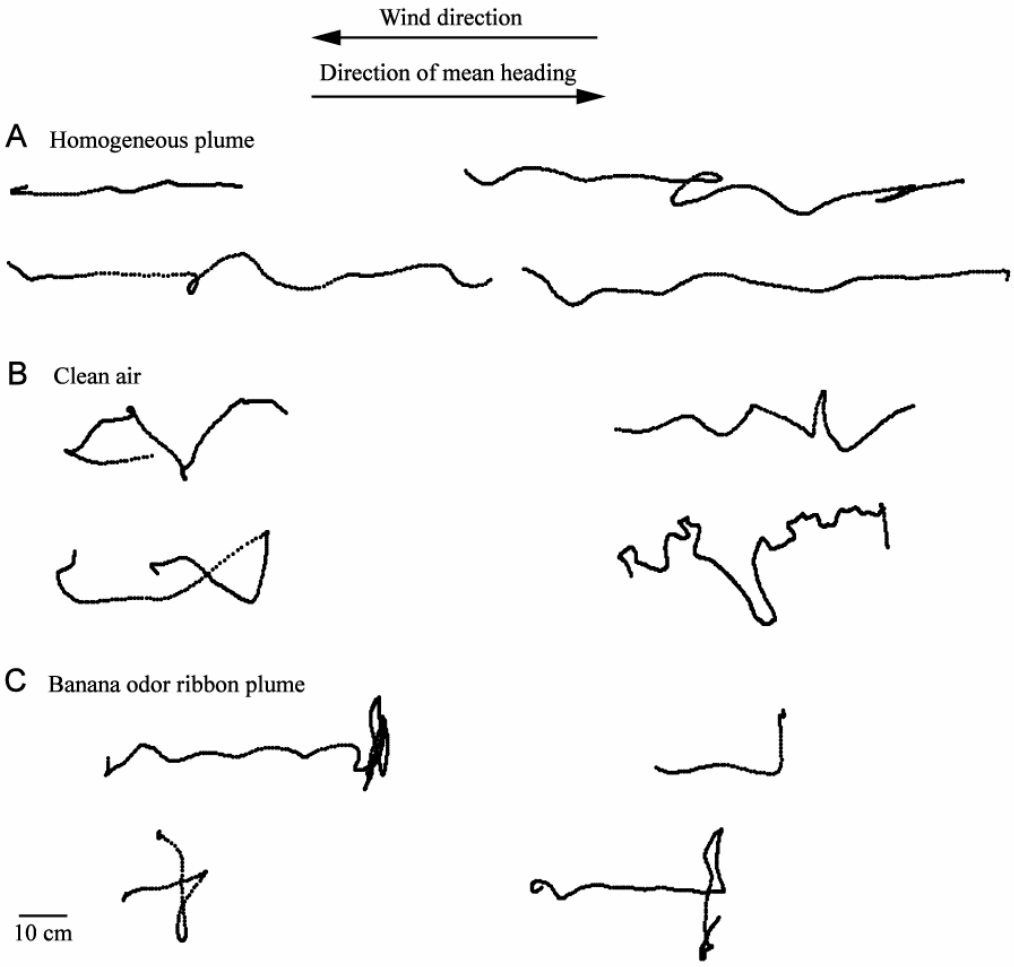

Figure 3.9. Representative trajectories illustrate the differences between flight in a homogeneous cloud, clean air, and a banana odor ribbon plume. Four representative, "post-contact," trajectories are shown from (A) a homogeneous cloud, (B) clean air and (C) a banana odor ribbon plume. Flight in the homogeneous cloud often gave rise to very straight upwind trajectories compared to clean air. Trajectories in clean air headed generally upwind, while those in the banana odor ribbon plume were largely characterized by upwind flight interspersed with cross-wind casts.

3.5.2 Results

Flies were allowed to fly in large-diameter pulsed or continuous odor plumes, in order to test the effects of plume truncation on flight behavior. Pulses were generated for 1 second with a 50:50 duty cycle. Flies were significantly more likely to land on the plume source when flying towards a pulsed odor plume (40%) than towards a pulsed clean air control (14%), (d.f.=1, χ^2=11.49, P<0.001). Flies were equally likely, however, to land on the plume source regardless of whether the odor plume was pulsed or continuous (46%) (d.f.=1, χ^2=1.90, P=0.17).

In order to test whether plume truncation was associated with cast initiation, casts were defined as a series of six consecutive velocity vectors with angles whose absolute values were between 50^o and 130^o. Flies were also required to travel at least 3 cm across the tunnel during a cast. While this definition is somewhat arbitrary, it captures the qualitative change in trajectory structure that an observer can subjectively identify as a cast. An automated implementation of this algorithm searched for casts that occurred following truncation of the pulsed plume, and for casts that were initiated while the fly remained within the continuous plume, allowing for the possibility that the cast itself may have carried the animal outside of the plume. The algorithm only searched for casts that occurred after the first episode of plume contact for each fly.

In the pulsed odor plume, trajectories often consisted of short upwind surges following plume contact, with casts frequently being initiated following plume truncation (Fig. 3.10A). In continuous plumes meanwhile, flight tended to consist of long periods of straight flight, as long as the fly remained within the odor plume (Fig. 3.10B). To test whether casting is causally related to plume loss, it is essential to make the appropriate comparison between the probability of cast initiation following plume loss and casting in a continuous plume. We thus calculated the mean duration that a fly spent in an odor pulse prior to its truncation, among flies that lost a pulsed plume due to truncation (Fig. 3.11A). We then compared the probability of cast initiation following plume truncation

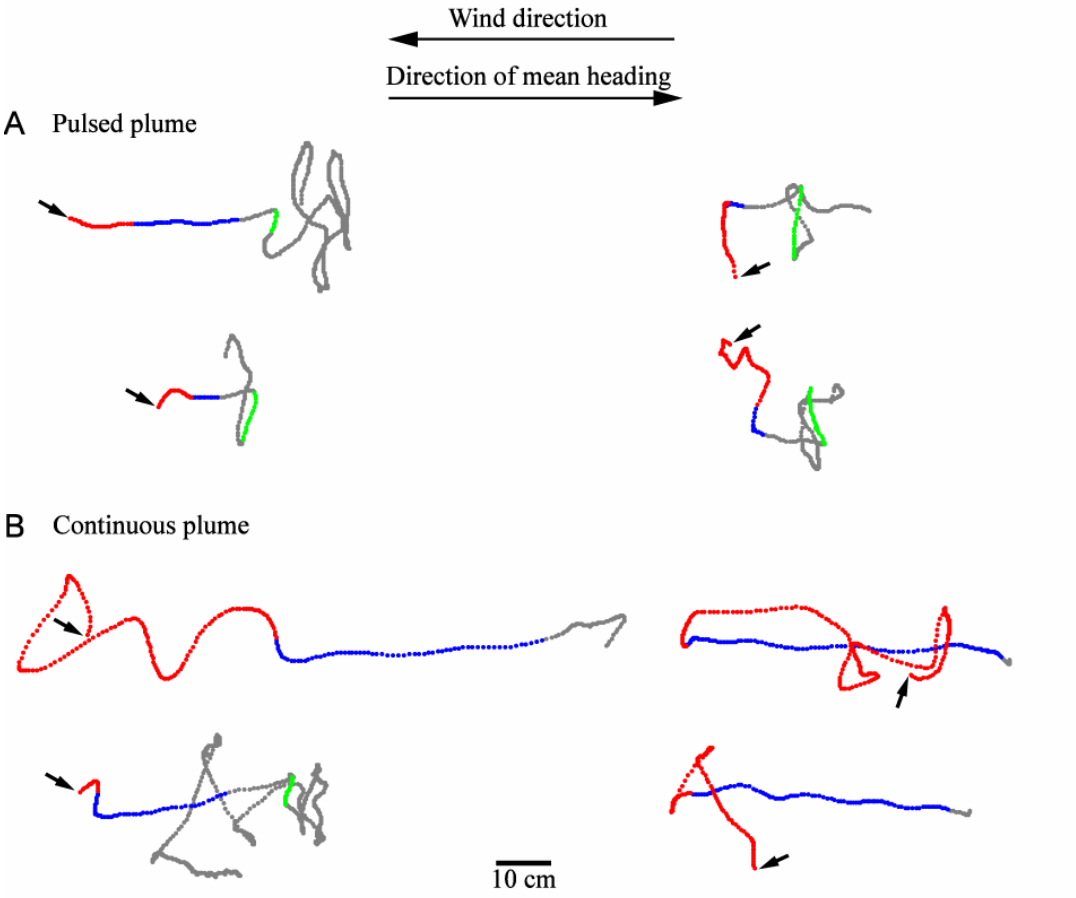

Figure 3.10. Casting frequently follows plume truncation. (A) Four representative trajectories from the large diameter pulsed banana odor plume illustrate flight prior to plume contact (red), within the plume (blue), and following plume loss due to truncation (gray). The first cast, as defined by our cast identification algorithm, is plotted in green. (B) In the continuous large diameter plume, casting rarely initiated within the plume (color designations as above except that gray indicates plume loss due to flight out of the plume rather than plume truncation). Arrows indicate the initiation of fly tracking, but in some cases several points were excised from the beginning of the track in order to enhance the clarity of the trajectory.

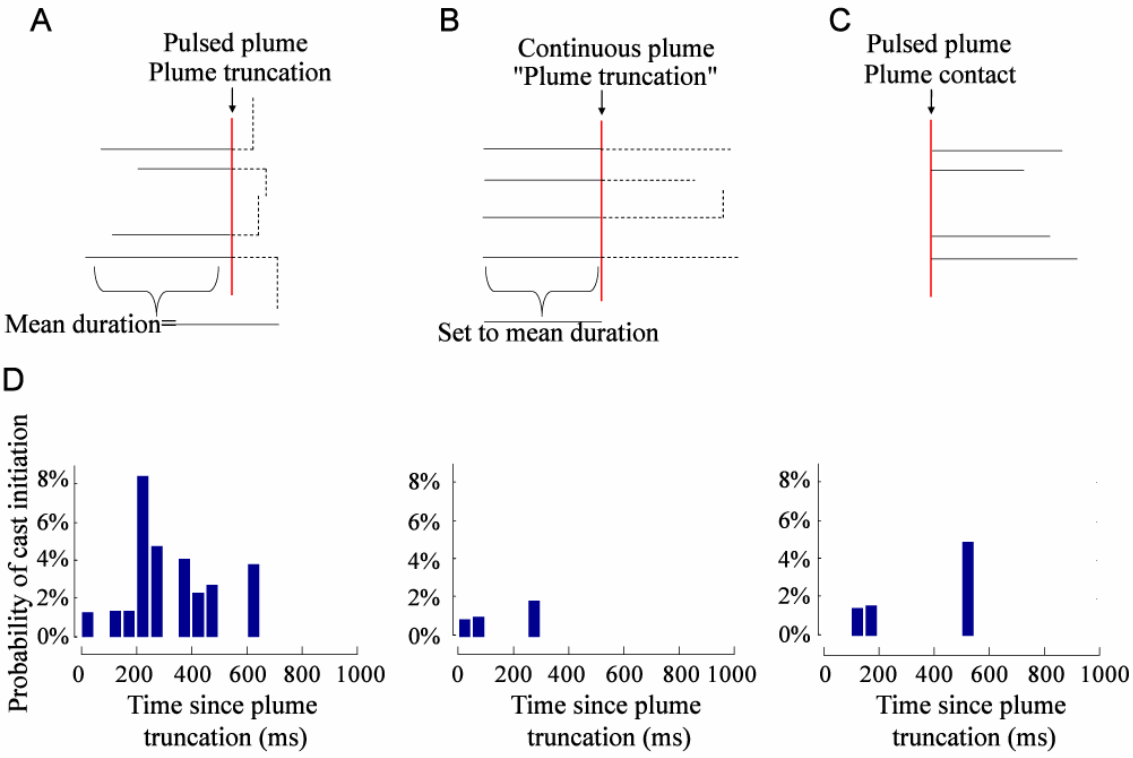

Figure 3.11. Plume loss increases the probability of casting. (A) To test the effect of plume truncation on the probability of cast initiation, we calculated the mean duration of contact with a pulsed plume prior to truncation (383 ms). (B) The probability of casting following plume truncation was compared to that following 383 ms exposure to the continuous plume. The probability of cast initiation within each 50 ms bin following plume truncation, or "pseudo-plume truncation," was then calculated as described in the text. Casting was significantly more likely following plume truncation than in the continuous plume (d.f.=1, χ^2=8.96, P<0.01) with 29.6% of flies initiating a cast within 1 second of plume truncation with a mean latency of 330±140 ms (D). For flies in the pulsed plume, cast initiation was significantly more likely following plume truncation (A) than following plume contact (C) (D, d.f.=1, χ^2=6.66, P<0.01).

to cast initiation following an equal duration spent in a continuous plume prior to "pseudo-plume truncation" (Fig. 3.11B) We further required that casts initiate with a latency of at least one frame (16.7 ms) following plume truncation in order to ensure that the animal had exited the plume.

Following actual or pseudo-plume truncation, some animals landed, were lost by the visualization system, or had already initiated casting, and thus were no longer "eligible" to initiate casting according to the definition provided above. Flies could also become ineligible to cast if, in a pulsed plume, they encountered a subsequent odor pulse, or exited a continuous plume. Thus, we calculated the probability of cast initiation in 50 ms bins following plume truncation only among those flies that were still competent to initiate casting. That is, we divided the number of casts initiated in each 50 ms bin by the number of flies that had not yet been excluded for any of the above reasons (Fig. 3.11D).

Flies were significantly more likely to initiate casting in the first second following plume loss due to plume truncation than due to pseudo-plume truncation of a continuous plume (d.f.=1, χ^2=8.96, P<0.01). Following plume truncation, 17 flies (29.6%) casted within 1000 ms of plume loss with a mean latency of 330±140 ms (Fig. 3.11D). In the continuous plume, only 3 flies (3.6%) initiated casting over the same duration. We carried out an analogous analysis within flies by comparing the probability of cast initiation following plume truncation to that following plume contact (while the fly still remained within the plume). The probability of cast initiation following plume contact was then calculated in every 50 ms bin following contact for those flies that had not yet suffered plume truncation. Flies were significantly more likely to initiate casting following plume loss than plume contact (d.f.=1, χ^2=6.66, P<0.01) with only three flies (7.7%) casting within 1000 ms of plume contact.

To quantify the effects of casting on trajectory kinematics, we plotted the same parameters from Fig. 3.7, aligned now relative to the moment of cast initiation (Fig. 3.12). The effects of casting are largely the inverse of plume contact which is not surprising given the definition of casting supplied above (that is, flight directed primarily across wind). It is important to note however that mean heading begins increasing approximately 40 ms prior to cast initiation,

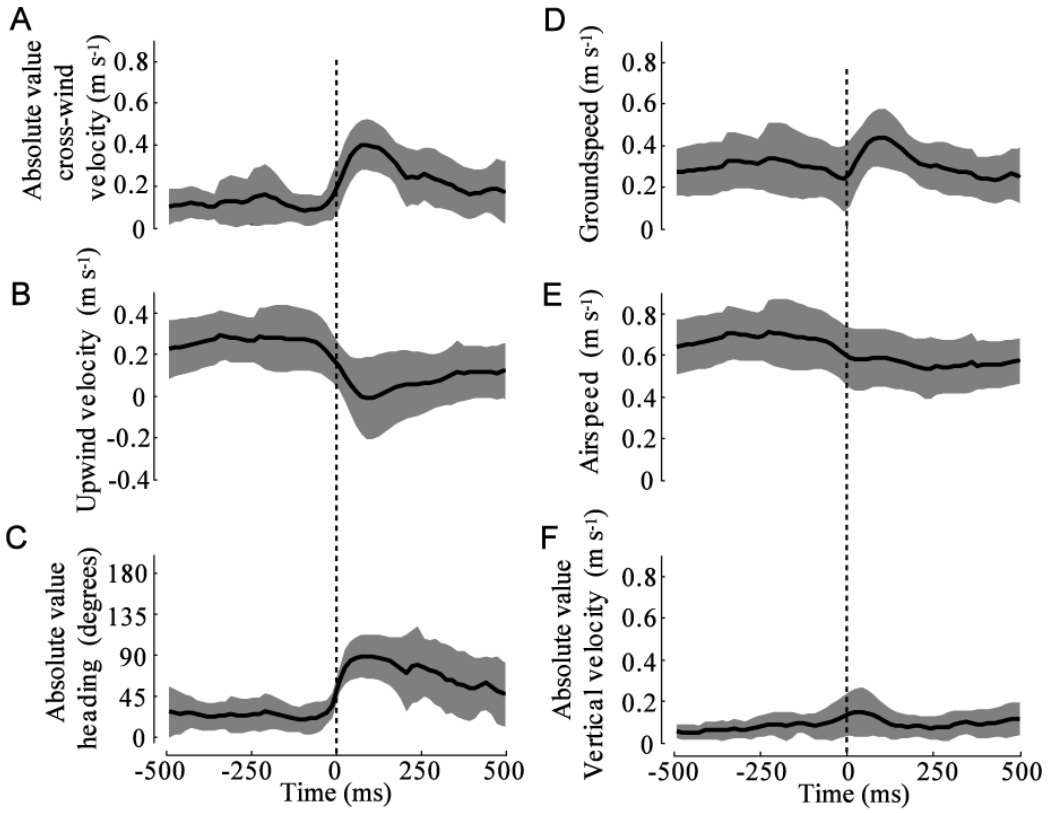

Figure 3.12. Effects of cast initiation on trajectory parameters. Kinematic parameters were aligned at the moment of cast initiation following plume loss due to truncation (mean and envelope of standard deviation are plotted). Casts manifested velocity profiles that were nearly the inverse of the plume contact response, with turns clearly initiating prior to reaching the 50° heading threshold necessary for the cast identification algorithm (C, 24 casts).

indicating that subtle alterations to the flight trajectory were initiated substantially earlier than our automated algorithm could detect (Fig. 3.12C).

3.6 Discussion

The results presented in §3.1.2 indicate that flies readily initiate flight and are anemotactic even in the absence of odor. Previous experiments on walking *D. melanogaster* had been somewhat inconclusive on whether this species polarized its locomotion upwind in the absence of odor (Flugge, 1934; Johnston, 1982). Work on *D. funebris* and *D. immigrans* has indicated that these species adopt a theoretically optimal search strategy by flying across a steady wind (Zanen et al., 1994). Further, as described in §1.1, when a wind shifts by at least $\pm 30^{o}$ around its mean direction, an embedded plume becomes wider than it is long, such that an insect is more likely to encounter the plume by flying up its time-averaged long axis. *D. funebris* and *D. immigrans* do appear to shift their search strategies accordingly (Zanen et al., 1994).

In this study, *D. melanogaster* flew primarily up a steady wind in the absence of odor, unlike *D. funebris* and *D. immigrans*. This discrepancy may partly be explained by differences in tunnel geometry. Zanen et al.'s tunnel had a square footprint, while ours was highly asymmetric, being relatively narrow. Given the existence of a strong expansion avoidance response in *D. melanogaster* (Bender and Dickinson, 2006b; Reiser, 2007; Tammero et al., 2004), which clearly had an impact on flight behavior in our experiments (see §3.3.2), it is entirely possible that this visual response inhibited a cross-wind search strategy in the absence of odor. Accordingly, flies tended to fly up the center of the wind tunnel, similar to the "centering response" described by Srinivasan and colleagues in honeybees flying along a tunnel (Srinivasan et al., 1991). This centering response is apparently accomplished in bees by balancing optic flow on the two eyes. While *D. melanogaster* did, on average, fly up the center of the tunnel, many trajectories meandered and included relatively close wall approach, with flies sometimes performing saccadic maneuvers similar to those observed in still air (Tammero and Dickinson, 2002b). Though superficially inconsistent with a

"centering response," these cross-tunnel flight trajectories are in fact not that unlike those illustrated in Srinivasan (1991), suggesting that a mean centering response may emerge despite a fair degree of variation in individual fly behavior.

While visual responses clearly played a large role in shaping trajectory structure, the anemotactic response was sufficiently strong to suppress another powerful visually mediated response, the attraction to conspicuous visual objects, such as a black post spanning the height of the tunnel (Maimon et al., in preparation). Furthermore, flies did cast in the wind tunnel, as discussed below, during which they approached the tunnel walls, tolerating substantial visual expansion in the process.

Interestingly, "pre-contact" headings during flight in a narrow banana plume were trimodally distributed, with modes directed upwind and crosswind. Because flies were immediately exposed to the banana stimulus on emergence into the wind tunnel, "pre-contact" flight did not imply a complete lack of previous odor exposure. The qualitative differences between "pre-contact" and "no odor" flight trajectories seem to imply a fundamental change in search strategies that accompanied odor exposure, with "pre-contact" trajectories more closely resembling the optimal, cross-wind search strategy predicted for flies attempting to localize a plume in steady wind (Dusenberry, 1989a).

For many years, odor-mediated flight in insects was thought of as the interplay between two tonically active behavioral programs triggered by odor contact—upwind anemotaxis and self-generated counterturning—with potential modulation by other stimulus parameters such as odor concentration (Kennedy, 1983; Kuenen and Baker, 1983). A good deal of research in recent years, primarily in two species of moths, *Cadra cautella* and *Heliothis virescens*, has suggested that flight trajectories may instead be modulated at fairly high frequencies by instantaneous stimulus experience. Experiments in both species have shown that plumes pulsed at high frequencies are capable of eliciting straight upwind flight, a behavior that was rarely, if ever, previously observed in Lepidopotera (Mafra-Neto and Cardé, 1994; Vickers and Baker, 1992; Vickers and Baker, 1994). These results were especially important in that they suggested

that the behavior could be understood, proximately, by understanding the dynamics of the olfactory stimuli.

These results led Baker (1990) to formulate a mechanistic model for moth behavior that incorporated these findings as well as the key result that many previously studied moth species cast across wind in the presence of a homogeneous plume (Kennedy et al., 1980; Willis and Baker, 1984). Baker suggested that two separate behavioral programs are triggered by odor contact: a phasically active "upwind surge," as well as a tonically active, self-generated counterturning program. If the phasic program is capable of suppressing the tonic one, but adapts rapidly to sustained stimulation, then a pulsed plume of the correct frequency could in theory elicit iterated surges, while avoiding adaptation, resulting in straight upwind flight. This theory of course requires an olfactory system capable of discriminating these high-frequency pulses and little work, unfortunately, has been performed on the relevant species. In other lepidopterans, including *Antheraea polyphemus* and *Manduca sexta*, the olfactory systems are capable of discriminating odor pulses up to 10 Hz at the level of projection interneurons in the antennal lobe (Christensen and Hildebrand, 1988; Rumbo and Kaissling, 1989) suggesting that, in principle, moth olfaction is capable of the performance implied by these behavioral results.

The degree to which these behaviors, and their underlying neural mechanisms, are shared with insects outside of the Lepidoptera is not yet clear. The results presented here for *D. melanogaster* indicate that these flies do respond to contact with a narrow banana odor plume by surging upwind. This response is the result of flies turning into the wind while increasing their airspeed. At the same time, flies also manifested a delayed, "surge-like" response even in the absence of olfactory stimulation. This surprising result can most likely be explained as a visual, collision-avoidance response turning the fly away from the tunnel walls, coupled with an anemotactic bias towards upwind flight. It seems likely that this visual response also played a role in odor-elicited surges, though it is difficult to disentangle their relative contributions given the relatively narrow dimensions of our wind tunnel. It should be noted, however, that such visual

contributions may be an important, and often overlooked, component of the behavioral response of any insect in wind tunnel studies.

Baker's model predicts that in an insect exposed to continuous olfactory stimulation, the counterturn-generating pathway should be engaged. That is indeed the case in the moth species *Adoxophyes orana* (Kennedy et al., 1980) and *Grapholita molesta* (Willis and Baker, 1984). It seems surprising therefore that when *H. virescens* and *C. cautella* are exposed to very high frequency pulses, where the olfactory stimulus must begin to approximate a continuous one, casting is not elicited. Certainly, if taken to its logical conclusion, the Baker model predicts that at some point, the surge response should adapt to these high frequency stimuli, resulting in the expression of the counterturning program. Justus & Carde (2002) tested this prediction by flying *C. cautella* in a homogenous plume, demonstrating that this species flies upwind under this condition and thus differs substantially from *A. orana*, *G. molesta* and *Pectinophora gossypiella*. Unfortunately, only mean trajectory headings are presented, making it difficult to compare the behavior in the homogenous and pulsed plumes and to determine how closely this species fits the Baker model. It would be extremely informative as well to study the behavior of *H. virescens* in a homogenous plume in hopes of observing a transition from straight upwind to casting flight at some critical pulse frequency.

In a homogenous odor plume, *D. melanogaster* does not initiate casting, but instead flies the straightest upwind trajectories that we observed under any condition. This result matches the anecdotal one reported by Wright and colleagues (Kellogg et al., 1962; Wright, 1964) and indicates a fundamental difference between *D. melanogaster* and commonly reported moth behavior—except possibly for *C. cautella*, as described above, and for walking *Bombyx mori* (Kanzaki et al., 1992). This result is consistent, however, with tethered-flight experiments where *D. melanogaster* maintains elevated wingbeat frequency and amplitude when subjected to sustained olfactory stimulation (Frye and Dickinson, 2004a, and Chapter 4 of this thesis). *D. melanogaster* thus seems to depart from the Baker model in that upwind flight does not adapt to sustained olfactory stimulation, at least in the short term. This characteristic,

interestingly, is shared with another dipteran, *Aedes aegypti* that also flies upwind in response to continuous stimulation by its preferred stimulus, human skin odor (Geier et al., 1999)

D. melanogaster, like many Lepidoptera, also occasionally casts cross-wind. This behavior is apparent among flies in a narrow banana odor plume and plume truncation experiments suggest that it is a causal consequence of plume loss. Casting follows plume loss with an average latency of about 290 ms, well within the range of values reported for other species. Individuals initiate casting within 150–220 ms of plume loss in *Grapholita molesta* (Baker and Haynes, 1987), 490 ms in *Manduca sexta* (Willis and Arbas, 1991), 710 ms in *C. cautella* (Mafra-Neto and Cardé, 1996), and 1 s in *Lymantria dispar* (Kuenen and Cardé, 1994). Based on their anecdotal results, Kellogg et al, suggested a value of about 100 ms in *D. melanogaste*r (Kellogg et al., 1962). It is somewhat remarkable that this feature of olfactory-mediated search is shared by such phylogenetically distant species and suggests either that this is an extremely ancient behavioral adaptation, or that it truly does represent an optimal strategy for localizing odor sources; one on which multiple species have independently converged.

The fact that *D. melanogaster* maintains upwind flight in the homogeneous odor plume suggests that the upwind surge response is tonically, rather than phasically activated in this species. Nevertheless, flies also initiate casting rapidly on plume loss. It is not possible from these results to determine whether casting is the output of a tonically active counterturn-generating program, as has been suggested for Lepidoptera, or whether it represents the output of a neural pathway that is only triggered by plume loss. It is thus possible that, as in moths, both an upwind response and a counterturn-generating mechanism are activated by odor contact, but that in this case, the surge response tonically suppresses counterturns in the continued presence of odor. Alternatively, the casting response might only be triggered by plume loss. In either case, it is very likely that the precise architecture of the casting response is largely a function of the structure of the visual environment as well as olfactory stimuli.

The present results are consistent with tethered-flight experiments where *D. melanogaster* increased its wingbeat frequency and amplitude in response to olfactory stimulation (Frye and Dickinson, 2004a, and Chapter 4 of this thesis). It is very difficult, however, to draw any conclusions on the free-flight consequences of the gross wing kinematic changes quantified in tethered flight experiments. In this study, insects rapidly increased their airspeed following odor contact, and did so with a time course very similar to that of the kinematic responses observed in tethered-flight (Frye and Dickinson, 2004a). Further, in tethered flight, wing responses to ongoing olfactory stimulation are sustained over long periods, again suggesting a parallel with the sustained, fast upwind flight observed in this study under continuous stimulation.

In tethered flight, experiments have indicated that responses to visual and olfactory cues are largely independent (Frye and Dickinson, 2004a). That is, the kinematic responses to simultaneous presentation of visual and olfactory stimuli are essentially equivalent to a linear summation of the unitary responses evoked by each stimulus modality. Additional experiments, however, have shown that olfactory stimulation does affect visual responses in that flies stabilize large-field image motion better when presented simultaneously with an attractive odor (Frye and Dickinson, 2004b). That result accords with those here in free-flight where insects fly extremely straight upwind trajectories in the homogeneous plume. It is thus difficult to gauge the degree to which free-flight behavior can be thought of as simply the result of thrust responses to olfactory stimulation superimposed on visually guided flight. In at least some cases, this does not appear to be the case. Casting, for instance, involves flight directed across wind and close approach to the tunnel walls prior to very large magnitude turns. This behavior is unlikely to be the product of a visually mediated response, since it specifically orients flies in a way that maximizes visual expansion. This suggests that in at least some cases, flight trajectories are likely to represent a complex interaction between visual- and olfactory-mediated guidance, rather than a simple additive sum of the two behaviors.

There do appear to be some discrepancies between the results of free- and tethered-flight studies. Most obviously, based on the free-flight results, one

might expect to see some signature of casting behavior in tethered flies, perhaps in the form of fictive turns, following the cessation of olfactory stimulation. Frye (2004b), however, did not see any evidence of increased steering variance following the termination of odor pulses. That may, however, have resulted from the very long odor pulses used in that experiment, or from the absence of mechanical feedback in tethered-flight. In Chapter 4 of this thesis, I address this discrepancy and show that saccade rate may indeed be increased specifically following short odor pulses in tethered-flight.

Free-flight experiments are extremely powerful for their ability to assay behavior in a relatively naturalistic environment. At the same time, this strength is also a weakness, in that it does not permit precise control of the stimulus milieu. In the next chapter, I examine behavioral responses in a tethered-flight paradigm where we can address this shortcoming, but where we can also interpret the results in terms of their implications for free-flight. Inasmuch as it may be possible to explain free-flight behavior as a function of short-term stimulus experience, these results will hopefully further illuminate the neural mechanisms underlying odor-mediated flight in *D. melanogaster*.

Chapter 4

Tethered-flight responses to pulsed and continuous odor plumes

While free-flight experiments allow for behavioral analysis in a highly naturalistic setting, they suffer from an inherent lack of control over the animals' precise stimulus environment and history. Tethered-flight experiments, where stimulus presentation can be tightly controlled, are thus an ideal complement to free-flight studies. In this series of experiments, we exposed tethered flies to olfactory stimuli, in the same wind tunnel used in the free-flight experiments, in order to more closely study the dynamics of the olfactory-mediated flight response.

4.1 Responses to continuous and pulsed odor plumes

4.1.1 Experimental design

Flies were rigidly tethered in the wind tunnel and randomly exposed to a 6 trial block of olfactory stimuli in a 0.4 m s^{-1} wind. Four of the trials consisted of continuous plumes with durations of 120, 280, 1.16, or 5.13 seconds. The other two trials consisted of plumes pulsed at 3 Hz over a total duration of 1.15 or 5.13 seconds, where individual pulses lasted 150 and 130 ms respectively.

4.1.2 Results

Clear wing kinematic responses were observed at the minimum pulse length tested—a single 120 ms odor pulse (Fig. 4.1). Both wingbeat frequency (WBF) and summed wingbeat amplitude (WBA)—the sum of the left and right wingbeat signals—increased within several hundred milliseconds of odor contact, consistent with the time course of the responses observed in the free-flight experiments in Chapter 3 (Fig. 3.7). The magnitude of the responses in WBF and WBA increased with the duration of odor exposure, saturating at a pulse duration of approximately one second (Figs. 4.1, 4.2A, B). The time constant of the WBF response was shorter than that of WBA, with WBF saturating within approximately one second of odor exposure. WBA meanwhile did not reach its maximal value until at least five seconds after the onset of a one or five second odor pulse. WBA thus continued to increase beyond the termination of the olfactory stimulus, regardless of the pulse duration, with a one second pulse being sufficient to elicit the maximal responses in both parameters.

To determine whether flies respond differently to pulsed and continuous odor plumes, we presented them with continuous pulses with durations of approximately one (1.16) and five (5.13) seconds. Flies were also presented with pulsed plumes, where the odor was pulsed at 3 Hz, for either approximately one (1.15) or five (5.13) seconds with individual pulses lasting 150 and 130 ms respectively. Examination of the mean kinematic profiles indicates that pulsed plumes evoked responses of similar or smaller magnitude, in both WBF and WBA, than did continuous plumes presented over the same duration (Fig. 4.1). Indeed, approximately one second long continuous plumes evoked significantly greater responses, in both wing kinematic parameters, than did pulsed plumes presented over the same duration (WBF: N=49, Z=-2.44, P=0.015; WBA: N=49 Z=-2.36 P=0.018; Wilcoxon signed ranks test) (Fig. 4.2C, D). Flies responded with significantly greater WBF (N=49, Z=-2.44, P=0.015), but not WBA (N=49, Z=-0.37, P=0.71), to an approximately five second long continuous plume than to a pulsed one, suggesting that the responses to both plume types approached saturation following that long a period of plume exposure.

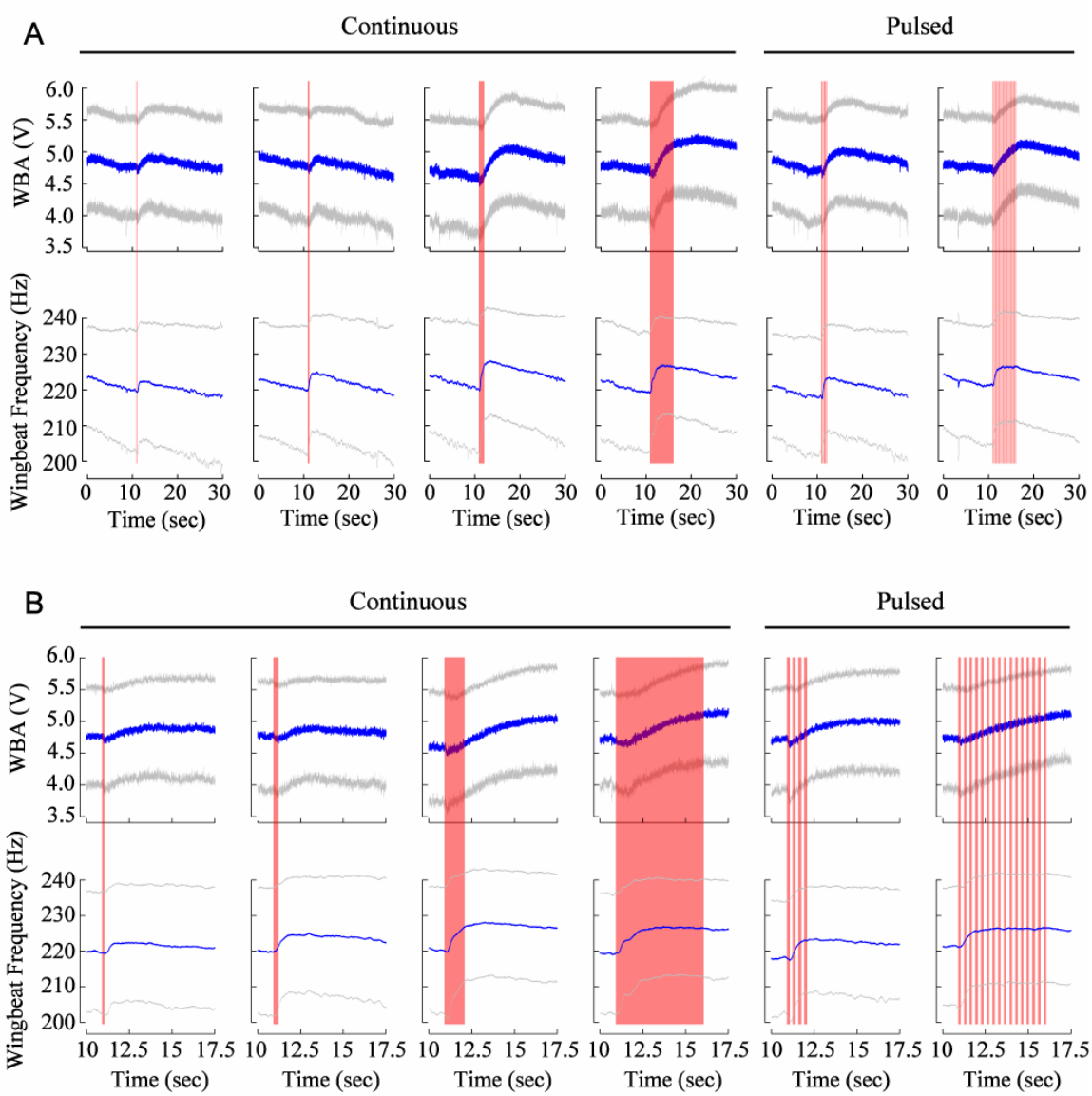

Figure 4.1. Flies increased their wingbeat frequency and amplitude in response to continuous and pulsed olfactory stimuli. (A) The mean responses (blue lines) and envelope of standard deviation (gray lines) for 49 flies exposed to pulsed and continuous stimuli. Shaded red bars represent the duration over which olfactory stimuli were presented. (B) The same data as in (A), but with an expanded view of the time period immediately surrounding the presentation of the odor stimulus.

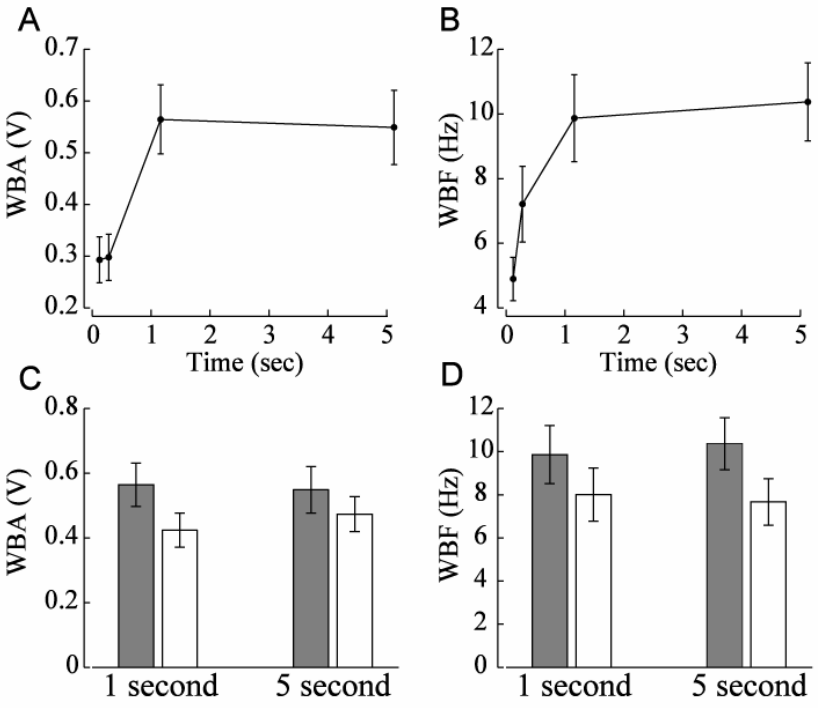

Figure 4.2. Response magnitude increases with odor exposure, saturating with long duration pulses. WBA and WBF signals were low-pass filtered at 2.5 Hz and the average value over the 500 ms preceding odor onset was subtracted from the maximal value attained between odor onset and 20 seconds following the beginning of the trial, yielding the response magnitudes for 49 flies. Mean response magnitudes±standard error in WBA (A) and WBF (B). Responses to continuous plumes±standard error, in both WBA (C) and WBF (D), were significantly greater than responses to plumes pulsed over approximately the same duration, except for WBA following the five second stimulation presentations (continuous plumes, shaded bars; pulsed plumes, empty bars).

As described in Chapter 3, casting, defined as wide cross-wind excursions with iterated large magnitude turns, frequently followed plume loss (Fig. 3.11). We were thus interested in whether olfactory stimulation is able to elicit a behavior analogous to casting following plume truncation in tethered-flight. To test this, we subtracted the left wingbeat amplitude from the right (L–R), low-pass filtering at 20 Hz, to yield a signal that is highly correlated with yaw torque and is thus an index of an animal's attempts to execute turns (Tammero et al., 2004).

During tethered-flight, flies often initiate saccades spontaneously, even in the absence of the visual stimuli that are known to elicit this behavior. In magnetically tethered experiments, these are manifested as high angular velocity turns (Bender and Dickinson, 2006b), while in rigidly tethered-flight, they take the form of "torque spikes" (Heisenberg and Wolf, 1979), or spikes in L–R when quantified with a wingbeat analyzer. Though the time course of these behaviors differs depending on the tethering paradigm (Bender and Dickinson, 2006b; Heisenberg and Wolf, 1979), due to the presence or absence of mechanosensory feedback (Bender and Dickinson, 2006a), they nevertheless represent either actual or intended episodes of yaw rotation. In these experiments, it was similarly the case that spikes in L–R frequently punctuated much slower drift in that signal (with the signal tending to drift since no visual stimulus was used to orient the flies in a particular direction).

We thus quantified the number of "spikes" in L–R by subtracting a 500 ms moving average from the L–R signal, removing the slow drift that occurred during each trial (Fig. 4.3). L–R spikes were then defined as fluctuations that exceeded a ± 0.2 V threshold. The time course of L–R spikes for all flies are raster plotted in Fig. 4.4A and corresponding histograms in Fig. 4.4B. In all cases, the number of amplitude spikes clearly declined during the period of odor presentation and for some duration following odor offset. In the case of the approximately one and five second presentations, whether pulsed or continuous, amplitude spikes were suppressed, compared to baseline, for the remainder of the 30 second trial. Interestingly, while amplitude spikes also suffered a temporary suppression following offset of the shorter odor pulses (120 and 280 ms), the

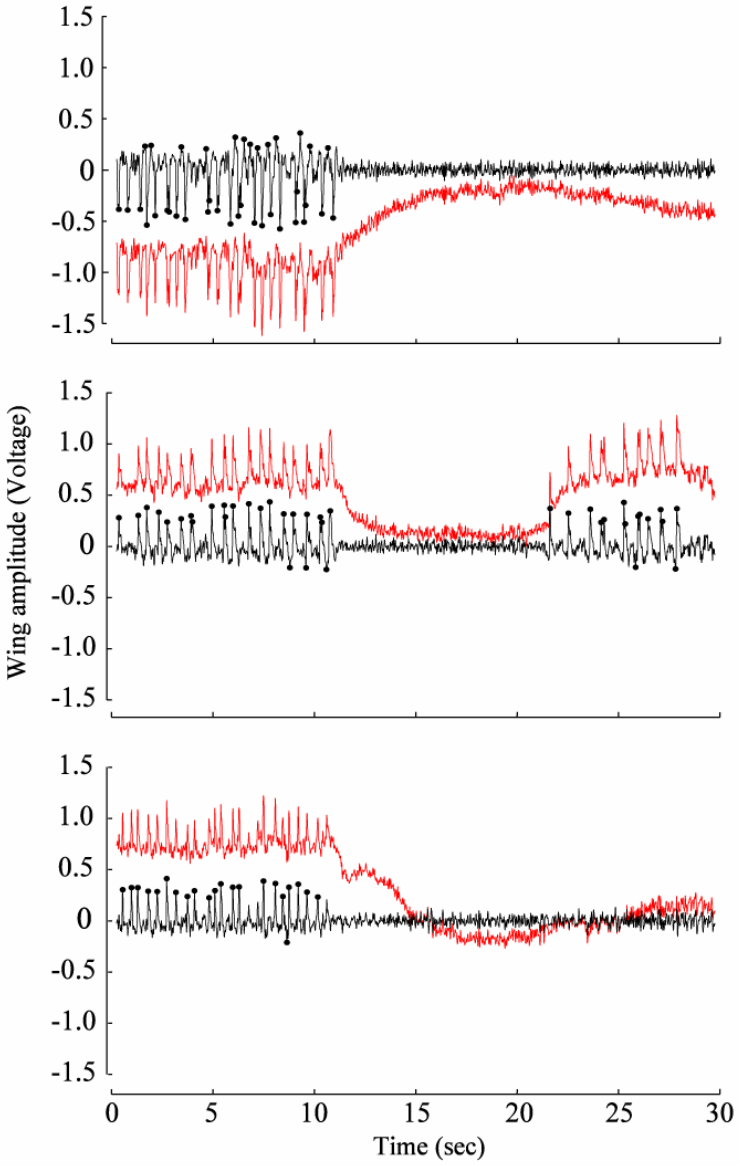

Figure 4.3. "Spikes" in L-R, suggestive of high angular velocity turns, were identified by an automated algorithm. In examples from three different flies, a 500 ms moving average was subtracted from the L-R signal, which had been low-pass filtered at 20 Hz (red) centering the mean at approximately 0 V (black). Amplitude spikes were then identified as fluctuations that exceeded a ± 0.2 V threshold (spikes indicated by filled black circles).

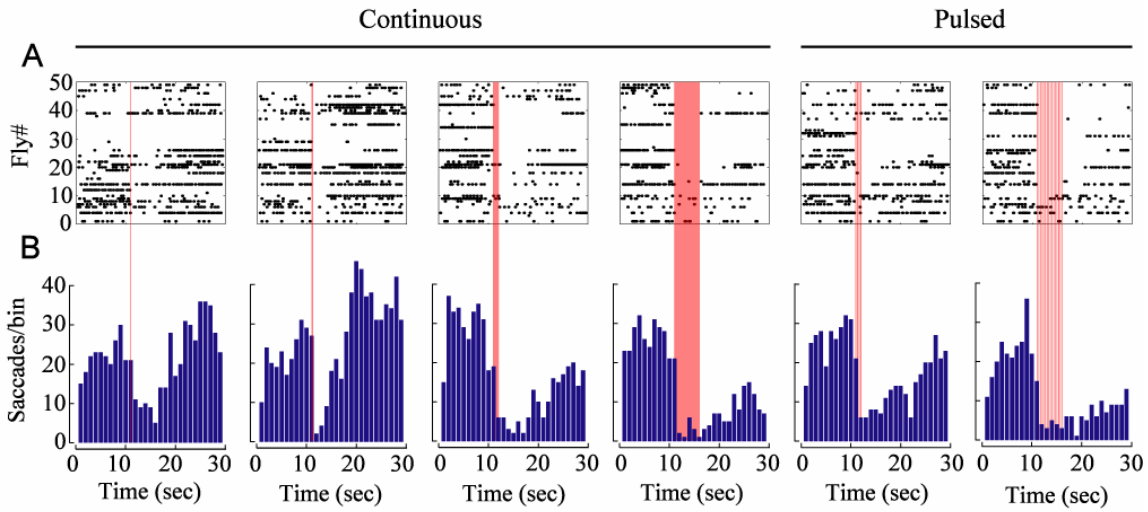

Figure 4.4. Spikes in L-R may serve as an index of cast initiation following odor offset. (A) Spontaneous amplitude spikes are raster plotted for all 49 flies before, during and after odor presentation in all treatments. Shaded red bars indicate the period of odor presentation. (B) The same data collapsed into histograms.

number of spontaneous spikes rebounded relatively quickly, within several seconds in both cases, returning to levels comparable to, or even exceeding those that preceded odor presentation. More extensive experimentation is clearly necessary to explore this relationship, but these data suggest that amplitude spikes may be preferentially expressed following short odor stimuli, consistent with the idea that casts may result specifically from the loss of plume contact following relatively brief periods of odor exposure.

4.2 Discussion

As described in Chapter 3, recent studies of odor localization by flying insects have strongly emphasized the role of intermittent olfactory stimulation. Experiments have shown that species of moths that were thought to adopt exclusively zigzagging upwind flight trajectories are in fact capable of straight upwind flight under the appropriate stimulus conditions (Mafra-Neto and Cardé, 1994; Vickers and Baker, 1994). Those conditions include odor plumes pulsed at high frequencies, such that each pulse is in theory able to reiteratively elicit a unitary upwind surge response, with the combined effect of fusion into a consistently upwind flight track.

Those results and their interpretation accord with a general model where insects will only proceed upwind in the face of intermittent stimulation, whether in the form of straight or zigzagging trajectories (Baker et al., 1985; Mafra-Neto and Cardé, 1994; Vickers and Baker, 1994; Willis and Baker, 1984). The results of the experiments presented in Chapter 3, however, suggest that for *D. melanogaster*, intermittent stimulation may not be a prerequisite for upwind flight, at least in the short term. This result is consistent with older anecdotal data (Kellogg et al., 1962; Wright, 1964), recent results in another dipteran, *Aedes aegypti* (Geier et al., 1999), and also with data on walking in *Bombyx mori* (Kanzaki et al., 1992).

In the present tethered-flight experiments, flies responded to olfactory stimulation, regardless of its duration or pulse structure, by increasing WBF and WBA. Because even very slight modifications of wing kinematics can have large

effects on force production (Fry et al., 2003), it is difficult to infer the aerodynamic consequences of the kinematic modulations observed in tethered-flight. It was demonstrated in Chapter 3, however, that flies rapidly surge upwind within several hundred milliseconds of plume contact, increasing their airspeed and thus their thrust. It may thus be reasonable to interpret increases in WBF and WBA following odor contact as at least a rough index of increased thrust in these flies. It is thus interesting to note that these wing parameters remain elevated in the face of ongoing olfactory stimulation, and that they persist even for long periods following odor offset. It is attractive to draw a parallel between this result and the consistently fast upwind flight that was observed in the homogeneous odor plume, as well as in flies flying within wide-diameter continuous odor plumes. These tethered-flight results thus appear to lend additional support to a model whereby flies continue to fly fast upwind trajectories so long as they remain within an odor plume.

If pulsed odor plumes are essential to upwind flight in *Drosophila*, one might expect that tethered-flight responses to such plumes would differ in a qualitative fashion from those to continuous odor plumes. One might, for instance, have suggested that the WBF and WBA responses would reach a greater magnitude, or increase at a greater rate, in pulsed rather than continuous plumes. This, however, was not the case, as continuous plumes, applied over the same duration as pulsed ones, elicited significantly greater responses, with the single exception of the WBA response to five second pulses. In that case, it is likely that the total duration of odor contact, in both plume types, was able to elicit a saturating response. These results are thus consistent with the hypothesis that *D. melanogaster* need not experience intermittent stimulation in order to sustain high velocity upwind progress.

At the same time, flies in free-flight do clearly respond to plume loss by initiating casting, indicating that upwind responses to odor can be rapidly modified by odor loss. Consistent with this finding, an analysis of "spikes" in L–R—a signal analogous to the "torque-spikes" described by Heisenberg and Wolf (1979), and reminiscent of free-flight saccades (Tammero and Dickinson, 2002b)—detected a conspicuous drop in spikes during and following odor

presentation. Interestingly, exposure to brief odor pulses may have elicited a substantially different response than that to longer pulses, with the rate of amplitude spikes recovering very rapidly following exposure to short ($\leq$280 ms) pulses, perhaps exceeding baseline levels. These spikes may thus represent a signature of casting, one that is preferentially expressed following brief odor pulses.

It is still perhaps surprising that fictive casts were not even more apparent following plume truncation in this paradigm. One possible explanation is that casting, in our free-flight experiments, is very likely a function of both olfactory and visual stimulation. That is, in free-flight, casting turns (aside from the initial one) typically occurred as a fly approached the tunnel walls while flying cross-wind following plume loss. This might suggest that the turns themselves are largely the result of a collision avoidance response rather than the output of the sort of self-generated counterturning mechanism generally ascribed to moths (though the occurrence of casting in moths flying in outdoor settings certainly suggests that collision avoidance may be only one component of a turn-initiating mechanism (e.g., Baker and Haynes, 1996)). Indeed, our tunnel geometry, being relatively narrow, makes it difficult to disambiguate the output of a metronomic turn generator from a purely visual response.

These data, together with those presented in Chapter 3, appear to suggest a relatively simple search strategy for *D. melanogaster*, such that fast upwind flight follows contact with an odor; a trajectory sustained so long as the animal remains in contact with the plume. Following the loss of an odor plume with which the insect had maintained contact over a relatively long duration, the tethered-flight results suggest that a fly may benefit from not substantially altering its wing kinematics, perhaps continuing the upwind trajectory that it followed while exposed to the odor plume. This strategy may make intuitive sense, since a plume that had been aligned with the wind over a long period may be less likely to suddenly change its orientation relative to the wind. On the other hand, following the loss of an odor plume with which an animal had only briefly been in contact, it appears that a fly may preferentially initiate casting. It may be the case that a plume that is lost shortly after contact is relatively less

likely to be uniformly oriented in the direction of the wind, due to frequent shifts in wind direction. A fly that merely heads upwind after plume contact may, in that case, be quickly carried away from the plume, making a rapid shift to crosswind flight favorable under those conditions.

CHAPTER 5

The role of visual and mechanosensory cues in structuring forward flight

In this chapter, we test the role of mechanosensory and visual cues in orienting flight in loosely tethered *D. melanogaster*. We consider the dependence of this behavior on wind velocity and decompose the responses of tethered flies into their passive aerodynamic and active behavioral components. We then test the contribution of the Johnston's organs (JOs) to mechanosensory mediated flight orientation and finally attempt to quantify the relative contributions of the visual and mechanosensory responses. The results described in this chapter have recently been submitted for publication (Budick et al., in review).

5.1 Effect of wind velocity on orientation

5.1.1 Experimental design

Flies were randomly presented with wind at 0, 0.2, 0.4, 0.6, 0.8, and 1.0 m s^{-1}, in 10 second trials. Trials were interspersed with 10 second periods when the wind was stopped and the flies were presented with an expanding visual pattern of vertical stripes with a spatial frequency of 36°, the focus of contraction being at the downwind end of the tunnel. The purpose of this visual stimulus was to realign the flies at a standardized downwind orientation at the start of each trial. Analysis covered the first five seconds of these 10 second trials as behavior was essentially unchanged over the final five seconds.

5.1.2 Results

Flies responded to a wind stimulus by orienting into the wind (Fig. 5.1A). In order to quantify this response, we defined a metric, the orientation response, which was calculated based on the fly's mean circular orientation over the trial's first 100 ms (initial orientation) and final two seconds (final orientation). The absolute value of the initial orientation was subtracted from the absolute value of the final one, such that positive values of the orientation response indicated final orientations that were more closely aligned with upwind than their corresponding initial ones (Fig. 5.1B). Because the magnitude of the orientation response is limited by the fly's initial orientation, we plotted the response as a function of the absolute value of the initial orientation (Fig. 5.1C, D). We also devised a second metric, the response index, which was defined as (90°-|final orientation|)/90°, and thus was not confounded by the scatter in initial orientation. By this measure, a turn that aligned the fly perfectly with upwind received a score of +1, a response that turned the fly precisely downwind received a score of -1, and a turn yielding a final orientation of ±90° yielded a score of 0 (Fig. 5.1E). The orientation index was significantly above baseline at all wind velocities (0.2 m s^{-1}: N=33, Z=-4.08, P<0.001; 0.4 m s^{-1}: N =33, Z =-3.83, P <0.001; 0.6 m s^{-1}: N =33, Z =-4.32, P <0.001; 0.8 m s^{-1}: N =33, Z =-4.58, P <0.001; 1.0 m s^{-1}: N =33, Z =-4.78, P <0.001; Wilcoxon signed ranks test), and was significantly dependent on wind velocity between 0.2 and 1.0 m s^{-1} when fly identity was controlled by including it as a nominal variable in a multiple regression (b=0.28, t=5.49, P<0.001)(Fig. 5.1F).

5.2 Passive and active components of the orientation response

5.2.1 Experimental design

Flies were divided into three groups. One group was tethered normally, a

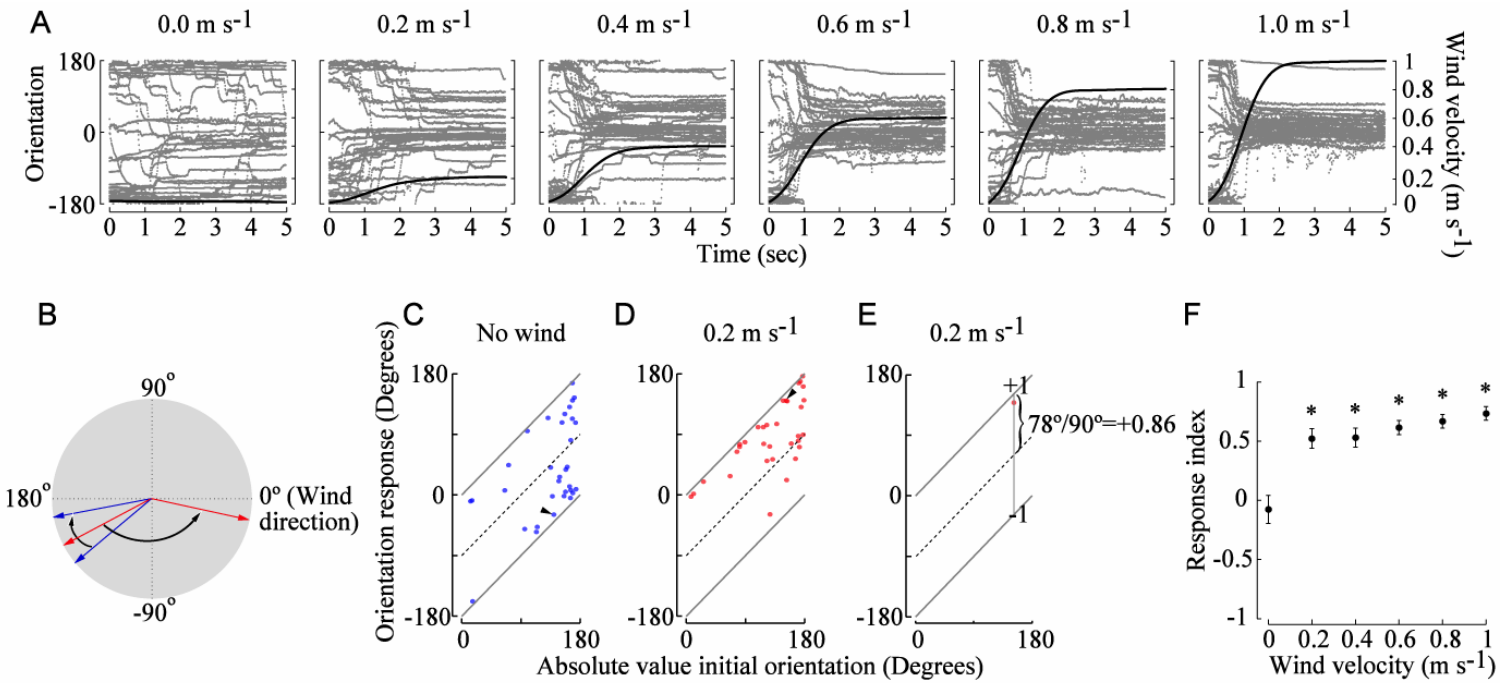

Figure 5.1. Loosely tethered *D. melanogaster* orient upwind. Flies randomly presented with wind velocities between 0 and 1.0 m s^{-1} orient progressively more tightly around 0° (upwind) with increasing wind velocity (A). The heavy black lines indicate the time course of wind velocity. Orientation changes were quantified in two different metrics: orientation response and response index. The mean circular orientation was calculated over the first 100 ms (initial orientation) and the final two seconds (final orientation) of each trial. Orientation response is then given by |initial orientation|-|final orientation|. For example, a fly responded to the onset of a 0.2 m s^{-1} wind by turning from an initial angle of -150° to a final angle of -12°, an orientation response of 138° (B, red arrows). In the absence of wind, the same fly turned from -140° to -169°, an orientation response of -29° (B, blue arrows). Plotting orientation response as a function of the absolute value of the initial orientation provides evidence for orientation to wind (C, D arrowhead indicates the fly whose responses are shown in A). Responses falling along the upper solid line represent perfect upwind orientation, while those along the lower line indicate responses diametric from upwind. A response index, independent of initial orientation, was calculated as (90°-|final orientation|)/90° where +1 indicates a response with final orientation of 0°, -1 corresponds to a final orientation of 180° and 0 indicates a response with final orientation of ±90°. For the fly in A, the response index is thus (90°-12)/90°=0.86 (E, dashed line indicates response index=0). Response index varied significantly with wind velocity between 0.2 and 1.0 m s^{-1}, with responses at all velocities being significantly greater than at 0 wind (F).

second group was frozen for one hour and then tethered, and a third group was also frozen, prior to having their wings clipped at the hinge. All three groups were then presented with wind at 0, 0.2, 0.4, 0.6, 0.8 and 1.0 m s^{-1}, in 5 second trials, where the trials were separated by 5 second periods when the wind was turned off and no visual stimulus was presented (since the dead flies would be unable to respond).

5.2.2 Results

Because it was possible that the wind-based orientation response in §5.1.2 was in part due to passive aerodynamic effects, we compared the responses of live flies to those of flies that had been freshly killed. To further parse the aerodynamic effects on the wings and the body, another group of dead flies had their wings clipped at the level of the hinge. From the raw orientation traces, it is apparent that dead flies also turned into an oncoming wind, particularly flies with intact wings at high wind velocities (Fig. 5.2). Dead flies did not adopt perfect upwind orientations, perhaps as a result of friction between the pin and jewel bearing, small irregularities in the magnetic field, or non-uniform tethering. Plotting the orientation responses of all three groups as a function of the absolute value of initial orientation, it is clear that the orientation response was particularly pronounced in dead flies with intact wings at velocities of 0.6 m s^{-1} and above (Fig. 5.3). Response indices were significantly higher in live flies than in dead flies with intact wings between 0.2 and 0.6 m s^{-1} and were almost significant at 0.8 m s^{-1} (0.2 m s^{-1}: t= 3.11, d.f.=36, P<0.005; 0.4 m s^{-1}: t=2.24, d.f.=36, P<0.05; 0.6 m s^{-1}: t=2.28, d.f.=36, P<0.05; 0.8 m s^{-1}: t=1.58, d.f.=36, P=0.06; 1.0 m s^{-1}: t=1.37, d.f.=36, P=0.09; one tailed, homoscedastic t-tests) (Fig. 5.4A).

To offer a rough quantification of the contribution of the wings to the passive aerodynamic response, we subtracted the mean response index, at each wind velocity, of the dead, wingless flies, from the corresponding values for the dead, winged flies. We then divided this value by the mean response of the dead, winged flies, to yield the percentage of their response attributable to the presence

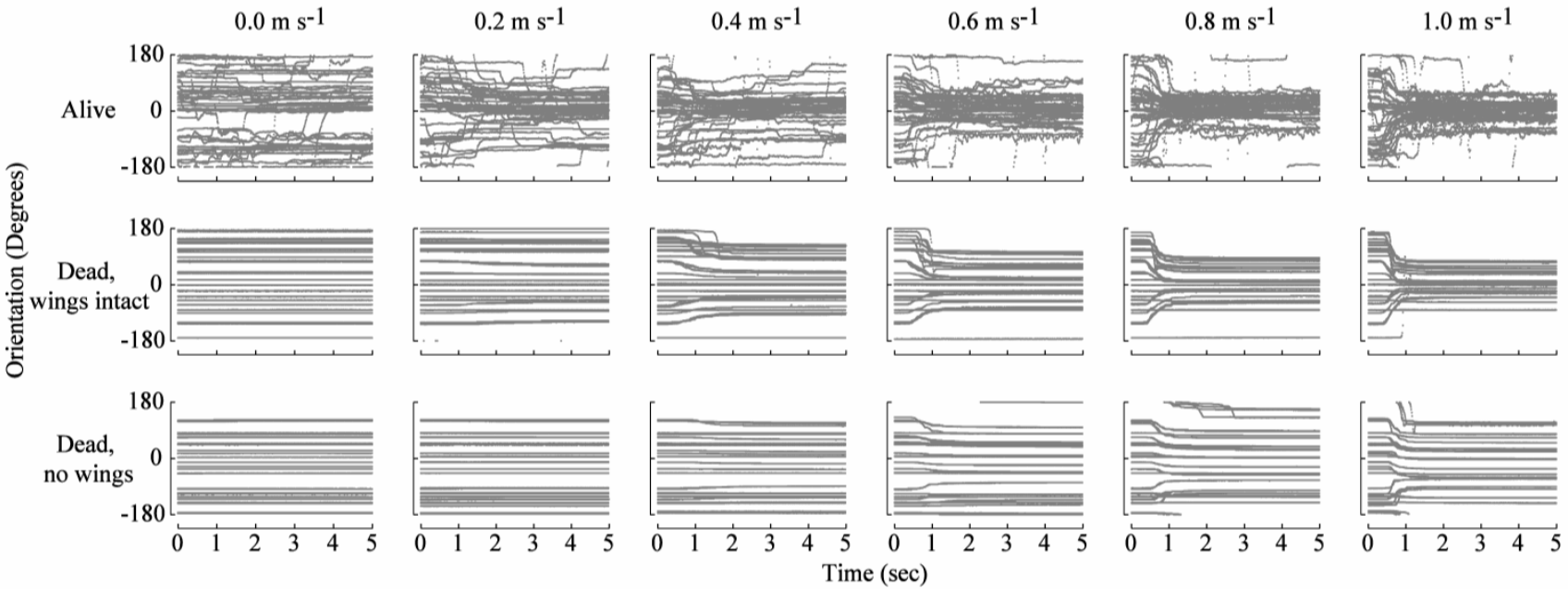

Figure 5.2. A passive aerodynamic response is apparent with increasing wind velocity. Dead flies with their wings intact and, to a lesser extent, dead flies without wings, evinced an orientation response to wind onset.

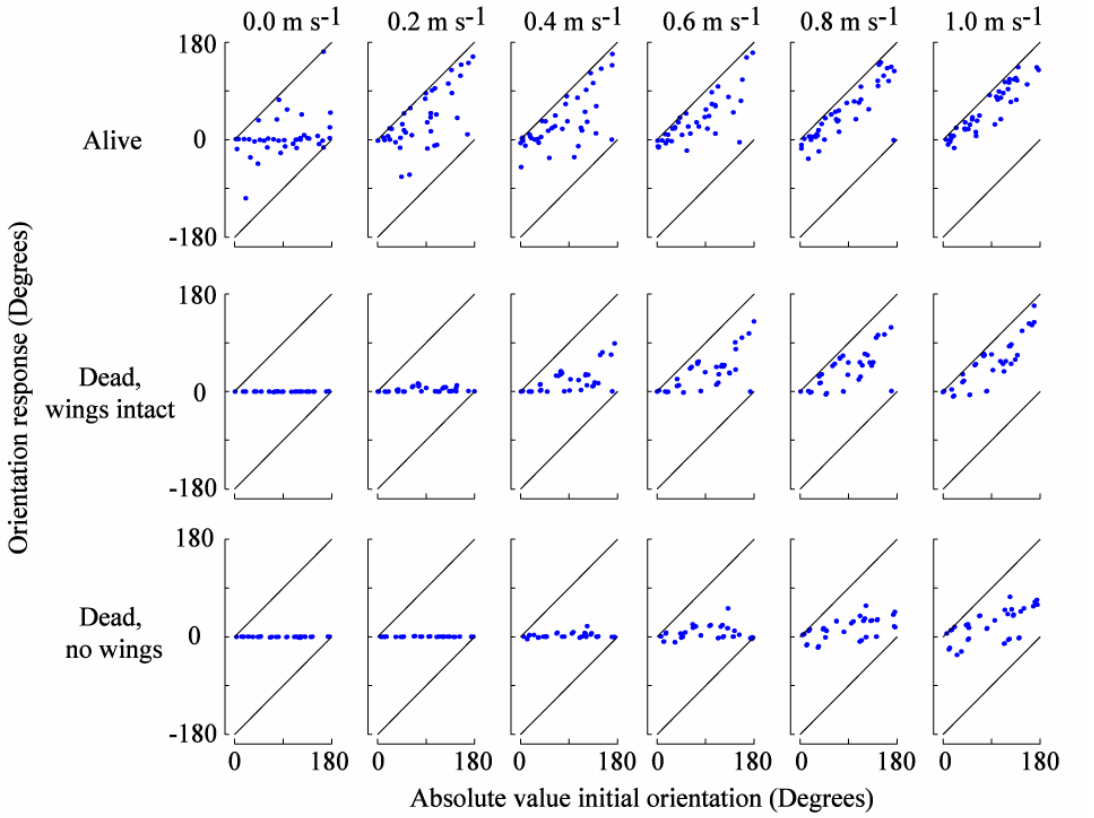

Figure 5.3. Orientation responses were much more pronounced in live flies, particularly at low wind velocity. Plotting orientation response as a function of |initial orientation| makes it apparent that responses in dead flies without wings are quite small, even at high wind velocity, while dead flies with intact wings manifested moderately strong orientation, especially at the highest wind velocities.

of wings (thus assuming that the aerodynamic effects of the wings and body are purely additive). We similarly calculated the active, behavioral, contribution to the live fly responses based on the response indices of the live and dead, winged, flies. These analyses indicated that wings accounted for a declining fraction of the passive response, from nearly 100% at 0.2 m s^{-1} to 61% at 1.0 m s^{-1} (Fig. 5.4B). The active behavioral response meanwhile explained 85% of the total response of live flies at 0.2 m s^{-1}, declining to 14% at 1.0 m s^{-1}. The wings of the dead, winged flies, were generally extended laterally or dorsally, thus representing a "snapshot" of the full range of wing-stroke conformations that occur in flight. The aerodynamic forces on the wings are therefore likely to be only a rough approximation of those experienced during flapping flight.

Body saccades play a major role in the flight orientation of tethered and freely-flying flies (Bender and Dickinson, 2006b; Tammero and Dickinson, 2002b). We were thus interested in whether saccades played a part in the orientation responses of these flies into an oncoming wind. Saccades were identified by the same algorithm used in Bender & Dickinson (2006), and were defined as turns with angular velocities exceeding 300° s^{-1} and magnitudes of at least 15° (Fig. 5.5A, B). Saccades were indeed a conspicuous component of the responses of live flies, tending to cluster towards the onset of the wind stimulus and to orient the flies towards upwind (Fig. 5.5C). In the absence of wind, spontaneous saccades were distributed throughout the trial and did not preferentially turn the flies towards upwind. Saccades were comparatively very rare among the orientation traces of dead flies, further supporting the interpretation that upwind orientation includes an active behavioral response.

5.3 Antennal contribution to the orientation response

5.3.1 Experimental design

Flies were divided into four groups. One group had both antennae glued at the junction between the funiculus and pedicel. Two other groups had their antennae glued unilaterally (right or left), and the final group was mock glued.

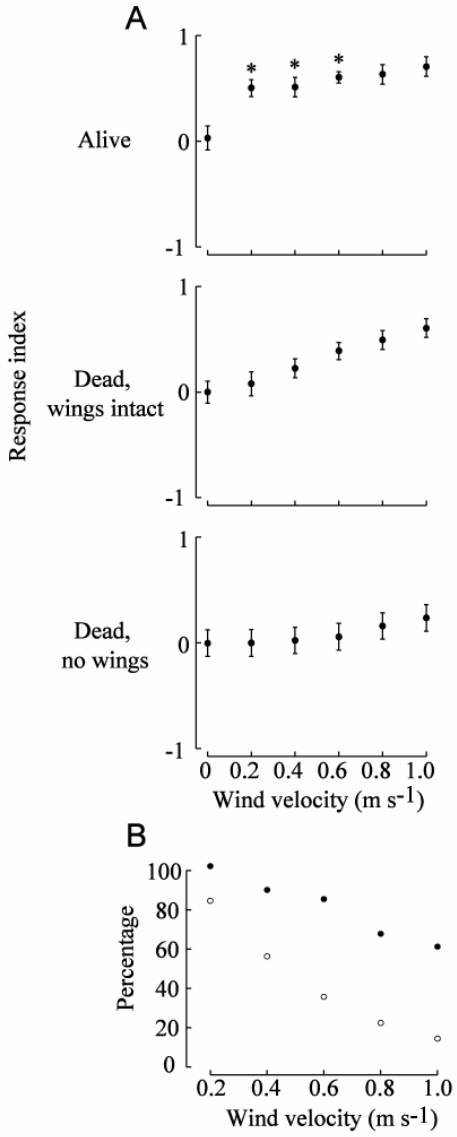

Figure 5.4. Response index scores permit a decomposition of the aerodynamic effect of wings and of the behavioral response. Response index scores were significantly higher in live flies compared to dead, winged flies, at velocities below 0.8 m s^{-1} (A) (0.2 m s^{-1}: t= 3.11, d.f.=36, P<0.005; 0.4 m s^{-1}: t=2.24, d.f.=36, P<0.05; 0.6 m s^{-1}: t=2.28, d.f.=36, P<0.05; 0.8 m s^{-1}: t=1.58, d.f.=36, P=0.06; 1.0 m s^{-1}: t=1.37, d.f.=36, P=0.09, one tailed, homoscedastic t-tests). The percentage of the response attributable to the aerodynamic effects of wings was quantified by subtracting the mean response index for dead wingless flies from the corresponding values for dead, winged flies and dividing by the mean, dead, winged response (B, filled circles). The effect of the live behavioral response was similarly quantified from the responses of live flies and dead, winged flies (B, open circles).

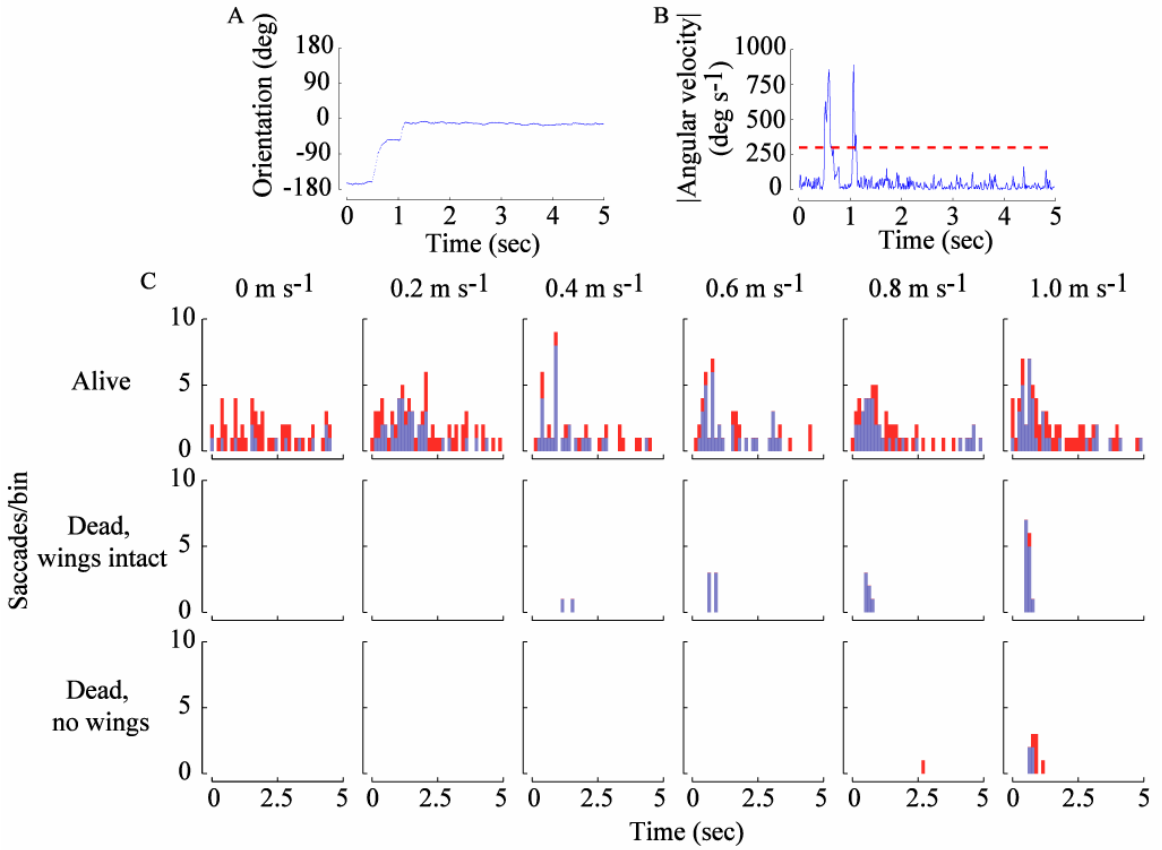

Figure 5.5. Saccades play a role in the active behavioral response. Saccades were quantified as turns with magnitudes greater than 15° and angular velocities exceeding 300° s^{-1}. Two successive saccades from a fly orienting in a 0.6 m s^{-1} wind are illustrated in A and B. In live flies, spontaneous saccades (i.e., those exhibited in the absence of wind) were distributed throughout the trial (C). Furthermore, those that improved the flies' orientation relative to upwind (blue bars) did not predominate compared to those that turned the flies away from upwind (red bars). In the presence of wind, saccades tended to cluster near the onset of the wind stimulus and also tended to improve the orientation relative to upwind. In dead flies, saccades were very rare under all conditions.

Flies were then exposed to wind at 0, 0.2, and 1.0 m s^{-1} in 10 second trials with trials interspersed with 10 second periods when the wind was turned off and a visual stimulus was again used to realign the flies facing downwind. Analysis again covered the first five seconds of the trials as behavior was essentially unchanged over the final five seconds.

5.3.2 Results

To test the effects of the Johnston's organs (JOs) on wind based orientation, the antennae were glued, either unilaterally or bilaterally, immobilizing them at the junction between the pedicel and funiculus. Because *D. melanogaster* lacks the campaniform sensillum present at this junction in some other Diptera (Miller, 1950; D. Eberl, personal communication), it is probably safe to ascribe any resulting behavioral deficits to the loss of directional sensitivity by the JOs. The raw traces indicate that, at 0.2 m s^{-1}, the orientation response was substantially degraded in the case of bilaterally glued flies, and, to a lesser extent, in unilaterally glued flies (Fig. 5.6A). At high wind velocity, however, the orientation responses were largely restored, probably due to the participation of the passive aerodynamic response. Flies with neither antenna glued oriented significantly better than baseline at both wind velocities (0.2 m s^{-1}: t=-4.84, d.f.=26, $P<0.001$; 1.0 m s^{-1}: t=-5.26, d.f.=26, $P<0.001$) (Fig. 5.6B). At 0.2 m s^{-1}, neither the bilaterally glued (t=0.24, d.f.=31, P=0.49), left glued (t=-0.35, d.f.=28, P=0.37), nor right glued (t=-2.77, d.f.=25, P=0.055) flies performed significantly better than baseline, though the performance of the right glued flies was almost significant. At 1.0 m s^{-1}, all groups oriented significantly better than baseline (bilateral: t=-3.65, d.f.=31, $P<0.001$; left: t=-3.61, d.f.=28, $P<0.001$; right: t=-4.04, d.f.=25, $P<0.001$).

We quantified the behavioral contributions of the JOs to the orientation response in a manner analogous to that used in §5.2.2 where we estimated the contributions of the passive and active components of the orientation response (Fig. 5.4B). Here, we similarly calculated the contribution of a single JO by subtracting the bilaterally glued responses from the mean unilateral ones and

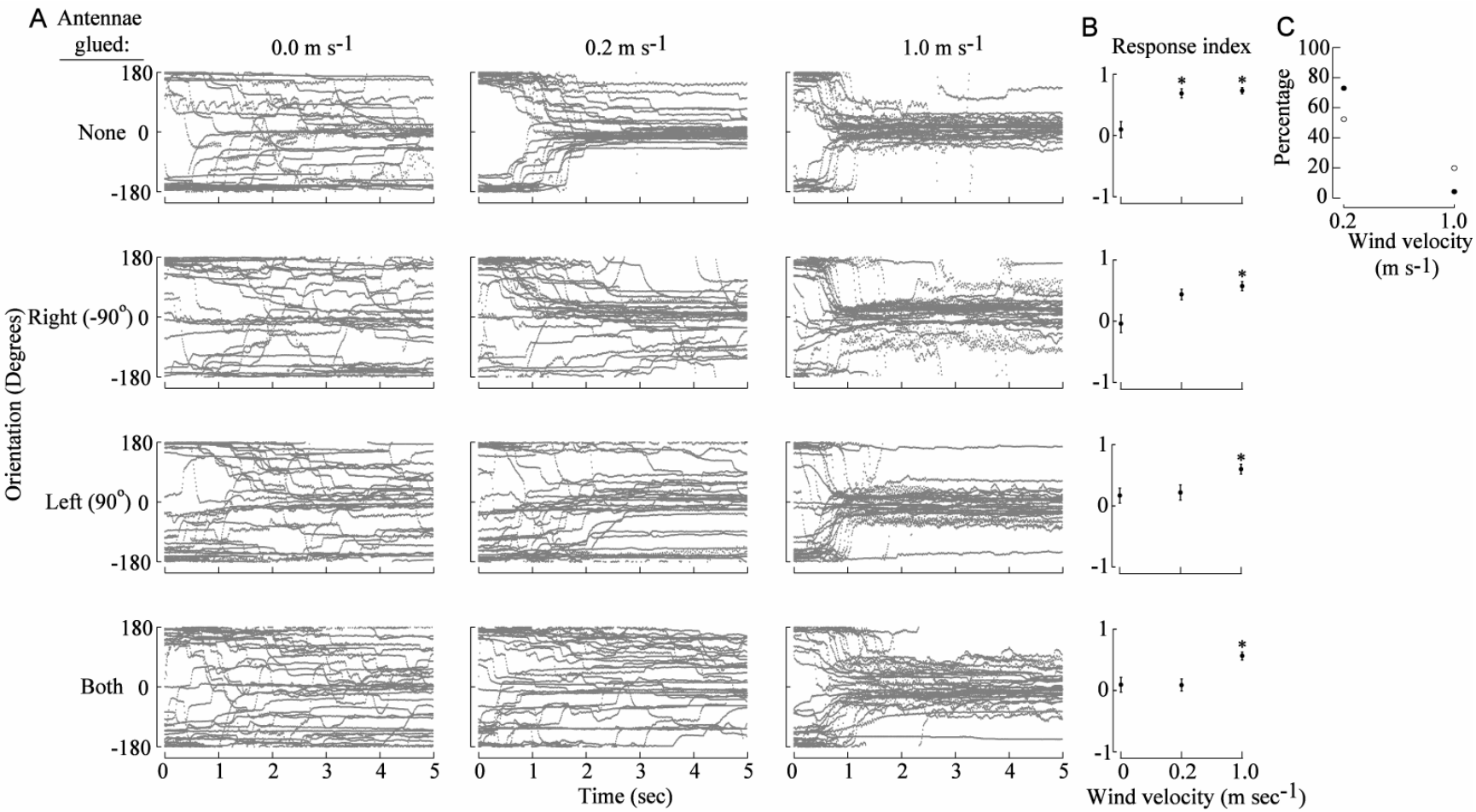
A
Antennae glued:
0.0 m s-1
0.2 m s-1
1.0 m s-1
None
Right (-90°)
Left (90°)
Both
180
0
-180
Orientation (Degrees)
0 1 2 3 4 5
Time (sec)
B
Response index
1
0
-1
0 0.2 1.0
Wind velocity (m sec-1)
C
Percentage
100
80
60
40
20
0
0.2 1.0
Wind velocity (m s-1)

Figure 5.6. Antennal immobilization greatly reduces the orientation response (A). Flies had their antennae glued at the junction of the pedicel and funiculus either unilaterally or bilaterally. At 0.2 m s^{-1}, orientation was not significantly different from baseline in bilaterally glued flies (t=0.24, d.f.=31, P=0.49), nor in flies with the right (t=-2.77, d.f.=25, P=0.055) or left (t=-0.35, d.f.=28, P=0.37) antennae unilaterally glued (B). Non-glued flies however did orient significantly better than baseline at the lower velocity (t=-4.84, d.f.=26, P<0.001). At 1.0 m s^{-1}, all groups oriented significantly better than baseline (none glued: t=-5.26, d.f.=26, P<0.001, right glued: t=-4.04, d.f.=25, P<0.001, left glued: t=-3.61, d.f.=28, P<0.001, both glued: t=-3.65, d.f.=31, P<0.001). The percentage of the response attributable to visual responses and mechanoreceptors other than the JOs was quantified by subtracting the mean response index for dead, winged flies (data from experiment 2) from the corresponding values for bilaterally glued flies and dividing by the bilaterally glued response (C, plus signs). The effect of a single JO was similarly quantified from the mean responses of unilaterally and bilaterally glued flies (C, filled circles). Finally, the effect of the second JO was calculated from the responses of none-glued flies and the mean unilaterally glued responses (C, open circles).

dividing those values by the mean unilateral responses. In this case, a single JO was responsible for 73% of the unilateral response at 0.2 m s^{-1} and 4% at 1.0 m s^{-1} (Fig. 5.6C). Comparing the responses of unilateral and control flies in the same way, the second JO contributed 52% and 20% of the response of control flies at 0.2 and 1.0 m s^{-1} respectively. It appeared as though there was a bias in the turn directions of unilaterally glued flies in that left and right glued flies tended to turn from -180° and 180° respectively towards 0°. In both cases, the flies apparently had oriented asymmetrically during the inter-trial presentation of visual stimuli and then minimized the total turn magnitude as they reoriented towards upwind. There was no apparent asymmetry however in the final orientations adopted by these flies.

5.4 Interaction of visual and mechanosensory stimuli

5.4.1 Experimental design

Flies were presented with 39 different combinations of wind velocity, visual expansion rate and location of the focus of expansion (FOE). The flies were tested at wind velocities of 0, 0.2, or 0.6 m s^{-1}. The visual stimulus was composed of two half-fields consisting of a square wave pattern (spatial frequency of 36°) that moved away from the FOE at angular velocities of 9, 36, or 180° s^{-1},

yielding temporal frequencies of 0.25, 1.0, or 5.0 Hz. The FOE was positioned either at 0° (upwind), ±90°, or 180°. Every wind velocity was paired with every expansion rate and FOE position, yielding 36 different treatments. The wind stimuli were also presented in the absence of visual stimuli, for a total of 39 treatments per fly.

5.4.2 Results

Recent experiments have indicated that expanding visual stimuli elicit robust turning responses in freely-flying flies (Tammero and Dickinson, 2002b). In tethered-flight, this results in fixation of a focus of contraction (FOC) as flies turn away from a FOE (Tammero et al., 2004). This result is somewhat paradoxical since forward flight must be accompanied by expanding stimuli, suggesting that flies are able to overcome this avoidance response under the appropriate conditions. Reiser (2007) has provided several possible solutions to this paradox. One is that the temporal frequencies of image expansion experienced by flies in free-flight are much lower than those used in tethered-flight experiments and thus are less likely to elicit avoidance responses. Another possibility is that fixation of a conspicuous visual object may be capable of suppressing the aversive reaction towards expanding large-field motion.

It may also be the case that toleration of expanding visual motion requires the input of other sensory modalities, namely the perception of the headwind that would be generated during forward flight. We thus tested the relative contributions of visual and mechanosensory cues to flight orientation to determine whether the strong mechanosensory preference for orientation into a headwind might help to explain free-flight behavior. This was accomplished by presenting flies with combinations of multiple wind velocities, expansion rates, and orientations of the expansion pattern.

To quantify the relative contributions of the two sensory modalities, we calculated a preference index based on the fly's relative orientation towards the FOC and the upwind direction (Fig. 5.7). The preference index was calculated by dividing the number of instantaneous heading vectors falling within ±45° of

upwind (0^o) by the total number of heading vectors falling within this interval and $\pm 45^o$ of the FOC. This metric thus ranged between +1 (perfect wind orientation) and -1 (perfect FOC orientation). A preference index could only be calculated when the FOC was offset from 0^o by at least 90^o, namely at $\pm 90^o$ and 180^o.

In the absence of visual stimulation, orientation towards upwind improved with wind velocity as described in §5.1.2 (Fig. 5.8, bottom row). When paired with a visual stimulus, preference indices increased with wind velocity, within a given expansion rate and across FOC locations. At the same time, within a given wind velocity, fixation indices declined with the rate of visual expansion as flies increasingly oriented towards the FOC. When the wind and visual stimuli both favored orientation towards 0^o, flies oriented relatively uniformly upwind, except at the highest rates of visual expansion. The competition between the two stimuli can be seen clearly, for example, in rows two and three of columns four through nine in Fig. 5.8, where preference indices increase with wind velocity and decrease with expansion rate.

It is clear from Fig. 5.8 that orientation is a multivariate function of wind velocity, expansion rate, and position of the FOC. To quantify the relative contributions of these three cues, we multiply linearly regressed preference index on these three parameters while controlling for fly identity by including it as a nominal variable. The results, given in Table 5.1, indicate that all three contributed significantly to a combined model with standard partial regression coefficients of similar magnitudes. This result indicates that orientation can be thought of as a tradeoff between an attraction to the mechanical stimuli associated with forward flight and an aversion towards expanding visual stimuli. Further, FOC location also had a strong effect on orientation. When the FOC was positioned at $\pm 90^o$ relative to the wind, flies were able to adopt a compromise orientation, but when the FOC moved to a downwind position, flies were increasingly forced to choose between the two attractive poles.

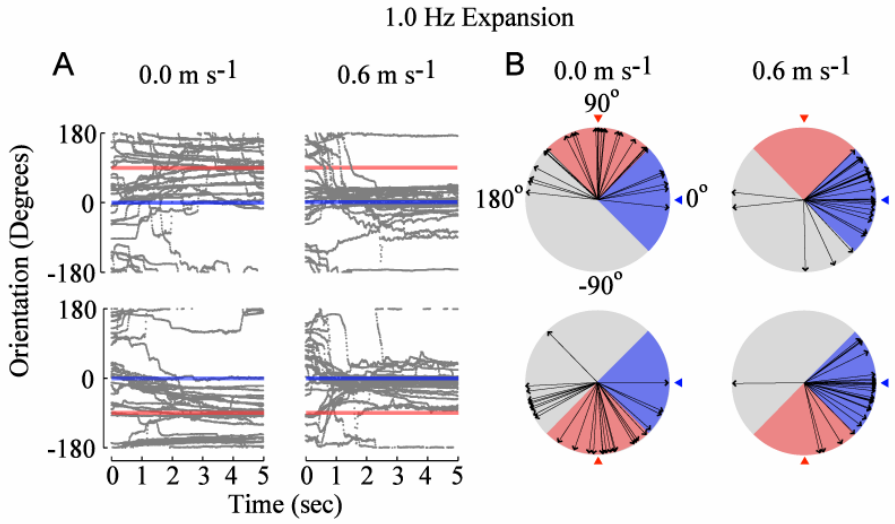

Figure 5.7. Orientation towards a wind or visual stimulus. Flies were presented with 39 different combinations of wind velocity, expansion rate and location of the FOC. Exemplar responses to a stripe pattern expanding at 1.0 Hz at $\pm 90°$ in the absence and presence of a 0.6 m s^{-1} wind are shown (A, location of the FOC is indicated by the red bar, orientation favored by wind is indicated by the blue bar). To quantify the preference for the visual or wind stimulus, the number of instantaneous heading vectors in the final two seconds of each trial that fell within $\pm 45°$ of $0°$ (B, blue shaded area) was divided by the total number falling within $\pm 45°$ of $0°$ and the number falling within $\pm 45°$ of the FOC (B, red shaded area). This yielded a preference index between 1 (wind preferred) and 0 (FOC preferred). In B, the arrows represent the mean orientation vectors of each fly in A over the full five second trial.

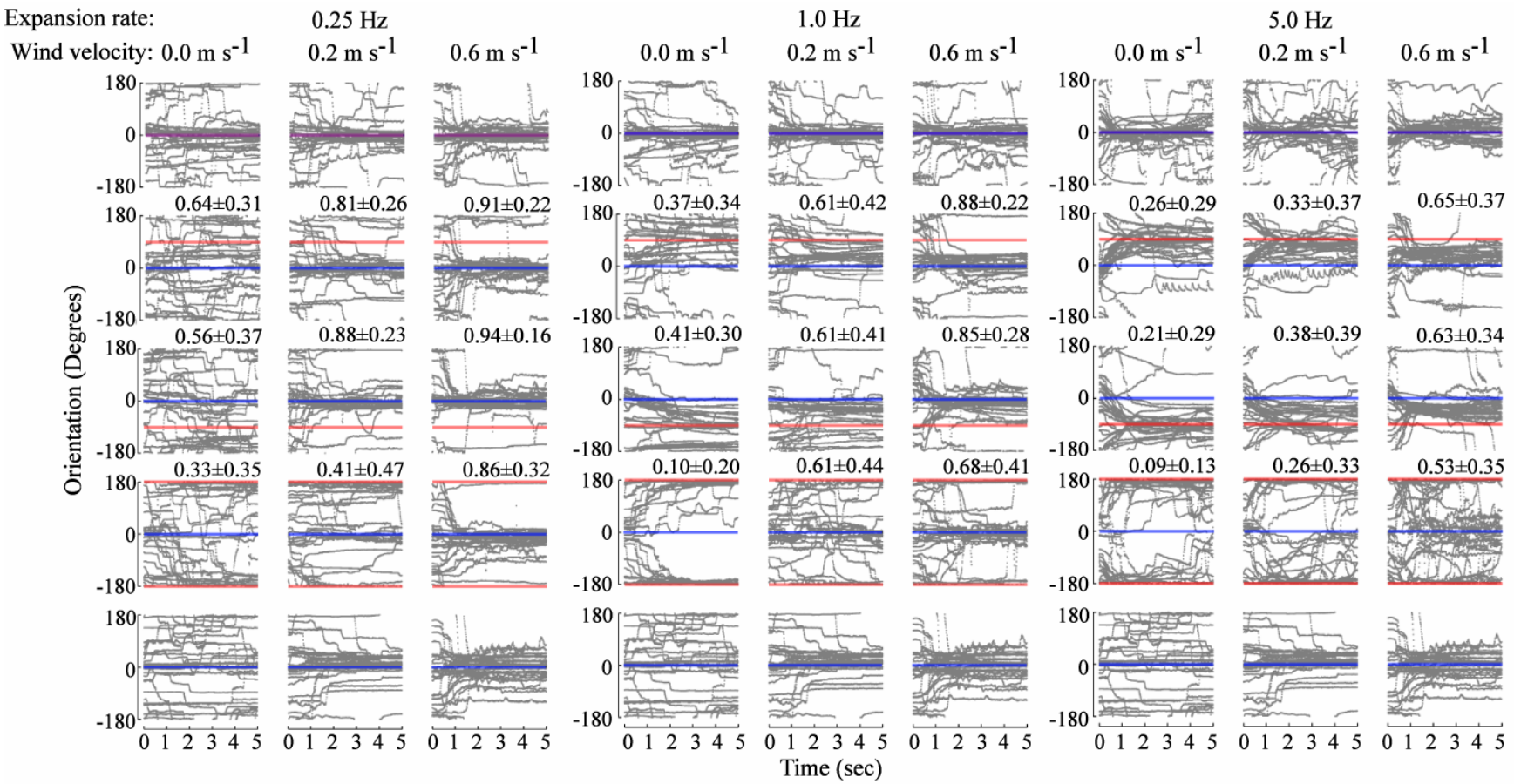

Figure 5.8. Both the visual and wind stimuli shaped fly orientation. The orientation predicted by a preference for wind is indicated by the blue bars and that predicted by expansion avoidance is indicated by the red bars. Numerical values above and to the right of the labeled panels are mean preference indices ± standard deviation. Orientation could, in general, be described as a compromise between the two competing stimuli with orientation being increasingly biased towards the wind with increasing wind velocity and increasingly favoring the FOC with increasing expansion velocity.

Table 5.1. *Multiple regression of preference index on visual expansion rate, wind velocity and FOC location*

	t	ß	P	R^2
Expansion	-10.70	-0.325	<0.001	0.33
Wind velocity	14.22	0.431	<0.001	
FOC location	-6.73	-0.204	<0.001	

Finally, we were interested in whether saccades played a role in FOC orientation, as they did with the wind stimulus alone (Fig. 5.5). Indeed, saccades were a conspicuous component of the visual response, tending to occur towards the beginning of each trial and to orient the flies towards, rather than away from, the FOC (Fig. 5.9). It is also clear that saccades were common towards the end of trials when the FOC was located at 0^o and 180^o, especially at 5.0 Hz. That this was the case is apparent from examination of the raw orientation traces. Aside from timing differences, saccade dynamics were very similar in all conditions (data not shown).

5.5 Discussion

D. melanogaster, loosely tethered so that it is able to rotate about its yaw axis, rapidly orients into an oncoming wind, as would be experienced during forward flight. This response is sustained for the duration of each trial and its magnitude is correlated with wind velocity over a range of speeds that a fly is likely to encounter in free-flight (Budick and Dickinson, 2006; Tammero and Dickinson, 2002b). Wind-based orientation in this species is consistent with observations in tethered *Schistocerca gregaria* (Weis-Fogh, 1948; Weis-Fogh, 1949) and *Locusta migratoria* (Gewecke and Philippen, 1978), and probably

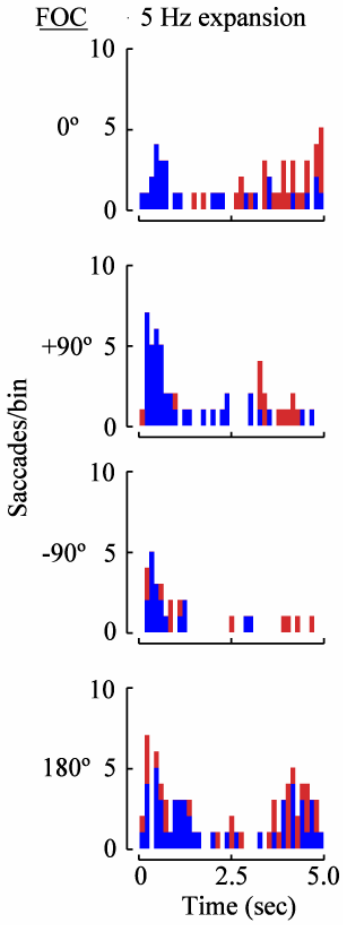

Figure 5.9. Saccades were employed, as with the wind stimuli (Fig. 5.5) to orient towards an attractive visual stimulus. A visual pattern, expanding at 5 Hz in the absence of a wind stimulus, tended to elicit saccades that oriented flies towards the FOC (blue bars) compared to those orienting flies away from the FOC (red bars), particularly at the beginning of the trial. Flies also exhibited a large number of saccades towards the end of trials with expansion rates of 5 Hz, particularly when the FOC was at either the up or downwind ends of the arena.

should not be surprising since a headwind is a natural consequence of forward flight.

A fraction of this orientation response could be attributed to passive "wind vane" effects on the body and wings, particularly at high wind velocity. It is difficult to estimate the degree to which this complementary passive effect may also be involved in free-flight. Its extent will be determined in part by the relative position of the fly's center of mass, and the center of pressure acting on its body and wings. In this study, the fly was likely tethered at a point anterior to its center of mass, which is located at the anterior end of the abdomen in a gravid female (W. Dickson, personal communication). This would most likely exaggerate the forces experienced by a fly in free-flight since it situates a greater proportion of the fly's surface area posterior to the axis of rotation. A second source of uncertainty in evaluating the role of passive forces in free-flight is in estimating the average force on two flapping wings, which is only very roughly approximated by those on the stationary wings of the dead flies used in these experiments.

Despite the presence of a passive aerodynamic effect, there was also a significant active behavioral response, largely mediated through the fast saccadic maneuvers that are known to play a role in visually based flight control (Frye et al., 2003; Tammero and Dickinson, 2002b). The active component of orientation explained a progressively greater fraction of the total response with decreasing wind velocity. Inasmuch as flies may rarely attain the high airspeeds at which passive forces play a more prominent role, their effect in free-flight may be relatively small (Budick and Dickinson, 2006; Tammero and Dickinson, 2002b). Finally, when visual and wind stimuli were presented in opposition, flies often oriented diametric to the wind stimulus, indicating that passive aerodynamic effects cannot account for the orientation responses observed here.

Antennal mechanoreceptors are clearly involved in flight control in a number of insect species, both in velocity control and in orienting flight relative to the wind. This has been established via gluing and ablation studies, usually involving the junction between the pedicel and flagellum, and thus deafferenting any mechanoreceptors sensitive to motion about that joint. In most species, this

non-specific manipulation may implicate the JOs as well as a variety of other mechanoreceptors. For instance, in *Locusta migratoria*, the JOs, a ring of 70 campaniform sensillae, and another chordotonal organ are all sensitive to deflections of the flagellum relative to the pedicel (Gewecke, 1972), with the campaniform sensillae specifically encoding information on directional displacements (Gewecke and Heinzel, 1979). Similarly, in *C. erythrocephala*, the JO is sensitive to high-frequency vibrations of the antennae at the joint between the pedicel and the basal annulus of the flagellum, known as the funiculus in Diptera, while an accompanying campaniform sensillum is tonically sensitive to lateral deflections of the funiculus (Gewecke, 1967a; Gewecke, 1974). In that species, wind direction seems to be encoded by the differential activation of scolopidia across the JO, this varying as a function of funicular deflection (Gewecke, 1974). Unilateral projections from these antennal mechanoreceptors terminate in the mechanosensory lateral deutocerebrum (Straussfeld and Bacon, 1983), where they are capable of inducing changes in wing stroke amplitude in response to asymmetric wind stimulation, resulting in yaw-corrective maneuvers (Gewecke, 1967b; Gewecke, 1974).

It has been known for some time that the JOs play a role in near-field sound detection during *Drosophila* courtship (Ewing, 1983) during which they also detect relative displacements of the pedicel and funiculus (Eberl et al., 2000; Ewing, 1978; Gopfert and Robert, 2002). The role of these chordotonal organs, and the antennae generally, in wind-based orientation has heretofore been unexplored in this species however. *D. melanogaster* makes an especially attractive target in which to address this question since it lacks any other mechanoreceptors sensitive to movement at the pedicellar-funicular joint (Miller, 1950; D. Eberl, personal communication), unlike *C. erythrocephala*. Immobilizing this joint thus suggests an attribution of any resulting behavioral deficits to deafferentation of the JO. In only one other species, to my knowledge, the Odonate *Orthetrum cancellatum*, has the JO specifically been implicated as the sole mediator of a behavioral response to wind stimulation (Gewecke et al., 1974; Gewecke and Odendahl, 2004).

When the JOs were bilaterally deafferentated, *D. melanogaster*'s low-velocity wind orientation was significantly impaired. With unilateral antennal gluing, flies also failed to orient significantly better than in the absence of wind, though that difference was nearly significant in right-antennal glued flies. At high wind velocity, orientation responses were largely restored in both groups of flies and this could probably be accounted for by passive mechanisms, since those responses resembled those of dead, winged flies. The JOs thus seem to play an essential role in wind-mediated orientation.

While unilaterally deafferentated flies failed to orient significantly above baseline at 0.2 m s^{-1}, this difference was almost significant in the case of right glued flies, as noted above. Further, restoration of a single JO resulted in a 73% improvement in orientation, suggesting a significant, but incomplete loss of orientation responses in these flies. This result implies that directional detection does not entirely rely on comparisons of the relative deflections of the two antennae and further suggests that a single chordotonal organ has the ability to detect wind direction. Restoration of the second JO accounted for an additional 52% and 20% improvement in orientation, at 0.2 and 1.0 m s^{-1} respectively, which may represent the unitary contribution of the second JO, or the output of a supplemental mechanism involving an inter-antennal comparison of deflections. We attempted to completely eliminate JO feedback by using the chordotonal mutant *Beethoven* (Eberl et al., 2000), but those flies were unable to fly in our apparatus.

The results in §5.4.2 indicate that, under the appropriate stimulus conditions, flies are able to overcome the otherwise robust expansion avoidance reflex and orient into a headwind. This wind-based orientation response increases with wind velocity across expansion rates and declines with visual expansion rate across wind velocities. It thus appears as though neither sensory modality is able to exert complete control over the fly's final orientation, and that the total response can be described as a relatively simple multivariate function of wind velocity, visual expansion rate, and position of the FOC. Diametric opposition of the FOC and the wind stimulus generally forced the

animal to choose between one of the attractive poles, while moderate misalignment permitted the fly to choose a compromise orientation.

These results suggest that during free-flight, the expansion avoidance response may be largely suppressed by a mechanically induced preference for forward flight. For example, flies tracking plumes of attractive odors routinely reach airspeeds of 0.6 m s^{-1} (Budick and Dickinson, 2006). If the resulting real-world temporal frequencies experienced by these flies fall into the range tested in this study, then these results could easily explain how flies are able to fly forward despite this antagonistic visual reflex. These results might then suggest a model of flight control whereby a preference for wind-induced mechanical stimulation promotes forward flight in *D. melanogaster*. At high rates of visual expansion, however, as would occur when collision with an object becomes imminent, the visual avoidance response is able to overcome its suppression by the mechanosensory one, eliciting a turn away from the FOE.

CHAPTER 6

Concluding Remarks

The previous three chapters have documented the results of experiments, in three different paradigms, on the role of the visual, olfactory, and mechanosensory systems in structuring the flight trajectories of *Drosophila melanogaster*. In this final chapter, I will review the key results of those experiments and consider how they contribute to a general understanding of flight control in this species.

6.1 Significant results

6.1.1 Chapter 3: Free-flight responses to olfactory and visual stimuli

- *D. melanogaster* is strongly anemotactic, biasing its flight upwind even in the absence of olfactory stimuli. The anemotactic response is capable of suppressing the otherwise robust attraction to conspicuous visual objects, causing flies to largely ignore a black post as they fly upwind.
- When a narrow plume of attractive odor is superimposed on the wind, flies readily track the plume to its source. In the process, their search strategy involves cross-wind flight that becomes directed upwind following plume contact.
- Flies respond to plume contact by decreasing their cross-wind velocity and increasing their upwind velocity such that they are maximally oriented upwind within about 250 ms of plume contact. This response, together

with an increase in airspeed, constitutes an "upwind surge," not unlike that manifested by various species of Lepidoptera.

- The upwind surge is echoed, on a slower time scale, by control flies flying in clean air, indicating that this response has a substantial visual component. This is likely the result of flies turning to avoid wall collision and orienting upwind due to the baseline anemotactic response. This result reminds us of the potential for confounding the effects of multiple sensory modalities in free-flight experiments.
- In a homogenous odor cloud, flies fly relatively fast and straight upwind, suggesting that intermittent stimulation is not necessary for sustained upwind flight in this species, at least in the short term. Similarly, flies in large-diameter continuous odor plumes rarely initiate casting flight—trajectories oriented primarily perpendicular to the wind direction with iterated, large angle turns.
- Casting appears to be a causal consequence of plume loss, as flies preferentially cast after losing an odor plume due to its truncation. These casts initiate with a mean latency of about 290 ms.

6.1.2 Chapter 4: Tethered-flight responses to pulsed and continuous odor plumes

- Flies manifest wing kinematic responses to odor pulses as brief as 120 ms, in the form of increased wingbeat frequency and stroke amplitude. Wing responses increase logarithmically with pulse duration, saturating after about one second of odor exposure.
- Wingbeat frequency increases with a shorter time constant than does amplitude, such that stroke amplitude may continue to increase for several seconds following odor exposure. Both remain elevated during the period of exposure and for some duration following it.
- Wing responses to pulsed and continuous plumes are qualitatively similar, with responses to continuous plumes being equal to or greater than those to pulsed plumes delivered over approximately the same duration.

- Flies reduce their rate of spontaneous fictive "saccades" during odor presentation, with saccades remaining suppressed for some duration following plume offset in the case of long (one second or longer) pulses. Saccade rate rebounds quickly after the offset of short pulses, possibly reflecting the tendency to initiate casting following plume loss in free-flight.

6.1.3 Chapter 5: The role of visual and mechanosensory cues in structuring forward flight

- Loosely tethered flies respond to a wind stimulus by orienting into the wind. The fidelity of this response is a function of wind velocity.
- The wind-orientation response depends on both a passive aerodynamic "wind-vane" effect as well as an active behavioral response. The active component explains a progressively greater fraction of the total response as wind velocity decreases, and is largely mediated by fast "saccadic" turns into the wind.
- The active orientation response is mediated by the Johnston's organs (JOs), a pair of antennal chordotonal organs sensitive to relative displacements of the pedicel and funiculus. Orientation is completely abolished by bilateral deafferentation of the JOs, but is partially restored by a single JO, suggesting that this orientation mechanism is not completely dependent on a comparison of signals originating from each antenna.
- The wind-orientation response is capable of suppressing the robust avoidance of visually expanding objects. This may help to explain how flies are able to fly forward in the face of an omnipresent stimulus that they should otherwise find highly aversive.

6.2 A multimodal approach to understanding resource localization in D. melanogaster

These results collectively demonstrate that multiple sensory modalities are involved in controlling *Drosophila* flight, and that the interactions between them can appear to be relatively simple or quite complex. If we consider a fly searching for an odor plume, for example, that fly must be able to overcome its inherent avoidance of expanding visual flow fields simply in order to accomplish the most basic task of forward flight. It appears, from these results, that this may largely be accomplished via the linear summation of a mechanosensory mediated preference for forward flight and a visually mediated avoidance of the attendant visual stimuli. At intermediate airspeeds, and in the absence of high-contrast nearby objects, the wind-induced response may be quite capable of suppressing the otherwise robust avoidance reflex.

Another important mechanism that may help to suppress the avoidance of an FOE is the attraction towards conspicuous visual objects. When a vertical stripe is superimposed on a FOE (Reiser, 2007), flies are far more willing to tolerate that visual expansion, and the results of the experiments presented here confirm that, in the absence of wind, flies are strongly attracted to high-contrast objects. Nevertheless, in the real world, flies may rarely fly in still air environments, instead being subjected to low velocity winds. In that situation, flies become anemotactic and strongly polarize their flight in the upwind direction. This response must be mediated by a visual mechanism, since flies cannot mechanically detect the direction of an externally imposed wind (David, 1986). Instead, they presumably rely on the motion of the visual world to determine the wind direction and to fly in the opposite direction. Interestingly, this visual response is capable of suppressing that same object fixation response which was so evident in the absence of wind and indeed, was posited above to play an important role in the toleration of visual expansion. In simply trying to explain upwind flight in the presence of a visual object, we have thus already recruited an expansion avoidance response, object fixation, visually based anemotaxis, and mechanically favored forward flight. Understanding the

relationships among these algorithms and their role in shaping behavior in a particular stimulus environment is clearly a formidable problem, but the results here suggest that it may nonetheless not be an intractable one.

Of course, the situation becomes increasingly complex if this fly contacts an odor plume. Its behavior is then modified once again so as to additionally favor direct upwind flight at increased airspeed, thus necessarily feeding back on the visual flight-control pathways. This result is consistent with that of Frye & Dickinson (2004b), where tethered flies exposed to odor reduced their steering variance as they more precisely controlled the position of a large-field visual stimulus. In the free-flight case, flies similarly seem to tolerate less rotation of the visual surround as they head directly upwind. While the olfactory and visual responses may thus appear to be independent in some situations (Frye and Dickinson, 2004a), there are also clearly cases where the interactions are more complex.

This is particularly apparent if a fly loses the odor plume, fundamentally altering its flight control strategy such that it now flies crosswind before executing large angle turns. This shift from upwind to crosswind flight is perhaps the most obvious example of a complex interaction between stimulus modalities. The loss of the odor plume, mediated by the olfactory system, is capable of modifying the response to visual stimuli such that instead of minimizing transverse optic flow, as may occur during upwind flight, flies now adopt a preference for a radically different structure of visual motion, one that includes a substantial transverse component. Furthermore, the avoidance of expanding flow fields, which had previously served an apparently important role in structuring flight, must be greatly suppressed by olfactory modulation of the response to visual stimuli. Needless to say, recontacting the odor plume is capable of triggering a return to upwind flight and an additional remodeling of the flight trajectory. At the same time, so long as the fly remains within the plume, this olfactory-mediated flight control strategy continues to carry the fly upwind, thus tonically modifying the flight control system.

These results demonstrate the diversity of interactions that are possible between flight control mechanisms mediated by different stimulus modalities. At

one extreme, forward flight may represent a relatively simple tradeoff between the visual and mechanosensory systems, with their antagonistic interaction determining whether a fly will fly forward or avoid expanding visual objects. At the other extreme, loss of an odor plume is capable of eliciting an alteration in trajectory structure that is so profound as to suggest fundamental change in the way that the flight control system responds to visual cues.

6.3 Future directions

For years, models of olfactory search in Lepidoptera implicated two complementary behavioral algorithms: optomotor anemotaxis and self-generated counterturning. These control systems were thought to operate without reference to instantaneous fluctuations in stimulus conditions, instead shaping the behavioral response more slowly as a function of average stimulus conditions. With the recent discovery that at least some species of moths modify their flight trajectories in response to short-term stimulus experience, it appears increasingly likely that search behavior can be understood as an input-output relationship on much shorter time scales. This is, of course, an extremely promising development since it implies that the delineation and characterization of the intermediate pathways leading from stimulus to behavior could yield a description of behavior in terms of current stimulus conditions. The results presented in this thesis will hopefully constitute another step in this direction, towards the goal of an explicit understanding of flight behavior as the product of the immediate stimulus environment. In so doing, the hope is to develop clear predictive models for behavior, models that imply explicit neural pathways amenable to physiological analysis.

Bibliography

Arbas, E. A. (1986). Control of hindlimb posture by wind-sensitive hairs and antennae during locust flight. *J. Comp. Physiol. [A].* **159**, 849–857.

Baker, P. S., Gewecke, M. and Cooter, R. J. (1981). The natural flight of the migratory locust *Locusta migratoria* L. III. Wingbeat frequency, flight speed and attitude. *J. Comp. Physiol.* **141**, 233–237.

Baker, T. C. (1990). Upwind flight and casting flight: Complimentary phasic and tonic systems used for location of sex pheromone sources by male moths. In *International Symposium on Olfaction and Taste X*, (ed. K. B. Doving), pp. 18–25. Oslo.

Baker, T. C. and Haynes, K. F. (1987). Manoeuvres used by flying male oriental fruit moths to relocate a sex pheromone in an experimentally shifted wind-field. *Physiol. Entomol.* **12**, 263–279.

Baker, T. C. and Haynes, K. F. (1996). Pheromone-mediated optomotor anemotaxis and altitude control exhibited by male oriental fruit moths in the field. *Physiol. Entomol.* **21**, 20–32.

Baker, T. C., Willis, M. A., Haynes, K. F. and Phelan, P. L. (1985). A pulsed cloud of sex pheromone elicits upwind flight in male moths. *Physiol. Entomol.* **10**, 257–265.

Balkovsky, E. and Shraiman, B. I. (2002). Olfactory search at high Reynolds number. *Proc. Natl. Acad. Sci. U. S. A.* **99**, 12589–93.

Batschelet, E. B. (1981). Circular Statistics in Biology. New York: Academic Press.

Bender, J. A. and Dickinson, M. H. (2006a). A comparison of visual and haltere-mediated feedback in the control of body saccades in *Drosophila melanogaster*. *J. Exp. Biol.* **209**, 4597–4606.

Bender, J. A. and Dickinson, M. H. (2006b). Visual stimulation of saccades in magnetically tethered *Drosophila*. *J. Exp. Biol.* **209**, 3170–3182.

Budick, S. A. and Dickinson, M. H. (2006). Free-flight responses of *Drosophila melanogaster* to attractive odors. *J. Exp. Biol.* **209**, 3001–3017.

Budick, S. A., Reiser, M. B. and Dickinson, M. H. (in review). The role of visual and mechanosensory cues in structuring forward flight in *Drosophila melanogaster*.

Cardé, R. T. and Minks, A. K. (1997). Insect pheromone research: New directions, pp. 684. New York: Chapman & Hall.

Carson, H. L. and Heed, W. B. (1986). Methods of collecting *Drosophila*. In *The Genetics and Biology of Drosophila*, vol. 3e eds. M. Ashburner H. L. Carson and J. N. Thompson), pp. 1–28. New York: Academic Press.

Christensen, T. A. and Hildebrand, J. G. (1988). Frequency coding by central olfactory neurons in the sphinx moth *Manduca sexta*. *Chem. Senses* **13**, 123–130.

Couto, A., Alenius, M. and Dickson, B. J. (2005). Molecular, anatomical, and functional organization of the *Drosophila* olfactory system. *Curr. Biol.* **15**, 1535–1547.

David, C. T. (1982). Compensation for height in the control of groundspeed by *Drosophila* in a new, 'barber's pole' wind tunnel. *J. Comp. Physiol. [A].* **147**, 485–493.

David, C. T. (1986). Mechanisms of directional flight in wind. In *Mechanisms in Insect Olfaction*, eds. T. L. Payne M. C. Birch and C. E. J. Kennedy), pp. 49–57. Oxford: Clarendon Press.

de Bruyne, M., Clyne, P. J. and Carlson, J. R. (1999). Odor coding in a model olfactory organ: The Drosophila maxillary palp. *J. Neurosci.* **19**, 4520–4532.

de Bruyne, M., Foster, K. and Carlson, J. R. (2001). Odor coding in the *Drosophila* antenna. *Neuron* **30**, 537–552.

Dickinson, M. H., Lehmann, F. O. and Götz, K. G. (1993). The active control of wing rotation by *Drosophila*. *J. Exp. Biol.* **182**, 173–189.

Dusenberry, D. B. (1989a). Optimal search direction for an animal flying or swimming in a wind or current. *Journal of Chemical Ecology* **15**, 2511–2519.

Dusenberry, D. B. (1989b). Ranging strategies. *J. Theor. Biol.* **136**, 309–316.

Dusenberry, D. B. (1992). Sensory Ecology. New York: W.H. Freeman & Company.

Eberl, D. F., Hardy, R. W. and Kernan, M. J. (2000). Genetically similar transduction mechanisms for touch and hearing in *Drosophila*. *J. Neurosci.* **20**, 5981–5988.

Egelhaaf, M. (1985a). On the neuronal basis of figure-ground discrimination by relative motion in the visual system of the fly. I. Behavioural constraints imposed on the neuronal network and the role of the optomotor system. *Biol. Cybern.* **52**, 123–140.

Egelhaaf, M. (1985b). On the neuronal basis of figure-ground discrimination by relative motion in the visual system of the fly. II. Figure-detection cells, a new class of visual interneurones. *Biol. Cybern.* **52**, 195–209.

Egelhaaf, M. (1987). Dynamic properties of two control systems underlying visually guided turning in house-flies. *Journal of Comparative Physiology [A]* **161**, 777–783.

Ewing, A. W. (1978). The antenna of *Drosophila* as a 'love song' receptor. *Physiol. Entomol.* **3**, 33–36.

Ewing, A. W. (1983). Functional aspects of *Drosophila* courtship. *Biol. Rev.* **58**, 275–292.

Fisher, N. I. (1993). Statistical analysis of circular data. Cambridge: Cambridge University Press.

Fishilevich, Y. and Vosshall, L. B. (2005). Genetic and functional subdivision of the *Drosophila* antennal lobe. *Curr. Biol.* **15**, 1548–1553.

Flugge, C. (1934). Geruchliche raumorientierung von *Drosophila melanogaster*. *Z. Vergl. Physiol.* **20**, 463–500.

Fry, S., Bichsel, M., Muller, P. and Robert, D. (2000). Tracking of flying insects using pan-tilt cameras. *J. Neurosci. Methods* **101**, 59–67.

Fry, S., Sayaman, R. and Dickinson, M. H. (2003). The aerodynamics of free-flight maneuvers in *Drosophila*. *Science* **300**, 495–498.

Frye, M. A. and Dickinson, M. H. (2004a). Motor output reflects the linear superposition of visual and olfactory inputs in *Drosophila*. *J. Exp. Biol.* **207**, 123–131.

Frye, M. A. and Dickinson, M. H. (2004b). Visuo-motor responses to attractive odorants during tethered flight in *Drosophila*. In *7th Congress of the International Society for Neuroethology*, pp. PO103. Nyborg, Denmark: University of Southern Denmark.

Frye, M. A., Tarsitano, M. and Dickinson, M. H. (2003). Odor localization requires visual feedback during free flight in *Drosophila melanogaster*. *J. Exp. Biol.* **206**, 843–855.

Geier, M., Bosch, O. J. and Boeck, J. (1999). Influence of odour plume structure on upwind flight of mosquitoes towards hosts. *J. Exp. Biol.* **202**, 1639–1648.

Gewecke, M. (1967a). Der Bewegungsapparat der Antennen von *Calliphora erythrocephala*. *Z. Morphol. Okol. Tiere.* **59**, 95–113.

Gewecke, M. (1967b). Die Wirkung von Luftströmung auf die Antennen und das Flugverhalten der Blauen Schmeissfliege (*Calliphora erythrocephala*). *Zietschrift fur Vergleichende Physiologie* **54**, 121–164.

Gewecke, M. (1970). Antennae: another wind receptor in locusts. *Nature* **225**, 1263–1264.

Gewecke, M. (1972). Bewegungsmechanismus und Gelenkrezeptoren der Antennen von *Locusta migratoria* L. (Insecta, Orthoptera). *Z. Morphol. Tiere.* **71**, 128–149.

Gewecke, M. (1974). The antennae of insects as air-current sense organs and their relationship to the control of flight. In *Experimental analysis of insect behaviour*, (ed. B. Brown), pp. 100–113. Berlin: Springer-Verlag.

Gewecke, M. and Heinzel, H. G. (1979). Directional sensitivity of the antennal campaniform sensilla in locusts. *Naturwissenschaften* **66**, 212–213.

Gewecke, M., Heinzel, H. G. and Philippen, J. (1974). Role of antennae of the dragonfly *Orthetrum cancellatum* in flight control. *Nature* **249**, 584–585.

Gewecke, M. and Niehaus, M. (1981). Flight and flight control by the antennae in the small tortoiseshell (*Aglais urticae* L., Lepidoptera): I. Flight balance experiments. *J. Comp. Physiol.* **145**, 249–256.

Gewecke, M. and Odendahl, A. (2004). Der Bewegungsapparat der Antennen des Großen Blaupfeils *Orthetrum cancellatum* (Odonata: Libellulidae). *Entomol. Gen.* **27**, 73–85.

Gewecke, M. and Philippen, J. (1978). Control of the horizontal flight-course by air-current sense organs in *Locusta migratoria*. *Physiol. Entomol.* **3**, 43–52.

Gopfert, M. C. and Robert, D. (2002). The mechanical basis of *Drosophila* audition. *J. Exp. Biol.* **205**, 1199–1208.

Götz, K. G. (1964). Optomotorische untersuchung des visuellen systems einiger augenmutanten der fruchtfliege *drosophila*. *Kybernetik* **2**, 77–91.

Götz, K. G. (1987). Course-control, metabolism and wing interference during ultralong tethered flight in *Drosophila melanogaster*. *J. Exp. Biol.* **128**, 35–46.

Hallem, E. A., Ho, M. G. and Carlson, J. R. (2004). The molecular basis of odor coding in the Drosophila antenna. *Cell* **117**, 965–979.

Hanna, S. R. and Insley, E. M. (1989). Time series analyses of concentration and wind fluctuations. *Boundary-Layer Meteorology* **47**, 131–147.

Heisenberg, M. and Wolf, R. (1979). On the fine structure of yaw torque in visual flight orientation of *Drosophila melanogaster*. *J. Comp. Physiol.* **130**, 113–130.

Heran, H. (1959). Wahrnehmung und Regelung der Flugeigengeschwindigkeit bei *Apis mellifera* L. *Z. Vergl. Physiol.* **42**, 103–163.

Johnston, J. S. (1982). Genetic variation for anemotaxis (wind-directed movement) in laboratory and wild-caught populations of *Drosophila*. *Behav. Genet.* **12**, 281–293.

Jones, C. D. (1983). On the structure of instantaneous plumes in the atmosphere. *J. Hazard. Mater.* **7**, 87–112.

Justus, K. A. and Cardé, R. T. (2002). Flight behaviour of two moths, *Cadra cautella* and *Pectinophora gossypiella*, in homogeneous clouds of pheromone. *Physiol. Entomol.* **27**, 67–75.

Kanzaki, R., Sugi, N. and Shibuya, T. (1992). Self-generated turning of Bombyx mori males during pheromone-mediated upwind walking. *Zoolog. Sci.* **9**, 515–527.

Kellogg, F. E., Frizel, D. E. and Wright, R. H. (1962). The olfactory guidance of flying insects. IV. *Drosophila*. *Canadian Entomologist* **94**, 884–888.

Kennedy, J. S. (1940). The visual responses of flying mosquitoes. *Proc. Zool. Soc. London* **109**, 221–242.

Kennedy, J. S. (1983). Zigzagging and casting as a programmed response to wind-borne odour: a review. *Physiol. Entomol.* **8**, 109–120.

Kennedy, J. S., Ludlow, A. R. and Sanders, C. J. (1980). Guidance system used in moth sex attraction. *Nature* **288**, 475–477.

Kennedy, J. S., Ludlow, A. R. and Sanders, C. J. (1981). Guidance of flying male moths by wind-borne sex pheromone. *Physiol. Entomol.* **6**, 395–412.

Kuenen, L. P. S. and Baker, T. C. (1983). A non-anemotactic mechanism used in pheromone source location by flying moths. *Physiol. Entomol.* **8**, 277–289.

Kuenen, L. P. S. and Cardé, R. T. (1994). Strategies for recontacting a lost pheromone plume: casting and upwind flight in the male gypsy moth. *Physiol. Entomol.* **19**, 15–29.

Lehmann, F. O. and Dickinson, M. H. (1997). The changes in power requirements and muscle efficiency during elevated force production in the fruit fly *Drosophila melanogaster*. *J. Exp. Biol.* **200**, 1133–1143.

Lemon, W. C. and Getz, W. M. (1997). Temporal resolution of general odor pulses by olfactory sensory neurons in American cockroaches. *J. Exp. Biol.* **200**, 1809–1819.

Lemon, W. C. and Getz, W. M. (1998). Responses of cockroach antennal lobe projection neurons to pulsatile olfactory stimuli. In *Olfaction and Taste XII*, (ed. C. Murphy), pp. 517–520. San Diego, CA: New York Academy of Sciences.

Mafra-Neto, A. and Cardé, R. T. (1994). Fine-scale structure of pheromone plumes modulates upwind orientation of flying moths. *Nature* **369**, 142–144.

Mafra-Neto, A. and Cardé, R. T. (1996). Dissection of the pheromone-modulated flight of moths using single-pulse response as a template. *Experientia* **52**, 373–379.

Maimon, G., Straw, A. D. and Dickinson, M. H. (in preparation). A simple visual algorithm underlies attraction-repulsion decision in *Drosophila*.

Marsh, D., Kennedy, J. S. and Ludlow, A. R. (1978). An analysis of anemotactic zigzagging flight in male moths stimulated by pheromone. *Physiol. Entomol.* **3**, 221–240.

Miller, A. (1950). The internal anatomy and histology of the imago of *Drosophila melanogaster*. In *Biology of Drosophila*, (ed. M. Demerec), pp. 420–531. New York: John Wiley & Sons, Inc.

Murlis, J., Elkinton, J. S. and Cardé, R. T. (1992). Odor plumes and how insects use them. *Annu. Rev. Entomol.*, 505–532.

Murlis, J., Willis, M. A. and Cardé, R. T. (2000). Spatial and temporal structures of pheromone plumes in fields and forests. *Physiol. Entomol.* **25**, 211–222.

Ng, M., Roorda, R. D., Lima, S. Q., Zemelman, B. V., Morcillo, P. and Miessenböck, G. (2002). Transmission of olfactory information between three populations of neurons in the antennal lobe of the fly. *Neuron* **36**, 463–474.

Niehaus, M. (1981). Flight and flight control by the antennae in the small tortoiseshell (Aglais urticae L., Lepidoptera): II. Flight mill and free flight experiments. *J. Comp. Physiol.* **145**, 257–264.

Reiser, M. B. (2007). Visually mediated control of flight in *Drosophila*: not lost in translation. In *Computation and Neural Systems*, (PhD thesis), pp. 206. Pasadena: California Institute of Technology.

Reiser, M. B. and Dickinson, M. H. (in review). Modular displays for rapid development of behavioral stimuli.

Robertson, H. M., Warr, C. G. and Carlson, J. R. (2003). Molecular evolution of the insect chemoreceptor gene superfamily in *Drosophila melanogaster*. *Proceedings of the National Academy of Sciences* **100 (Suppl 2)**, 14537–14542.

Rumbo, E. R. and Kaissling, K. E. (1989). Temporal resolution of odour pulses by three types of pheromone receptor cells in *Antheraea polyphemus*. *Journal of Comparative Physiology [A]* **165**, 281–291.

Rützler, M. and Zwiebel, L. J. (2005). Molecular biology of insect olfaction: recent progress and conceptual models. *Journal of Comparative Physiology [A]* **191**, 777–790.

Sabelis, M. W. and Schippers, P. (1984). Variable wind directions and anemotactic strategies of searching for an odour plume. *Oecologia* **63**, 225–228.

Schneider, G. (1953). Die Halteren fer Schmeissfliege (*Calliphora*) als Sinnesorgane und als Mechanische Flugstabilisatoren. *Z. Vergl. Physiol.* **35**, 416–458.

Srinivasan, M., Lehrer, M., Kirchner, W. H. and Zhang, S. W. (1991). Range perception through apparent image speed in freely flying honeybees. *Vis. Neurosci.* **6**, 519–535.

Straussfeld, N. J. and Bacon, J. P. (1983). Multimodal convergence in the central nervous system of dipterous insects. *Fortschr. Zool.* **28**, 47–76.

Tammero, L. F. and Dickinson, M. H. (2002a). Collision-avoidance and landing responses are mediated by separate pathways in the fruit fly, *Drosophila melanogaster*. *J. Exp. Biol.* **205**, 2785–2798.

Tammero, L. F. and Dickinson, M. H. (2002b). The influence of visual landscape on the free flight behavior of the fruit fly *Drosophila melanogaster*. *J. Exp. Biol.* **205**, 327–343.

Tammero, L. F., Frye, M. A. and Dickinson, M. H. (2004). Spatial organization of visuomotor reflexes in Drosophila. *J. Exp. Biol.* **207**, 113–122.

Vickers, N. J. and Baker, T. C. (1992). Male *Heliothis virescens* maintain upwind flight in response to experimentally pulsed filaments of their sex pheromone (Lepidoptera: Noctuidae). *Journal of Insect Behavior* **5**, 669–687.

Vickers, N. J. and Baker, T. C. (1994). Reiterative responses to single strands of odor promote sustained upwind flight and odor source location by moths. *Proc. Natl. Acad. Sci. U. S. A.* **91**, 5756–5760.

Wang, J. W., Wong, A. M., Flores, J., Vosshall, L. B. and Axel, R. (2003). Two-photon calcium imaging reveals an odor-evoked map of activity in the fly brain. *Cell* **112**, 271–282.

Weis-Fogh, T. (1948). An aerodynamic sense organ in locusts. In *Eighth International Congress of Entomology*, pp. 584–588. Stockholm.

Weis-Fogh, T. (1949). An aerodynamic sense organ stimulating and regulating flight in locusts. *Nature* **164**, 873–874.

Willis, M. A. and Arbas, E. A. (1991). Odor-modulated upwind flight of the sphinx moth, *Manduca sexta* L. *Journal of Comparative Physiology A* **169**, 427–440.

Willis, M. A. and Baker, T. C. (1984). Effects of intermittent and continuous pheromone stimulation on the flight behavior of the oriental fruit moth, *Grapholita molesta*. *Physiol. Entomol.* **9**, 341–358.

Wilson, R. I., Turner, G. C. and Laurent, G. (2004). Transformations of olfactory representations in the *Drosophila* antennal lobe. *Science* **303**, 366–370.

Wright, R. H. (1964). The science of smell. London: G. Allen & Unwin.

Zanen, P. O., Sabelis, M. W., Buonaccorsi, J. P. and Cardé, R. T. (1994). Search strategies of fruit flies in steady and shifting winds in the absence of food odours. *Physiol. Entomol.* **19**, 335–341.